Doctoral Thesis

Semiclathrate-based post- and pre-combustion CO_2 capture: thermodynamic and spectroscopic analyses

Soyoung Kim

Department of Urban and Environmental Engineering
(Environmental Science and Engineering)

Graduate School of UNIST

2017

Semiclathrate-based post- and pre-combustion CO_2 capture: thermodynamic and spectroscopic analyses

Soyoung Kim

Department of Urban and Environmental Engineering
(Environmental Science and Engineering)

Graduate School of UNIST

Semiclathrate-based post- and pre-combustion CO_2 capture: thermodynamic and spectroscopic analyses

A thesis/dissertation
submitted to the Graduate School of UNIST
in partial fulfillment of the requirements for the degree of
Doctor of Philosophy

Soyoung Kim

12. 08. 2016 of submission

Approved by

Yongwon Seo

Advisor

Yongwon Seo

Semiclathrate-based post- and pre-combustion CO_2 capture: thermodynamic and spectroscopic analyses

Soyoung Kim

This certifies that the thesis/dissertation of Soyoung Kim is approved.

12/08/2016

Advisor: Yongwon Seo

Young-Nam Kwon

Sung-Deuk Choi

Chaenyung Cha

Seong-Pil Kang

ABSTRACT

The accumulation of CO_2 and other greenhouse gases in the atmosphere has led to global warming. These climate changes are threatening the earth and its inhabitants. So, the clathrate hydrates formation application is interesting to many researchers and experts.This research is focused on minimizing CO_2 capture using clathrate hydrates formation because CO_2 is attributed to a large portion of global warming.

Clathrate hydrates are are non-stoichiometric crystalline compounds formed by a physical reaction between small guest molecules and host water molecules at low temperature and high pressure conditions. Water molecules form a framework while the guest molecules are trapped. These two different molecules are mechanically intermingled but not chemically. Clathrate hydrates have many technological applications, such as separation processes, natural gas storage/transportation and carbon dioxide sequestration. These clathrate hydrate-based technologies are expected to be an innovative method for solving energy and environmental issues. However, the major drawback of the clathrate hydrate-based technologies is that they require the maintenance of a specific temperature and pressure for storing or capturing gas molecules in the hydrate cages.

Clathrate hydrates can be divided into true and semi clathrate hydrates. These hydrates have many similar physical and chemical properties, but the main difference between the two is that there exists a chemical interaction between the host and guest molecules. The chemical interaction between semiclathrate hydrates is not yet fully understood. Recently, semi-clathrate hydrates have been reported to be formed by the existence of a hydrate promotor such as quaternary ammonium salts (QASs), amines, and alcohols. The presence of a hydrate promotor forms semiclathrate hydrates under a higher temperature and lower pressure conditions when compared with the pure hydrate systems. Semiclathrate hydrates have unoccupied cages which can be applied to gas separation/sequestration for capturing CO_2. Quaternary ammonium salts (QASs) form semiclathrate hydrates under higher temperature and lower pressure conditions when compared with the pure hydrate systems. These semiclathrate hydrates have vacant small cages which can be used for capturing small-sized gas molecules, while the large cages are occupied by the TBA cation.

The main purpose of this study is to develop an innovative energy-efficient and eco-friendly CO_2 separation method using semiclathrate hydrates formation, formed by quaternary ammonium salts (QASs). This research is based on selective partitioning of the CO_2 and N_2 (or H_2) gases during hydrates formation. CO_2 has a higher occupancy in the hydrate phase, even though both gases can form hydrates, since CO_2 has a larger molecular diameter and more thermodynamic stability than N_2

(or H_2). The feasibility of the semiclathrate hydrates based CO_2 capture method will be examined with a focus on the macroscopic phase behavior and microscopic analytical methods such as NMR, and Raman spectroscopy to investigate the guest gas enclathration behavior. In addition, thermal properties will also be measured using a high pressure micro differential scanning calorimeter (HP μ-DSC) in order to provide heat of formation and dissociation values of semiclathrate hydrates.

□ In this study, clathrate-based CO_2 capture from flue and fuel gas was investigated in the presence of quaternary ammonium salts (QASs) as a semiclathrate former (tetra-n-butyl ammonium bromide (TBAB), chloride (TBAC), and fluoride (TBAF)), tetrahydrofuran (THF) as a water-soluble sII hydrate former, and cyclopentane (CP) as a water-insoluble sII hydrate former. The clathrate stabilities of the CO_2 (20%) + N_2 (80%) + promoter systems and the CO_2 (40%) + H_2 (60%) + promoter systems were measured using an isochoric method. The clathrate equilibrium pressures at a specified temperature were significantly reduced in the presence of these thermodynamic promoters. Gas storage capacity and CO_2 composition analysis in both vapor and clathrate phases were conducted using gas chromatography. The CO_2 in flue gas mixtures was found to be enriched approximately 61% in semiclathrate phase. In addition, the 5.6 mol% THF solution showed the largest gas storage capacity during the clathrate formation, but it demonstrated the lowest CO_2 concentration (35%) in the clathrate phase after the completion of clathrate formation. In addition, the CO_2 in fuel gas mixtures was found to be enriched approximately 95% in semiclathrate phase after the completion of semiclathrate formation. The inclusion of CO_2 in the clathrate phase was also confirmed via Raman spectroscopy. The overall experimental results are useful for the clathrate-based CO_2 capture process from flue and fuel gas.

CONTENTS

LIST OF FIGURES

LIST OF TABLES

Chapter I

Introduction

1.1. Introduction

Carbon dioxide (CO_2) and other greenhouse gases is suspected as a major source of global warming [1]. These climate changes are threatening the earth and its inhabitants. So, gas hydrates formation is interesting to many researchers and experts. There are a variety of technologies using gas hydrates formation, such as separation processes, natural gas storage/transportation and carbon dioxide sequestration (figure 1.1) [2-13]. This research is focused on minimizing CO_2 capture using hydrates formation because carbon dioxide is attributed to a large portion of global warming.

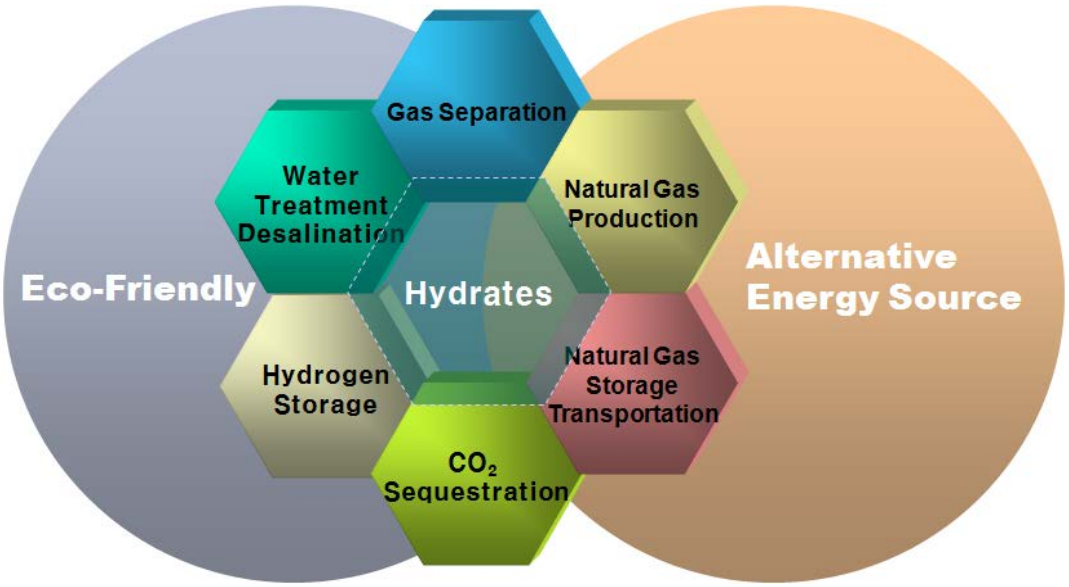

Figure 1.1. Gas hydrate-based applications.

My first goal is to uncover the principles and foundations related to the formation of gas hydrates and semiclathrate. Then, various experimental methods are conducted to reveal semiclathrate formation and dissociation mechanisms at suitable conditions because semiclathrate and their derivates tend to dissociate naturally in ambient conditions. The ultimate goal of this research is to find the optimal conditions needed for capturing CO_2 within semiclathrate to reduce suspected global warming gas.

1.1.1. Gas hydrates

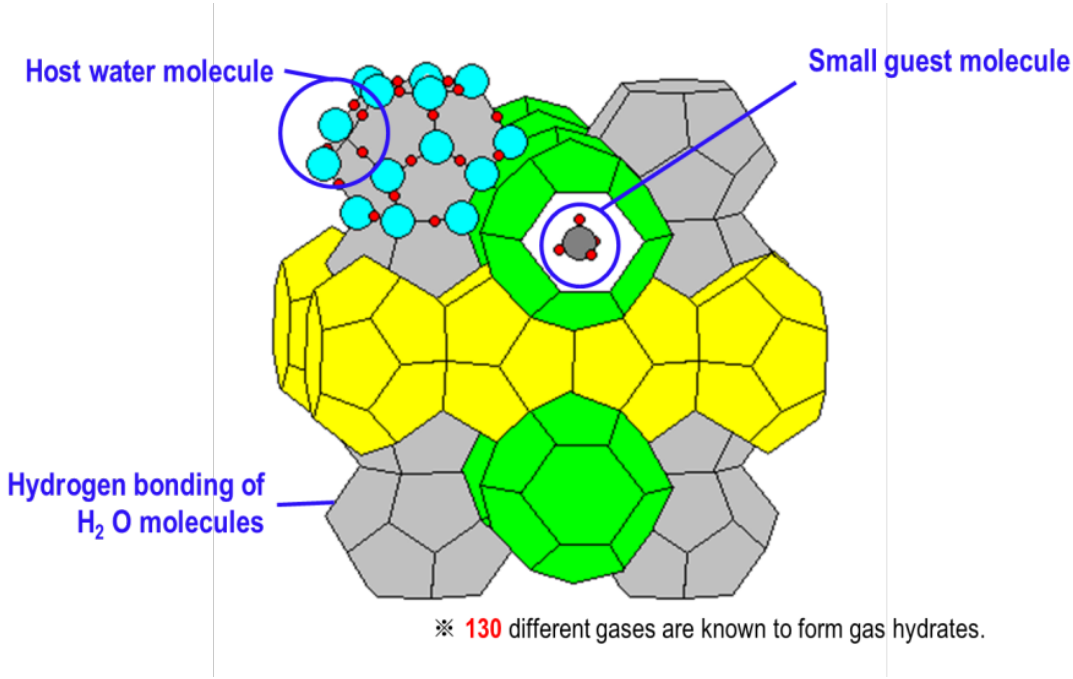

Figure 1.2. The inclusion compound of gas hydrate [28].

Gas hydrates are non-stoichiometric crystalline compounds formed by a physical reaction between small guest molecules and host water molecules at low temperature and high pressure conditions [14]. Water molecules form a framework while the guest molecules are trapped as shown in (Figure 1.2.). These two different molecules are mechanically intermingled but not chemically [15].

1.1.2. Crystal structures

Table 1.1. Characteristics of gas hydrate structure [14].

Hydrate structure	**I**		**II**		**H**		
Cavity	Small	Large	Small	Large	Small	Medium	Large
Structure	5^{12}	$5^{12}6^2$	5^{12}	$5^{12}6^4$	5^{12}	$4^35^66^3$	$5^{12}6^8$
No. of cavities/unit cell	2	6	16	8	3	2	1
Average cavity radius (Å)	3.95	4.33	3.91	4.73	3.91	4.06	5.71
Variation in radius (%)	3.4	14.4	5.5	1.73	4	8.5	15.1
No. of water molecules/cavity	20	24	20	28	20	20	36

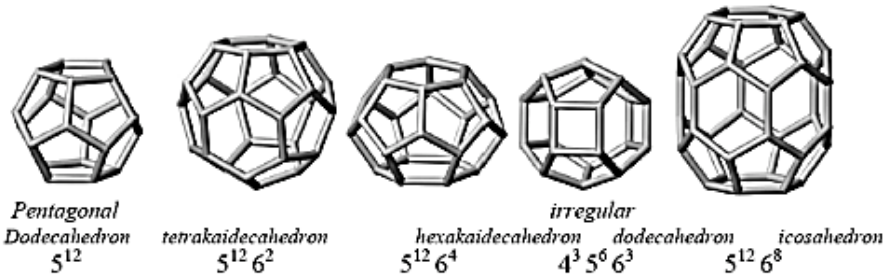

Figure 1.3. Unit cell of gas hydrate structures [29].

The host framework of gas hydrates is classified as structure I (sI), structure II (sII), and structure H (sH). The gas hydrate framework structure can take on different forms, the Structure I (sI) and Structure II (sII) is most common forms [14]. Gas hydrate structures are composed of different types of lattices and size. The all clathrate hydrates have pentagonal dodecahedron (5^{12}) cages of water molecules. It has 12 regular pentagonal faces, 20 vertices, and 30 edges. These are five representative cavities; pentagonal dodecahedron (5^{12}), tetrakaidecahedron ($5^{12}6^2$), hexakaidecahedron ($5^{12}6^4$), irregular dodecahedron ($4^35^66^3$), and icosahedron ($5^{12}6^8$). The cavities size and geometric information are shown in (Figure 1.3.), and the data are represented in (Table 1.1.).

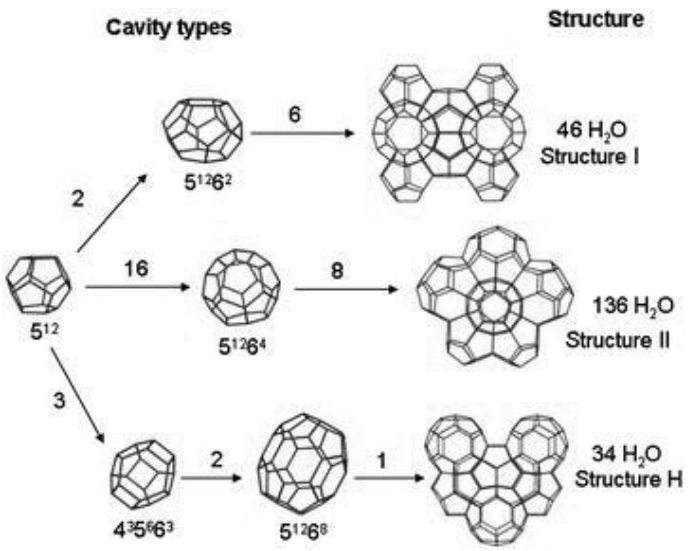

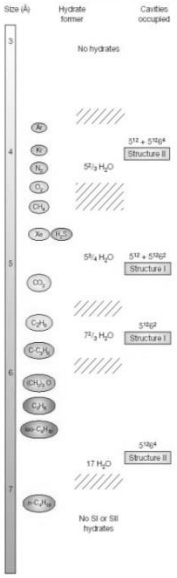

Figure 1.4. Gas hydrate structure sI, sII, and sH [30].

Each structure has a different unit of cavities which shown in (Figures 1.3. and 1.4.). The structures depend on the size of the guest gas molecule which is captured in empty cages of gas hydrate [14].

structure I: If the size of gas hydrate formers (guests gas) is in the range of 4.2 and 6.0; CH_4, C_2H_6, CO_2, and H_2S. Structure I (sI) hydrates are made up of 8 polyhedral cages; 6 large ones and 2 small [29].

structure II: If the size of gas hydrate formers (guests gas) is smaller than 4.2 or larger than 6.0; C_3H_8, iso-$_4H_{10}$, N_2. Structure II (sII) hydrates are made up of 24 polyhedral cages; 8 large ones and 16 small [29].

structure H: Ripmeester (1987) found a new hydrate structure, called structure H (sH). This structure has three sizes of cavities and are formed by larger molecules, but only in the presence of a smaller helper gas molecule, such as CH_4, Xe, and H_2. Structure H hydrates are made up of 6 polyhedral cages; 1 large, 3 medium, and 2 small. The large molecule occupies the large cage and the small molecule occupies the small and medium cages. Structure H formers include: 2-methylbutane, methylcyclopentane, methylcyclohexane, and cyclooctane [29].

1.1.3. Trend of applications

The consumption of fossil fuels such as natural gas, coal, and oil leads to climate changes. The worldwide energy demands are rapidly increasing for a decade and the CO_2 is exponentially produced. The CO_2 capture and disposal has become an important research for mitigating CO_2 emissions.

CCS (Carbon Capture and Storage) process can divide for separation, transportation, and underground deposit. In the CCS process, CO_2 separation has required a large amount of expense for handling. Moreover, there are comprehensive studies that are investigated for developing the energy efficient and environmentally friendly technology for separation of the CO_2 from large emission sources. CO2 can be separated and captured using absorption, adsorption, or membrane technologies from flue or fuel gas. Recently, the dominant CO_2 capture technology is absorption method with amines. Other technology such as membrane, adsorption, and Metal-Organic Frameworks (MOFs) technologies are still being investigated.

Clathrate-based CO_2 capture can be a novel approach as clean technology to reduce CO_2 because clathrate can form with only water and gas molecules. In addition, the clathrate-based technologies can be controlled by depressurization or heating. A recent study [21] provided a clathrate-based CO_2 separation can recover more than 99 % CO_2 with several clathrate formation processes. Park et al. [22] also studied the semiclathrate-based fuel gas separation at milder condition than that of gas hydrate formation condition. This study is targeting to find the confirmation of the feasibility for the semiclathrates-based post-and pre-combustion CO_2 capture. The experimental results provide fundamental key variables for designing and operating the semiclathrates-based CO_2 capture process.

1.2. Thermodynamic hydrate promotion

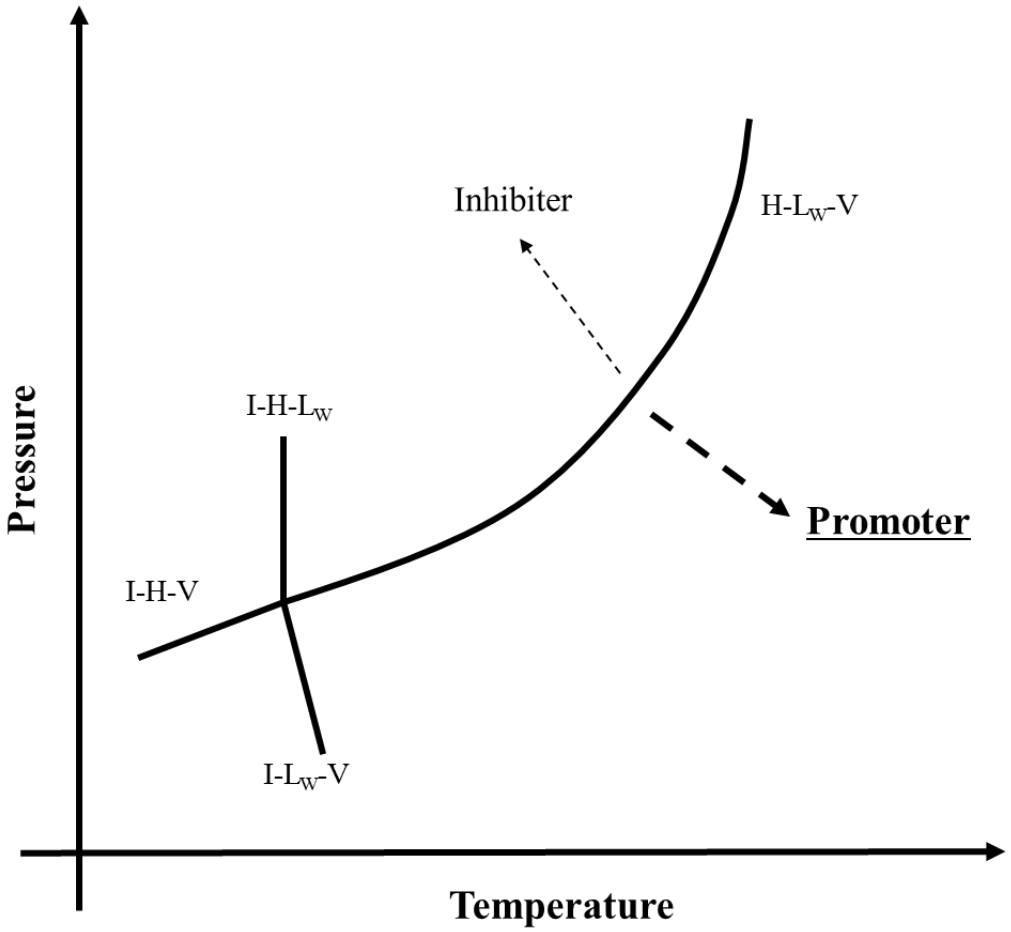

Figure 1.5. Gas hydrate phase equilibrium.

The (Figure 1.5.) shows a typical p-T diagram of a gas hydrate. This equilibrium data area is a very important to predict the conditions of their stability both theoretical and practical reasons. The equilibrium curve provides the hydrate stability region. The clathrate hydrates can form under the left of equilibrium line. If the curve shifted towards lower temperatures and higher pressure, it is more stable.

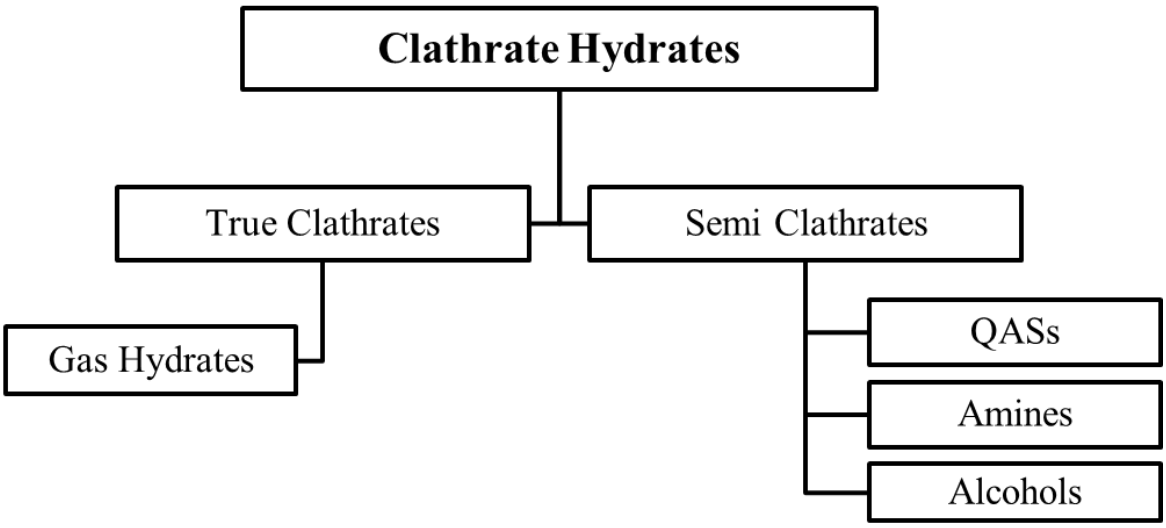

Figure 1.6. Classification of clathrate hydrate.

Clathrate hydrates are crystalline water-based solids physically resembling ice. Clathrate hydrates can be divided into true- and semi-clathrate hydrates. These hydrates have many similar physical and chemical properties, but the main difference between the two is that there exists a chemical interaction between the host and guest molecules. The chemical interaction between semiclathrates is not yet fully understood. This research will focus on the understanding semiclathrates formation and their role in capturing CO_2.

1.2.1. sII hydrates

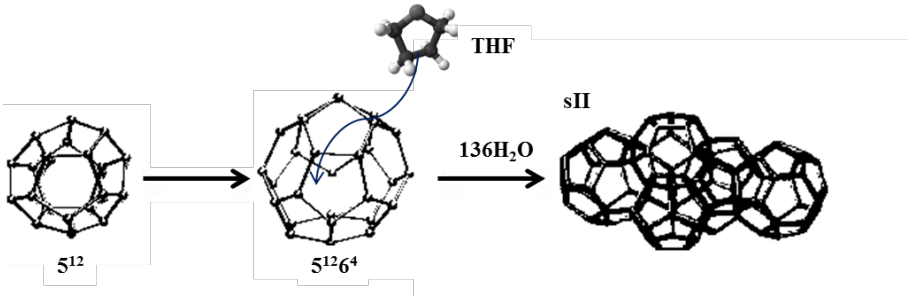

Figure 1.7. THF hydrate formation (sII structure) [31].

Tetrahydrofuran (THF), which is completely miscible in water, and cyclopentane (CP), which is immiscible in water, are well-known thermodynamic sII hydrate promoters and these sII hydrate former has been studied exhaustively and broadly [16-21, 23-24]. Adding THF and CP to the hydrate formation system, the gas hydrate equilibrium pressure can significantly decrease at a given temperature and pressure condition because they are enclathrated in large cages of sII hydrates, which results in significant thermodynamic stabilization. However, these conventional thermodynamic promoters, such as THF and CP, have several disadvantages to their use in actual processes. They are highly volatile and toxic, indicating that an additional process for further purification of the gas phase and complete recovery from the liquid phase is required after use [26, 27]. A significant loss after repeated use can also be expected because of their high volatility. When compared with water-miscible promoters, the liquid phase of CP needs more vigorous agitation to enhance the gas - liquid contact area for gas hydrate formation because of its immiscibility in water, which suggests a larger energy requirement for the actual application.

1.2.2. Semiclathrates

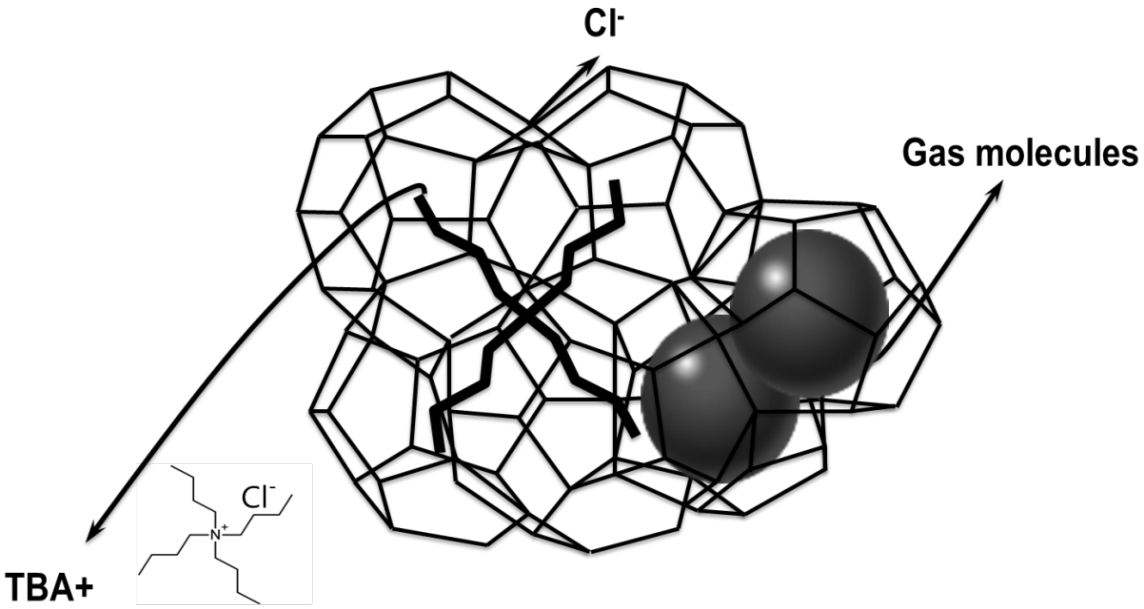

Figure 1.8. TBAC semiclathrate.

Recently, semiclathrates have been reported to be formed by the existence of a hydrate promotor known as quaternary ammonium salts (QASs), amines, and alcohols. In the presence of these hydrate promoter, semiclathrates have unoccupied small cages which can be applied for gas capturing, while the large cages are charged by the TBA cation. Tetra-n-butyl ammonium bromide (TBAB) and tetra-n-butyl ammonium fluoride (TBAF) well known as QASs promoters are broadly studied but TBAC are rarely attention. The TBAC semiclathrate is expected to have similar properties with TBAB and TBAF.

1.3. References

[1] Spigarelli BP, Kawatra SK. Opportunities and challenges in carbon dioxide capture. J CO_2 Util 2013;1:69-87.

[2] Khokhar AA, Gudmundsson JS, Sloan ED. Gas storage in structure H hydrates. Fluid Phase Equilib 1998;150-151:383-92.

[3] Eslamimanesh A, Mohammadi AH, Richon D. Thermodynamic modeling of phase equilibria of semi-clathrate hydrates of CO_2, CH_4, or N_2 + tetra-n-butylammonium bromide aqueous solution. Chem. Eng. Sci 2012;81:319-2.

[4] Linga P, Kumar R, Lee JD, Ripmeester J, Englezos P. A new apparatus to enhance the rate of gas hydrate formation: Application to capture of carbon dioxide. Int. J. Greenhouse Gas Control 2010;4:630-7.

[5] Tajima H, Yamasaki A, Kiyono F. Process design of a new injection method of liquid CO_2 at the intermediate depths in the ocean using a static mixer. Fuel Process. Technol 2005;86:1667-78.

[6] Lee H, Seo Y, Seo YT, Moudrakovski IL, Ripmeester JA. Recovering methane from solid methane hydrate with carbon dioxide. Angew. Chem. Int. Ed 2003;42:5048-51.

[7] Kang S-P, Lee H. Recovery of CO_2 from flue gas using gas hydrate: thermodynamic verification through phase equilibrium measurements. Environ. Sci. Technol 2000;34:4397-400.

[8] Linga P, Kumar R, Englezos P. The clathrate hydrate process for post and pre-combustion capture of carbon dioxide. J. Hazard. Mater 2007;149:625-9.

[9] Lee Y, Lee S, Lee J, Seo Y. Structure identification and dissociation enthalpy measurements of the CO_2 + N_2 hydrates for their application to CO_2 capture and storage. Chem. Eng. J 2014;246:20-6.

[10] Li XS, Xu CG, Chen ZY, Wu HJ. Tetra-n-butyl ammonium bromide semi-clathrate hydrate process for post-combustion capture of carbon dioxide in the presence of dodecyl trimethyl ammonium chloride. Energy 2010;35:3902-8.

[11] Lee Y, Lee S, Jin YK, Seo Y. 1-Propanol as a co-guest of gas hydrates and its potential role in gas storage and CO_2 sequestration. Chem. Eng. J 2014;258:427-32.

[12] Kang KC, Linga P, Park K-n, Choi S-J, Lee JD. Seawater desalination by gas hydrate process and removal characteristics of dissolved ions (Na^+, K^+, Mg^{2+}, Ca^{2+}, B^{3+}, Cl^-, SO_4^{2-}). Desalination 2014;353:84-90.

[13] Cha J-H, Seol Y. Increasing Gas Hydrate Formation Temperature for Desalination of High Salinity Produced Water with Secondary Guests. ACS Sustainable Chem. Eng. 2013;1:1218-24.

[14] Sloan ED, Koh C. Clathrate hydrates of natural gases, 3th ed. Boca Raton. Taylor & Fr ancis; 2007.

[15] Koh CA. Towards a fundamental understanding of natural gas hydrates. Chem Soc Rev. 2002;31:157-67.

[16] Torré J-P, Ricaurte M, Dicharry C, Broseta D. CO_2 enclathration in the presence of water-soluble hydrate promoters: Hydrate phase equilibria and kinetic studies in quiescent conditions. Chem Eng Sci 2012;82:1-13.

[17] Yang M, Song Y, Jiang L, Zhao Y, Ruan X, Zhang Y, et al. Hydrate-based technology for CO_2 capture from fossil fuel power plants. Appl Energy 2014;116:26-40.

[18] Kang S-P, Lee H, Lee C-S, Sung W-M. Hydrate phase equilibria of the guest mixtures containing CO_2, N_2 and tetrahydrofuran. Fluid Phase Equilib 2001;185:101-9.

[19] Delahaye A, Fournaison L, Marinhas S, Chatti I, Petitet J-P, Dalmazzone D, et al. Effect of THF on equilibrium pressure and dissociation enthalpy of CO_2 hydrates applied to secondary refrigeration. Ind Eng Chem Res 2005;45:391-7.

[20] Hashimoto S, Murayama S, Sugahara T, Ohgaki K. Phase equilibria for H_2 + CO_2 + tetrahydrofuran + water mixtures containing gas hydrates. J Chem Eng Data 2006;51:1884-6.

[21] Kang S-P, Lee H. Recovery of CO_2 from flue gas using gas hydrate: thermodynamic verification through phase equilibrium measurements. Env Sci Technol 2000;34:4397-400.

[22] Park S, Lee S, Lee Y, Seo Y. CO_2 capture from simulated fuel gas mixtures using semiclathrate hydrates formed by quaternary ammonium salts. Environ Sci Technol. 2013;47:7571-7.

[23] Seo Y, Kang S-P, Lee S, Lee H. Experimental measurements of hydrate phase equilibria for carbon dioxide in the presence of THF, propylene oxide, and 1,4-dioxane. J Chem Eng Data 2008;53:2833-7.

[24] Hashimoto S, Sugahara T, Sato H, Ohgaki K. Thermodynamic stability of H_2 + tetrahydrofuran mixed gas hydrate in nonstoichiometric aqueous solutions. J Chem Eng Data 2007;52:517-20.

[25] Sfaxi IBA, Durand I, Lugo R, Mohammadi AH, Richon D. Hydrate phase equilibria of CO_2 + N_2 + aqueous solution of THF, TBAB or TBAF system. Int J Greenhouse Gas Control 2014;26:185-92.

[26] Mayoufi N, Dalmazzone D, Fürst W, Delahaye A, Fournaison L. CO_2 enclathration in hydrates of peralkyl-(ammonium/phosphonium) salts: stability conditions and dissociation enthalpies. J Chem Eng Data 2009;55:1271-5.

[27] Mohammadi A, Manteghian M, Mohammadi AH. Dissociation data of semiclathrate hydrates for the systems of tetra-n-butylammonium fluoride (TBAF) + methane + water, TBAF + carbon dioxide + water, and TBAF + nitrogen + water. J Chem Eng Data 2013;58:3545-50.

[28] http://www.uwgb.edu/dutchs/petrology/Clathrate-0.HTM

[29] https://miktechnology.wordpress.com/2010/05/22/hydrates-a-novel-concept-for-plugging-deep-sea-severed-pipeline-proposed-scenario-for-bp-gulf-of-mexico-spill/

[30] http://pubs.rsc.org/en/content/articlehtml/2013/cs/c2cs35340g

[31] http://hubpages.com/education/Water-Desalination-Process-Using-Hydrates#

Chapter II

Experimental section

2.1. Experimental

2.1.1. Materials

The CH_4 with a purity of 99.95 % was purchased from Gasvally Co. (Republic of Korea) and the CO_2 with a purity of 99.99 % was supplied by the PSG Gas Co. (Republic of Korea). N_2 with a purity of 99.9% was supplied from MS Gas Co. (Korea). The gas mixture of CO_2 (20%) + N_2 (80%) and CO_2 (40%) + H_2 (60%) was supplied by MS Gas Co. (Republic of Korea). TBAB (99.9% purity), TBAC (97.0% purity), TBAF (75.0% solution in water), THF (99.0% purity), and CP (99.0% purity) were purchased from Sigma-Aldrich Chemical Co. (USA). Double distilled and deio -nized water was used in this experiment.

2.1.2. TiAAB synthesis

Tetra-iso-amyl ammonium Bromide (TiAAB): Triisopentylamine and isopentyl bromine were refluxed in acetonitrile under nitrogen for 72 h. The solvent was evaporated by heating under vacuum, and the crystals were then dissolved in ethyl acetate. The TBAB was recrystallized overnight at 275.0 K. The crystals were then filtered from the solution and the process was repeated twice. The crystalline mass was dried in a vacuum oven at 313.0 K.

2.2. Experimental apparatus & procedure

2.2.1. Stability condition measurements

The dissociation equilibrium temperatures of pure TBAC semiclathrate were measured under an atmospheric pressure condition by using an Erlenmeyer flask that was immersed in a water bath circulator (RW-2040G, JEIOTECH, Republic of Korea) with a magnetic bar inside. The temperature of the water bath was lowered until pure TBAC semiclathrate crystals appeared. The temperature was also maintained for more than 6 h for complete conversion. Then, it was slowly increased in steps of 0.1 K/h until the semiclathrate crystals disappeared. The point where the final semiclathrate crystal disappeared was considered as the dissociation equilibrium temperature of the pure TBAC semiclathrate at each TBAC concentration.

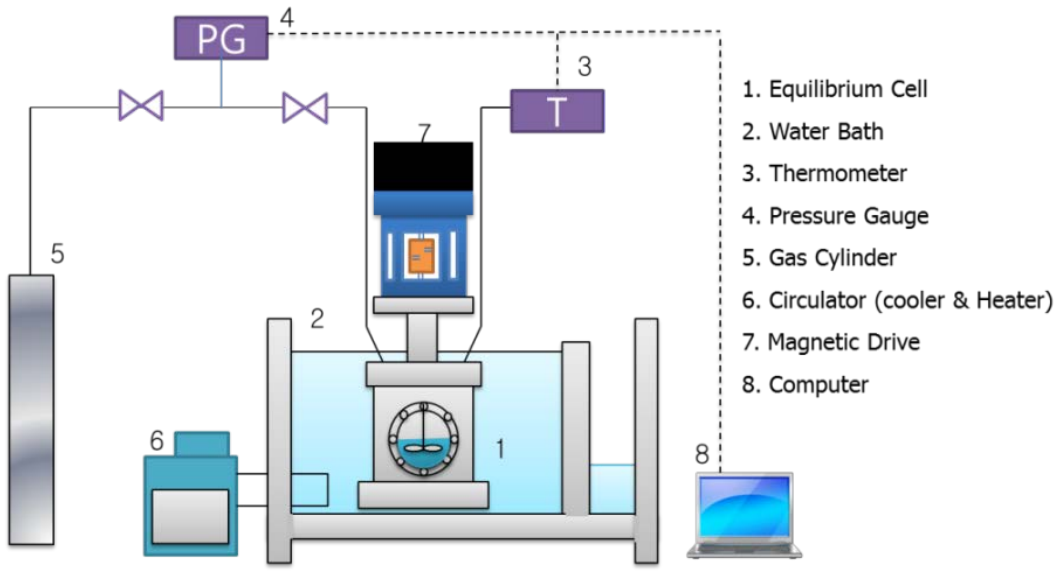

Figure 2.1. Schematic diagram of an experimental apparatus for measuring semiclathrate stability conditions.

(Figure 2.1.) shows an experimental apparatus for measuring semiclathrate stability conditions. The equilibrium cell was constructed of 316 stainless steel. It had an internal volume of approximately 250 cm^3. The cell has sapphire windows located at the front and opposite sides, which allow

for the visual observation of semiclathrate formation and dissociation processes. The equilibrium cell was immersed in a water bath, which was temperature-controlled using an external circulator (RW-2040G, JEIOTECH, Korea). During the experiment, an impeller-type stirrer was used to agitate the aqueous solution in the cell. The internal temperature was measured by a thermocouple with ± 0.1 K accuracy, which was calibrated with ASTM 63 C (H-B Instrument Company, USA) with ± 0.02 K accuracy from 265.15 to 305.15 K. The pressure in the cell was measured by a pressure transducer (S-10, WIKA, Germany), which was calibrated using a Heise Bourdon tube pressure gauge (CMM-140830, 0-20.0 MPa, Ashcroft, Inc. USA) with an error of ± 0.02 MPa.

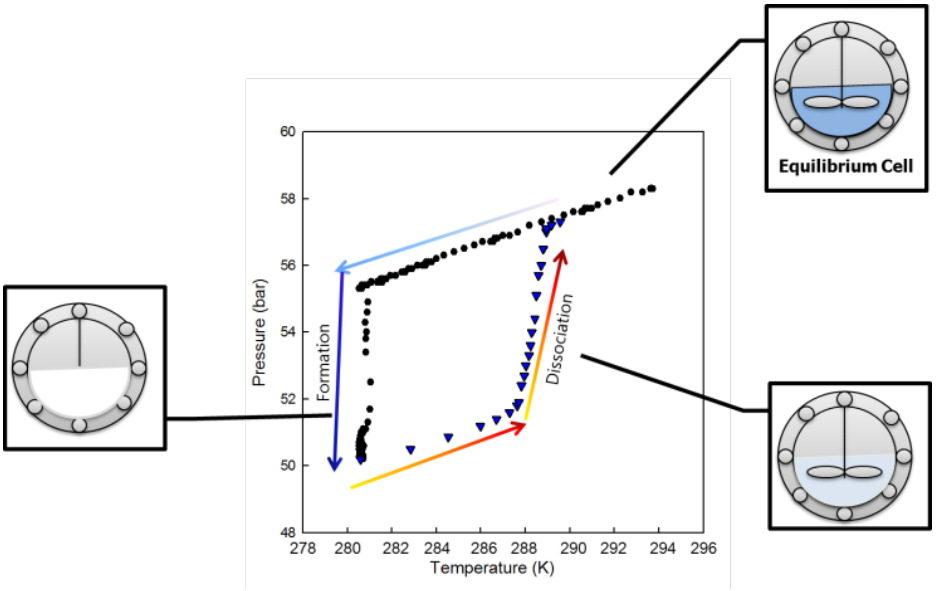

Figure 2.2. p-T trace for determination of equilibrium dissociation (CH_4 +TBAC + water).

The three-phase (H-L_W-V) clathrate equilibria were measured using an isochoric method (pressure variation versus temperature at constant volume (pVT)) with step heating and cooling (Figure 2.2.). The equilibrium cell was initially charged with 70 cm^3 of TBAB, TBAC, TBAF, TiAAB, THF, or CP solution. Then, gas was supplied into the cell up to the desired pressure. The cell was slowly cooled in steps of 1.0 K/h in order to initiate the clathrate formation, which could be detected by abrupt pressure decreases. After a sufficient time was given for the complete conversion of the solution into the clathrate, the temperature was raised in steps of 0.1 K/90 min until all clathrate crystals disappeared. The three-phase (H-L_W-V) equilibrium point at a given pressure was determined at the intersection of the clathrate dissociation and thermal expansion lines, and this procedure was repeated at each pressure condition.

2.2.2. Differential scanning calorimeter (DSC)

The onset temperature and dissociation enthalpy of pure TBAC and TiAAB semiclathrate was measured using a differential scanning calorimeter (DSC, Q 200, TA instruments, USA). 11.0 mg of the TBAC and TiAAB solution was encapsulated in a Tzero hermetic pan and lid using a sample press (Tzero, TA instruments, USA), and the pan was then loaded into the apparatus. Its temperature was reduced to 243.15 K for the nucleation of semiclathrate. After confirming the complete conversion of the TBAC and TiAAB solution to a TBAC and TiAAB semiclathrate, its temperature was raised to 323.15 K for the dissociation of the TBAC and TiAAB semiclathrate. The entire cooling and heating process was conducted at a rate of 1.0 K/min. The dissociation enthalpy of the TBAC and TiAAB semiclathrate was obtained from the integration of an endothermic peak generating from the TBAC and TiAAB semiclathrate dissociation.

A high-pressure micro-differential scanning calorimeter (HP μ-DSC VII evo, Setaram Inc., France) was used to measure the dissociation enthalpies (ΔH_d) of the N_2 + TBAC semiclathrates and CO_2 (40%) + H_2 (60%) + TBAC semiclathrates under high pressure (Figure 2.3.). The HP μ-DSC device consists of a reference cell and a sample cell, with an operating pressure range of 0 - 40 MPa and an operating temperature range of 228.15 - 393.15 K. The HP μ-DSC had a resolution of 0.02 μW with a temperature deviation of ± 0.2 K.

For the ΔH_d measurements, the sample cell was charged with approximately 10.0 mg of TBAC solutions, whereas the reference cell was left empty. Then, the cells were inserted into the furnace and pressurized with gas to the desired pressure. A multi-cycle mode of cooling and heating was applied to the cells in order to enhance the conversion of the TBAC solution to the TBAC semiclathrate because there was no agitation in the liquid phase in the sample cell. The HP μ-DSC cells were initially cooled to 263.15 K at a cooling rate of 1.0 K/min. Then, the cells were heated to a temperature lower than the equilibrium dissociation temperature of the N_2 + TBAC semiclathrates and CO_2 (40%) + H_2 (60%) + TBAC semiclathrate, but higher than the dissociation temperature of the pure TBAC semiclathrate at a heating rate of 1.0 K/min. Through repeating cycles of cooling and heating, the fraction of the N_2 + TBAC semiclathrate and CO_2 (40%) + H_2 (60%) + TBAC semiclathrate was gradually increased and the complete conversion of the TBAC solution to the N_2 + TBAC semiclathrate and CO_2 (40%) + H_2 (60%) + TBAC semiclathrate was confirmed via the disappearance of further formation and dissociation peaks for the pure TBAC semiclathrate from the heat flow curve. Then, the temperature was heated to 313.15 K for the dissociation of the N_2 + TBAC semiclathrate and CO_2 (40%) + H_2 (60%) + TBAC semiclathrate. The dissociation enthalpies of the CO_2 (40%) +

H_2 (60%) + TBAC semiclathrates at a specified pressure were obtained through the integration of each endothermic heat flow curve. The equilibrium dissociation temperatures of the CO_2 (40%) + H_2 (60%) + TBAC semiclathrates were also determined from the onset temperatures of the endothermic heat flow curves.

For ΔH_d measurements of the QAS semiclathrates, approximately 11.0 mg of QAS solution were charged into the sample cell. Then, the cells were pressurized with the CO_2 (20%) + N_2 (80%) to 3.1 MPa. Because no agitation is applied for mixing the liquid phase in the HP μ-DSC, a multi-cycle mode of cooling and heating was adopted to completely convert the QAS solution to the QAS semiclathrate. The HP μ-DSC cells were initially cooled down to 263.15 K with a cooling rate of 1.0 K/min and then, heated up to a temperature that was higher than the dissociation temperature for each pure QAS semiclathrate but lower than the equilibrium dissociation temperature for each semiclathrate with a heating rate of 0.5 K/min at 3.1 MPa. After repeating the cycles of cooling and heating, the temperature was raised up to 313.15 K for the dissociation of the QAS semiclathrates with CO_2 (20%) + N_2 (80%). The dissociation enthalpies of each CO_2 (20%) + N_2 (80%) + QAS semiclathrate were determined by the integration of each endothermic heat flow curve.

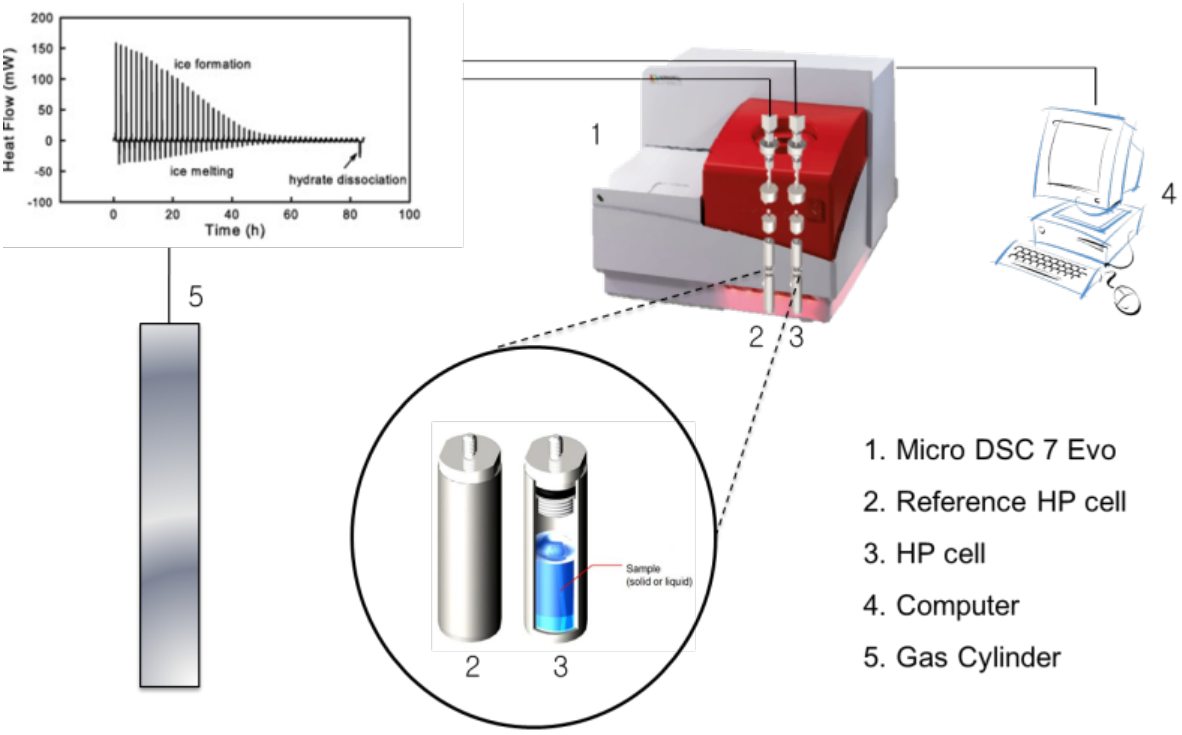

Figure 2.3. Schematic diagram of experimental apparatus for dissociation enthalpy.

2.2.3. Gas uptake and CO_2 composition measurements

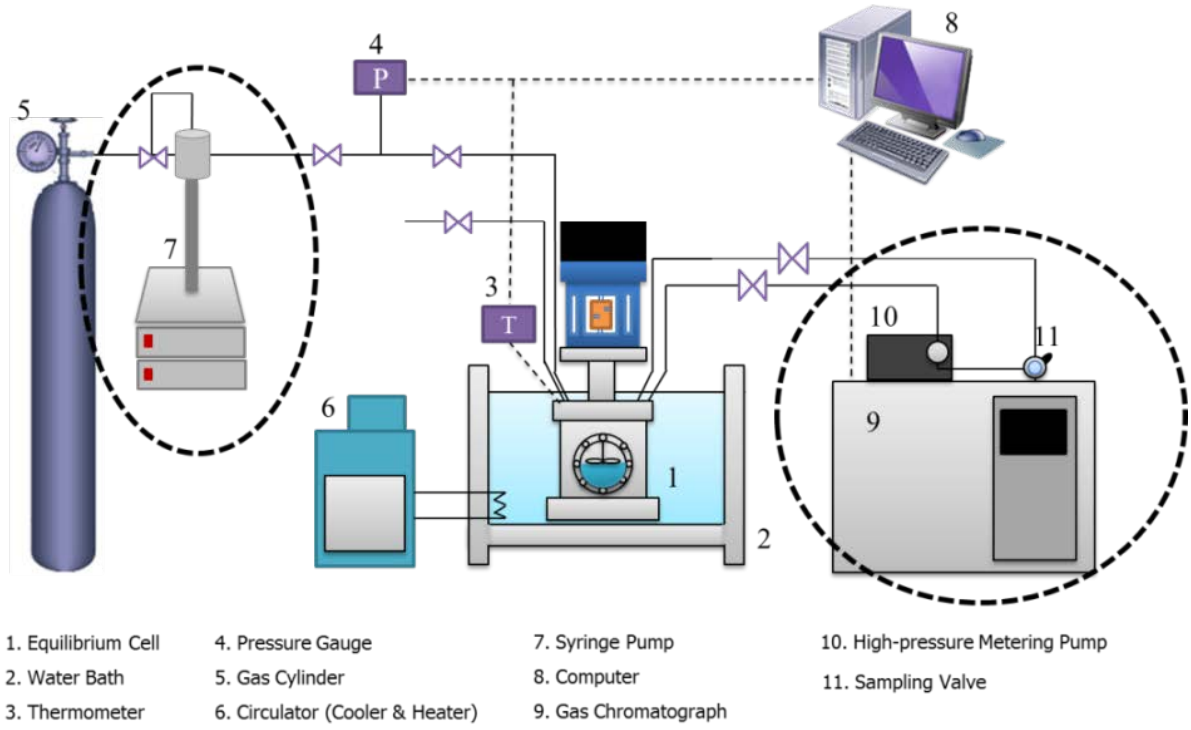

Figure 2.4. Schematic diagram of experimental apparatus for gas uptake and gas composition analysis.

The gas uptakes of the CO_2 (20%) + N_2 (80%) (or CO_2 (40%) + H_2 (60%)) + promoters + water systems were measured during clathrate formation. The volumetric gas consumption due to the enclathration of CO_2 and N_2 (or H_2) into the clathrates was measured under isothermal and isobaric conditions. A micro-flow syringe pump (ISCO, Model 500D, USA) was used to maintain the constant pressure of the reactor during the semiclathrate formation process. The gas uptake measurement was conducted in a batch manner with a fixed amount of the solutions. The volume of the supplemented gas to the reactor was recorded at a regular time interval of 5 min for 160 min, and was then converted to moles of gas consumed during clathrate formation.

CO_2 concentrations in the vapor and clathrate phases were measured with a gas chromatograph (7890A, Agilent, USA), which is equipped with a sampling valve (Rheodyne, Model 7010, USA) with a loop volume of 5 μl and connected to the reactor through a high-pressure metering pump (Eldex, USA). Changes in CO_2 concentration in the vapor phase were measured at regular time inter-

vals during semiclathrate formation, whereas CO_2 concentrations in the clathrate phase were measured after the completion of semiclathrate formation. In order to measure CO_2 concentrations retrieved from the clathrate phase, the vapor phase was evacuated after the reactor was cooled to approximately 173 K, and then, the entire clathrate phase was dissociated at 308.15 K. All the experiments for the gas uptake and CO_2 composition measurements were performed at 3.0 MPa for post combustion CO_2 capture and 4.0 (and 8.0) MPa for pre combustion CO_2 capture with a driving force (ΔT) of 5.0 K, which is defined as the temperature difference between the equilibrium and the experimental temperatures.

2.2.4. ^{13}C NMR & Micro Raman and *in-situ* Raman analyses

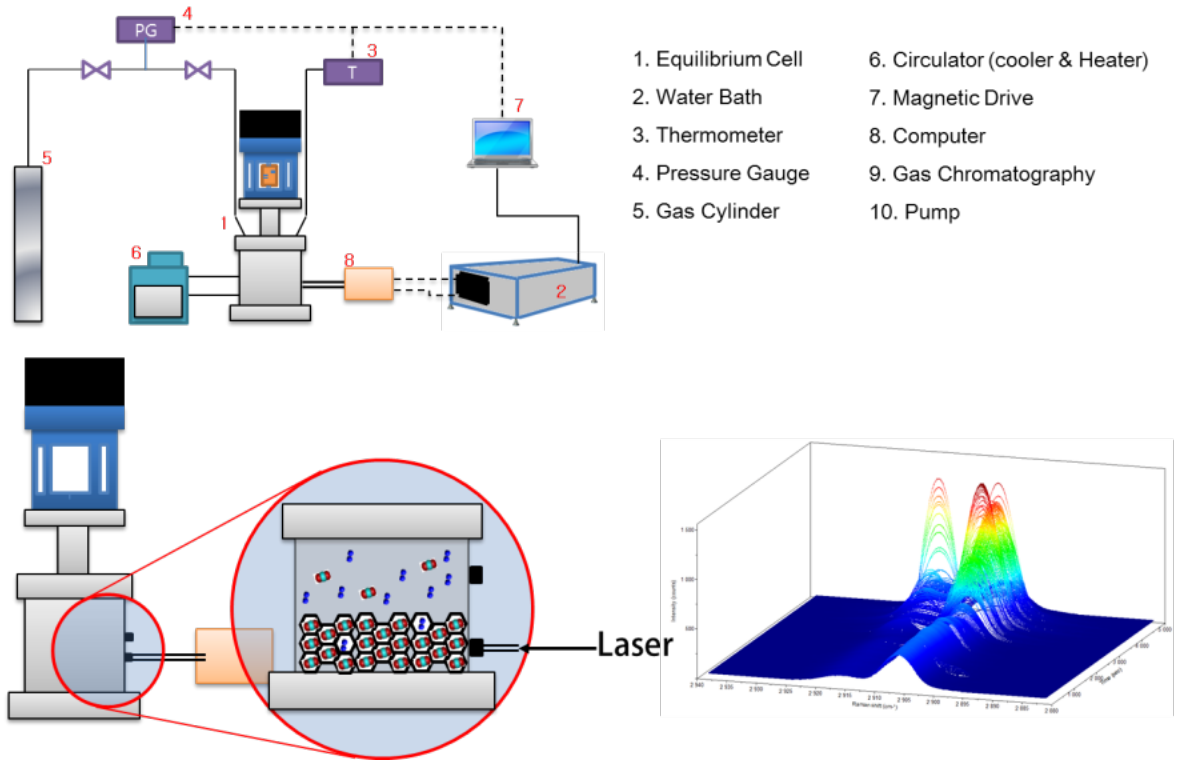

Figure 2.5. Schematic diagram of In-situ Raman apparatus.

Samples of clathrates for ^{13}C NMR and Raman analyses were prepared using the same apparatus as was used for stability condition measurements. The clathrates samples were ground into fine powder in a mortar filled with liquid nitrogen. The Korea Basic Science Institute (KBSI) provided a Bruker 400 MHz solid-state FT-NMR spectrometer to confirm the enclathration of guest gases in the clathrates. The powdered semiclathrate samples were placed into a 4 mm o.d. Zr rotor, which was inserted in a variable-temperature probe at 243 K. NMR spectra for the pure and double clathrates were obtained at a Lamor frequency of 100.6 MHz with magic angle spinning (MAS) between 2 and 4 kHz. The pulse length of 2 μs and pulse repetition delay of 10 s under proton decoupling were employed when a radio frequency field strength of 50 kHz corresponding to 5 μs 90˚ pulses was used. The external chemical shift reference was set to the downfield carbon resonance peak of adamantane (38.3 ppm at 300 K).

For Raman measurements, the clathrates sample was powdered and then, compacted into cylindrical pellets of 1.0 cm diameter and 0.3 cm height. The sample was then analyzed using a Raman spectrometer (Alpha 300R, WITec, Germany) with a thermoelectrically cooled CCD detector and 1800 grooves/mm holographic grating. The Raman spectra were recorded under an atmospheric condition at approximately 123 K to avoid semiclathrate dissociation. The low temperature condition was maintained using a liquid N_2 vapor-controlled freezing cryostat. Additional information about the experimental procedure and analytical methods can be found in our previous papers.

The semiclathrate formation process and the enclathration of the guest gas in the semiclathrate phase were monitored using an *in-situ* fiber coupled Raman spectrometer (SP550, Horiba, France) with a multichannel air cooled CCD detector and 1800 grooves/mm grating (Figure 2.5.). A fiber optic Raman probe that was installed in the high pressure reactor provided time dependent Raman spectra as semiclathrate formation proceeded. A more detailed description of the experimental methods and procedure are given in our previous papers [1-5].

2.4. References

[1] Kim, S., Baek I., You, J., Seo, Y. "Guest gas enclathration in tetra-n-butyl ammonium chloride (TBAC) semiclathrates: Potential application to natural gas storage and CO_2 capture" Applied Energy, 2015;140, 107-112.

[2] Kim, S., Kang, S., Seo, Y. "Semiclathrate-based CO_2 capture from flue gas in the presence of tetra-n-butyl ammonium chloride (TBAC)", Chemical Engineering Journal, 2015;276, 205–212.

[3] Kim, S., Seo, Y. "Semiclathrate-based CO_2 capture from flue gas mixtures: An experimental approach with thermodynamic and Raman spectroscopic analyses", Applied Energy, 2015;154, 987-994.

[4] Kim, S., Baek I., You, J., Seo, Y. “Phase equilibria, dissociation enthalpies, and Raman spectroscopic analyses of N_2 + tetra-n-butyl ammonium chloride (TBAC) semiclathrates”, Fluid Phase Equilibria, 2016;413, 86-91.

[5] Kim, S., Choi S-D., Seo, Y., “CO_2 capture from flue gas using clathrate formation in the presence of thermodynamic promoters”, Energy (In press).

Chapter III

QAS semiclathrates without/with a single guest (CH_4, CO_2, N_2)

3.1. Introduction

Semiclathrates are a promising alternative to gas hydrates for these technological applications because they generally form cage lattices under milder conditions. Quaternary ammonium salts (QASs) including tetra-n-butyl ammonium bromide (TBAB), fluoride (TBAF), chloride (TBAC), and tetra-iso-amyl ammonium bromide (TiAAB) form semiclathrates under atmospheric pressure [1-6]. These semiclathrates are chemically and physically similar to gas hydrates, but the primary difference is that in semiclathrates, there exist chemical or ionic interactions between the host water and guest molecules. The small dodecahedral (5^{12}) cages of QAS semiclathrates are typically left vacant, which can be used for storing or capturing small-sized gas molecules, while large cages are partially broken and occupied by large-sized cations [2-8].

TBAC semiclathrates have higher dissociation temperatures than TBAB semiclathrates under atmospheric pressure and can store a higher amount of gas molecules in vacant small cages than in TBAF semiclathrates [9-12]. Among the QASs, TBAB and TBAF have been broadly examined as a tool for gas storage or CO_2 capture [3, 9, 10, 13-18], whereas TBAC, which is expected to have better physico-chemical properties for technological applications, has not been thoroughly examined as a semiclathrate former [19, 20]. In addition, TiAAB as thermodynamic promotor has expected to have high thermodynamic stabilities than other quaternary ammonium salts. Therefore, this study was thoroughly investigated of QAS semiclathrates, concentrating on dissociation enthalpies analyses for their potential application to natural gas storage and CO_2 capture.

The thermodynamic stability conditions of pure QAS semiclathrates and double QAS semiclathrates were experimentally measured at different concentrations. A differential scanning calorimeter (DSC) was used to measure the dissociation enthalpy of the QAS semiclathrate. In addition, the enclathration of guest molecules in the clathrate lattices was confirmed via ^{13}C NMR and in-situ Raman spectroscopy.

3.2. Results and discussion

3.2.1. Phase equilibria of QAS semiclathrates and spectroscopic analysis

The dissociation equilibrium temperatures of pure TBAC semiclathrates were measured and found to be 282.3, 288.0, and 287.0 K at 1.0, 3.3, and 5.0 mol% of TBAC solutions, respectively, under atmospheric pressure conditions. The results are presented in (Figure 3.1) with data from previous studies [19, 21, 22]. Aladko et al. [23] and Rodionova et al. [5] revealed that pure TBAC semiclathrates have three crystal structures with different hydration numbers: TBAC·(32.2±0.4) H_2O (h32), TBAC· (29.7±0.4) H_2O (h30), and TBAC·(24.8±0.4) H_2O (h24). As can be seen in (Figure 3.1.), the TBAC semiclathrate is the most stable at a stoichiometric concentration (3.3 mol%) of TBAC·29.7H_2O, where the equilibrium temperature is 288.0 K. This result is in line with the measurements obtained by previous researchers. The dissociation temperature of the TBAC semiclathrate was increased with an increasing TBAC concentration from 1.0 to 3.3 mol %, but the temperature decreased when the concentration increased further to 3.3 mol %. The decrease in the dissociation equilibrium temperature of TBAC semiclathrates at a TBAC concentration more than 3.3 mol % can be attributed to the presence of unclathrated ions of TBAC. TBA^+ and Cl^-, which were not in the semiclathrate lattices, acted as inhibitors, disrupting the hydrogen bonding of water molecules in the host lattices.

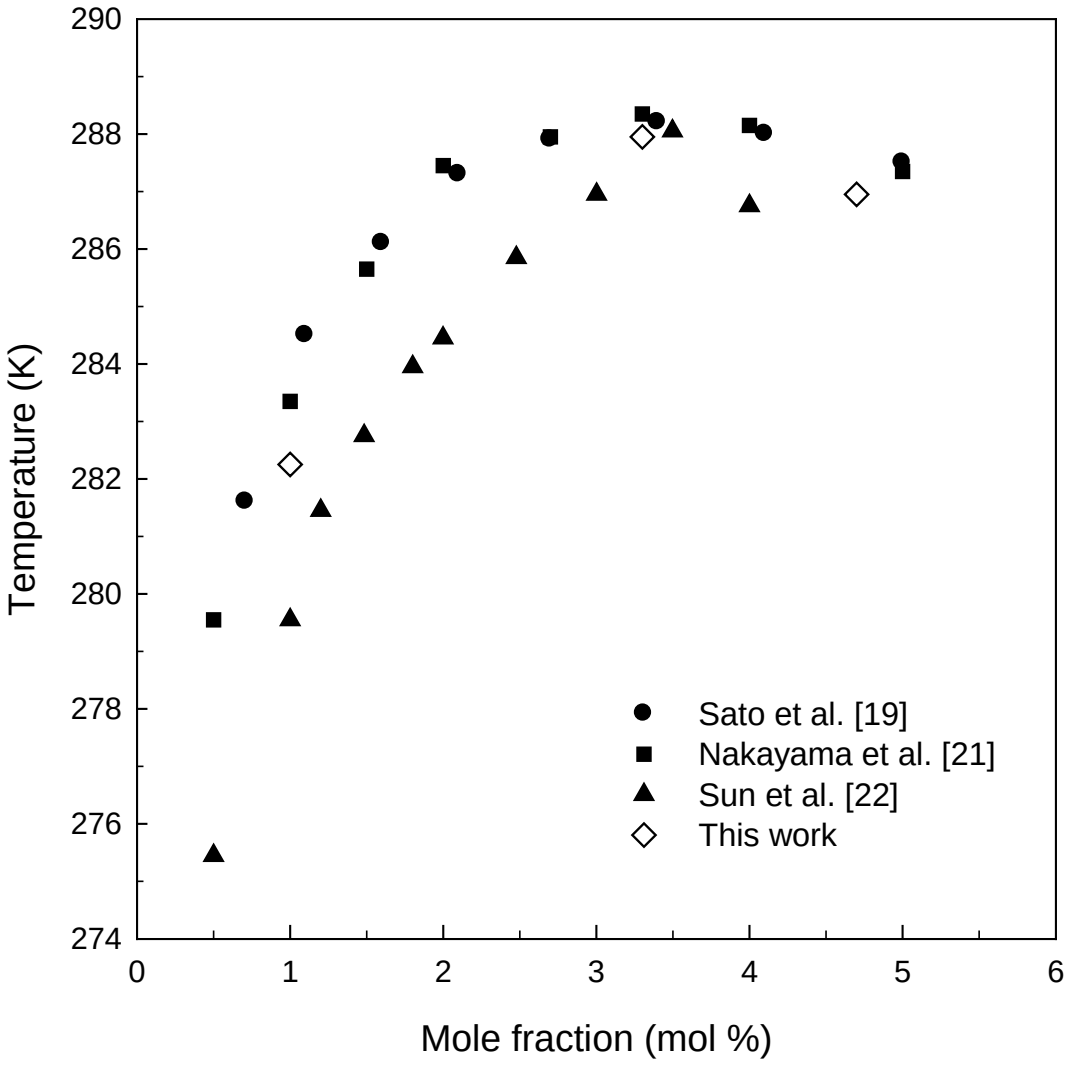

Figure 3.1. Dissociation equilibrium temperatures of pure TBAC semiclathrates under an atmospheric pressure condition.

(Figure 3.2.) shows the DSC thermogram of pure TBAC semiclathrate formed from a 3.3 mol% solution under an atmospheric pressure condition. The dissociation enthalpy of pure TBAC semiclathrate obtained from the integration of an endothermic dissociation peak was 204.8±1.7 J/g. The onset temperature of the endothermic peak, which is taken as the dissociation equilibrium temperature at a given pressure [24], was found to be 288.0 K. The onset temperature of the TBAC semiclathrate with 3.3 mol% was identical to the equilibrium temperature presented in (Figure 3.2.), which was measured in the conventional reactor. In (Figure 3.2.), no ice melting peak was observed around 273.15 K, which indicates the complete conversion of the TBAC 3.3 mol% solution to a semiclathrate of TBAC·29.7H_2O.

The measured dissociation enthalpy value 204.8±1.7 J/g of the TBAC semiclathrate was in good agreement with the values in previous studies [11, 21, 25, 26]. This can be a good criterion for estimating the thermodynamic stability of each QAS semiclathrate. The dissociation enthalpy of the TBAB·26.0H_2O semiclathrate is 193.0 J/g [4, 25] and that of the TBAF·28.6H_2O semiclathrate is 234.9 J/g [15]. Judging from both the dissociation temperature and enthalpy of each QAS semiclathrate, the semiclathrate with a higher dissociation enthalpy also has a higher dissociation equilibrium temperature, which corresponds to a higher thermodynamic stability. Therefore, the TBAC·29.7H_2O semiclathrate is more stable than the TBAB·26.0H_2O semiclathrate, but less stable than the TBAF·28.6H_2O semiclathrate. However, small cages of the TBAF·28.6H_2O semiclathrate are partially filled with the water molecules [4, 25], which means that a much smaller number of dodecahedral (5^{12}) cages is available for capturing target gas molecules compared with other QAS semiclathrates.

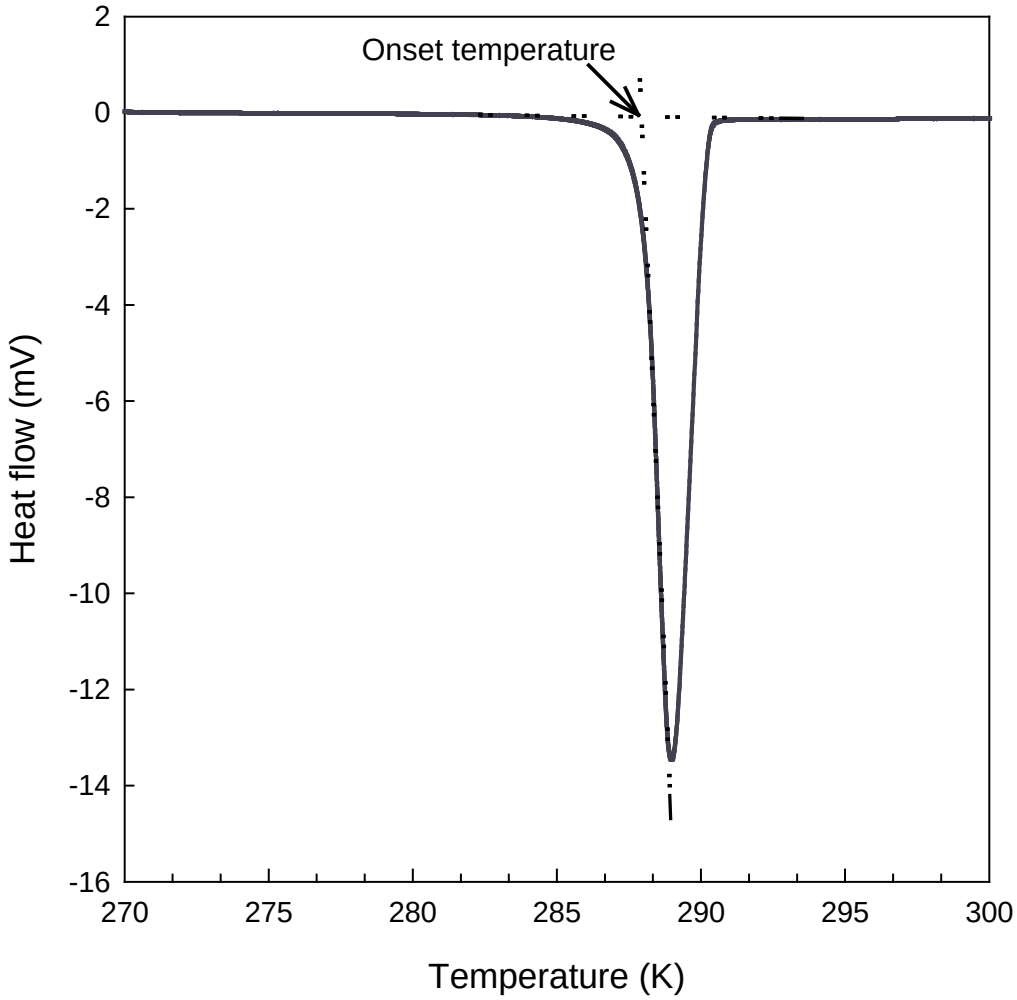

Figure 3.2. Dissociation thermogram of pure TBAC (3.3 mol%) semiclathrate in DSC under an atmospheric pressure condition.

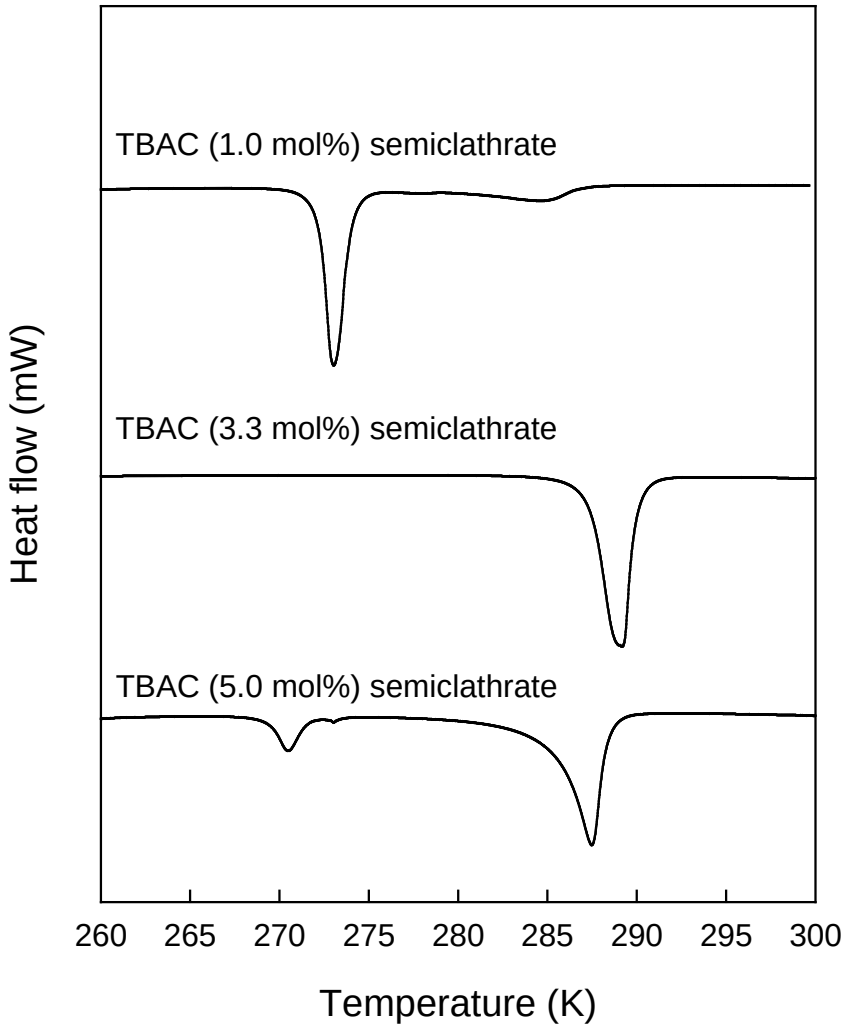

Figure 3.3. Dissociation thermograms of the pure TBAC semiclathrates (1.0, 3.3, and 5.0 mol%) under atmospheric pressure.

The phase equilibria and dissociation enthalpies of TBAC semiclathrates were investigated at three different TBAC solutions of 1.0, 3.3, and 5.0 mol% in order to confirm the effects of both excess water and TBAC molecules on the stability conditions of TBAC semiclathrates. The DSC thermograms obtained from the dissociation of pure TBAC (1.0, 3.3, and 5.0 mol%) semiclathrates under atmospheric pressure are presented in (Figure 3.3.). The TBAC (3.3 mol%) semiclathrate exhibited only one endothermic peak without an ice melting peak during the semiclathrate dissociation, which indicates that all water molecules reacted with TBAC molecules to form the TBAC semiclathrate

(TBAC·29.7H_2O) at the stoichiometric concentration of 3.3 mol%. However, the TBAC (1.0 mol%) semiclathrate demonstrated two distinct endothermic peaks. A large peak originated from the ice melting due to the presence of excess water in the 1.0 mol% solution and a small peak emanated from the TBAC semiclathrate dissociation. Interestingly, the TBAC (5.0 mol%) semiclathrate also exhibited a small ice melting peak as well as a large semiclathrate dissociation peak. The appearance of the ice melting peak for the TBAC (5.0 mol%) semiclathrate could be attributed to the unclathrated ions of both TBA^+ and Cl^-, which can inhibit the complete conversion of the TBAC solution into the TBAC semiclathrate.

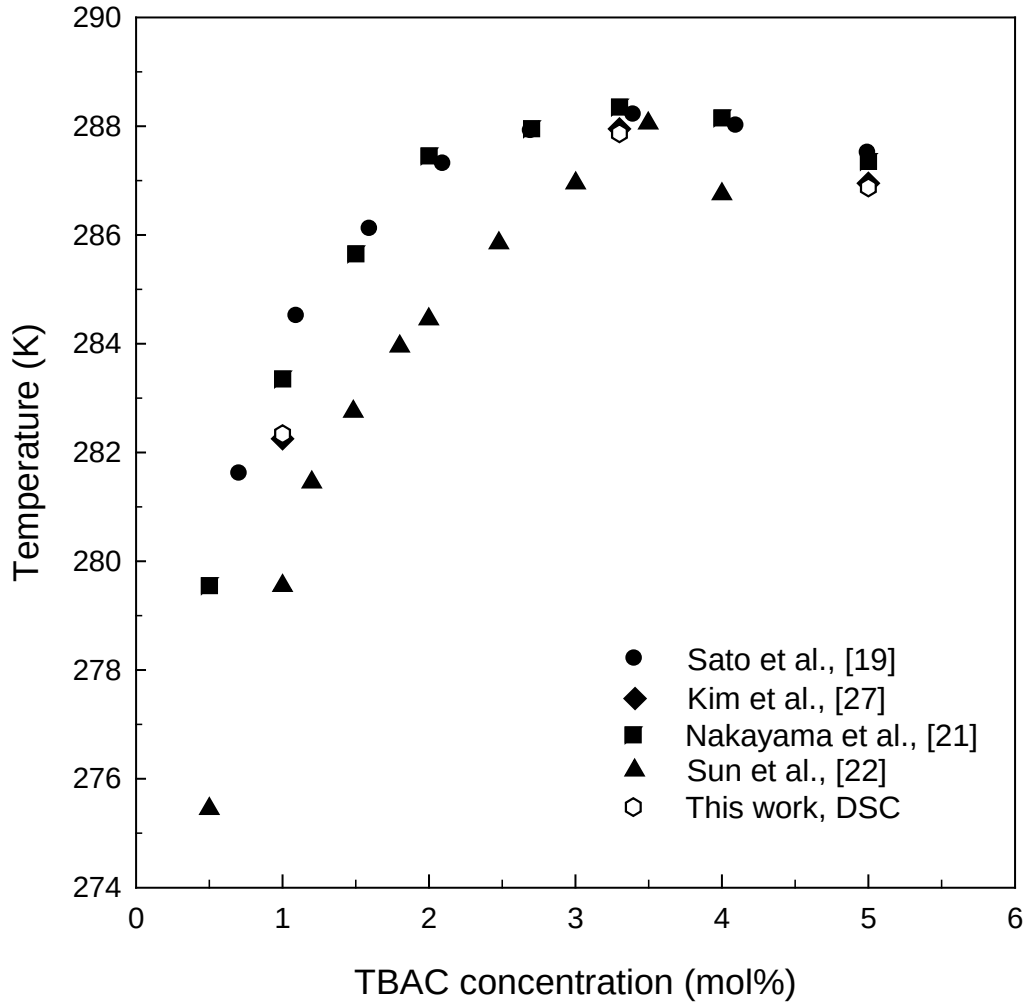

Figure 3.4. Dissociation equilibrium temperatures of the pure TBAC semiclathrates under atmospheric pressure using DSC.

The dissociation equilibrium temperatures of the pure TBAC semiclathrates obtained from the DSC thermograms under atmospheric pressure are presented in (Figure 3.4.) and are compared with the values reported in the literature [19, 21, 22, 27]. The onset temperature, which is defined as the intersection of an extrapolated baseline with a line tangent to the inflection point of the endothermic DSC curve, can be taken as the equilibrium dissociation temperature for each TBAC semiclathrate. As seen in (Figure 3.4.), the dissociation equilibrium temperatures of the TBAC (1.0, 3.3, and 5.0 mol%) solutions were 282.3, 288.0, and 286.7 K, respectively, and these are in good agreement with our previous results obtained using the conventional method, as well as other literature values [19, 21, 22, 27].

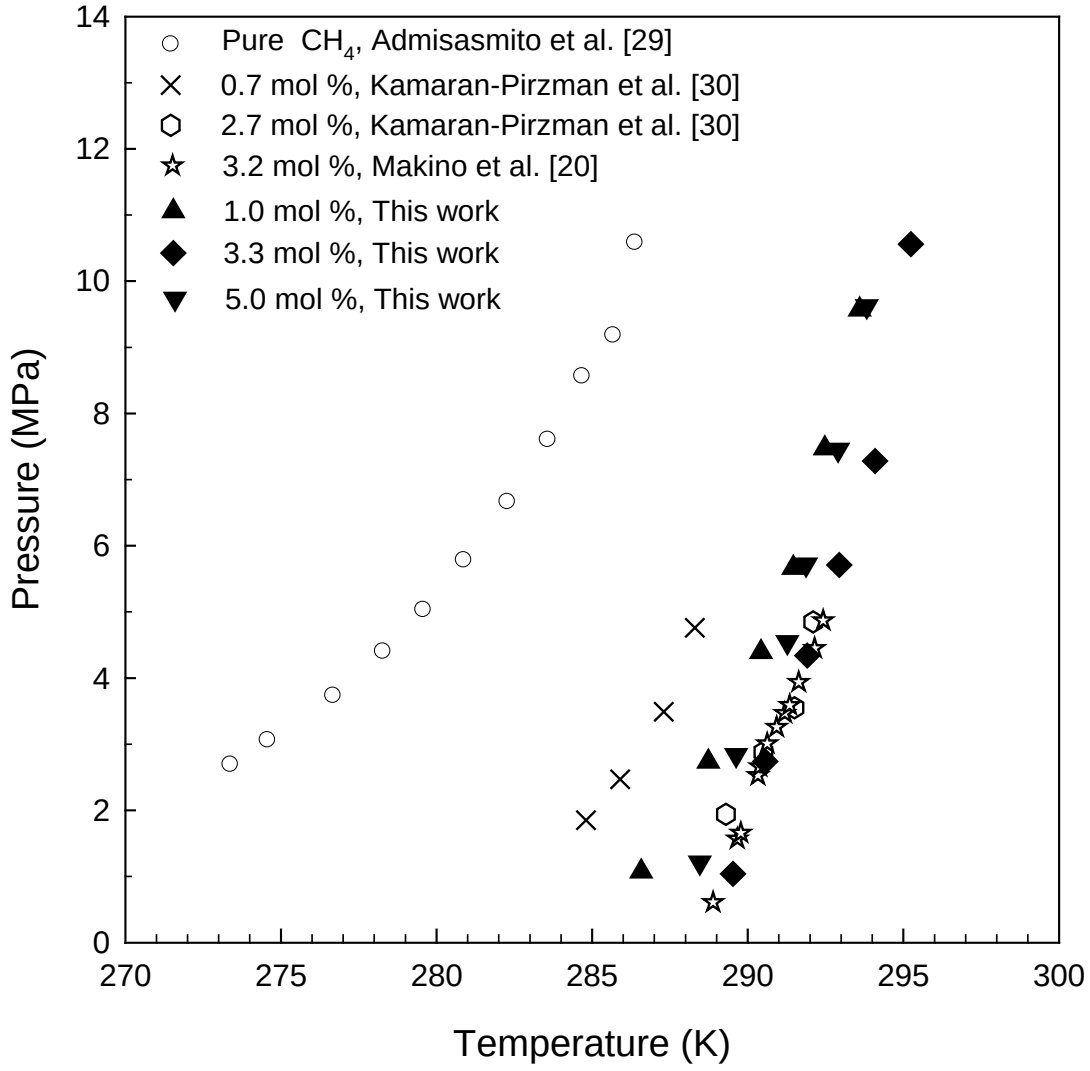

Figure 3.5. Three-phase equilibria of the CH_4 + TBAC (1.0, 3.3 and, 5.0 mol %) + water systems.

The three-phase equilibria (H - L_W - V) of the CH_4 + TBAC + water systems were measured at three different TBAC concentrations of 1.0, 3.3, and 5.0 mol%. The experimental results were tabulated in (Table 3.1.) and shown in (Figure 3.5.). The double CH_4 + TBAC semiclathrates showed a significantly enhanced thermodynamic stability compared to pure CH_4 hydrate. As can be seen in (Figure 3.5), at 3.0 MPa the equilibrium temperature of the CH_4 + TBAC semiclathrate formed from 3.3 mol% solution was higher by 15 K than the pure CH_4 hydrate. As was observed in (Figure 3.2), the maximum stabilization happened at TBAC 3.3 mol%, which is also the stoichiometric concentration of the TBAC·29.7H_2O semiclathrate.

Table 3.1. Semiclathrate phase equilibrium data for the CH_4 + TBAC + water systems.

1.0 mol %		3.3 mol %		5.0 mol %	
T/K	P/MPa	T/K	P/MPa	T/K	P/MPa
286.6	1.08	289.5	1.04	288.5	1.21
288.7	2.74	290.6	2.74	289.6	2.84
290.4	4.39	291.9	4.34	291.3	4.54
291.5	5.67	292.9	5.71	291.9	5.72
292.5	7.47	294.1	7.28	292.9	7.45
293.6	9.57	295.2	10.56	293.8	9.62

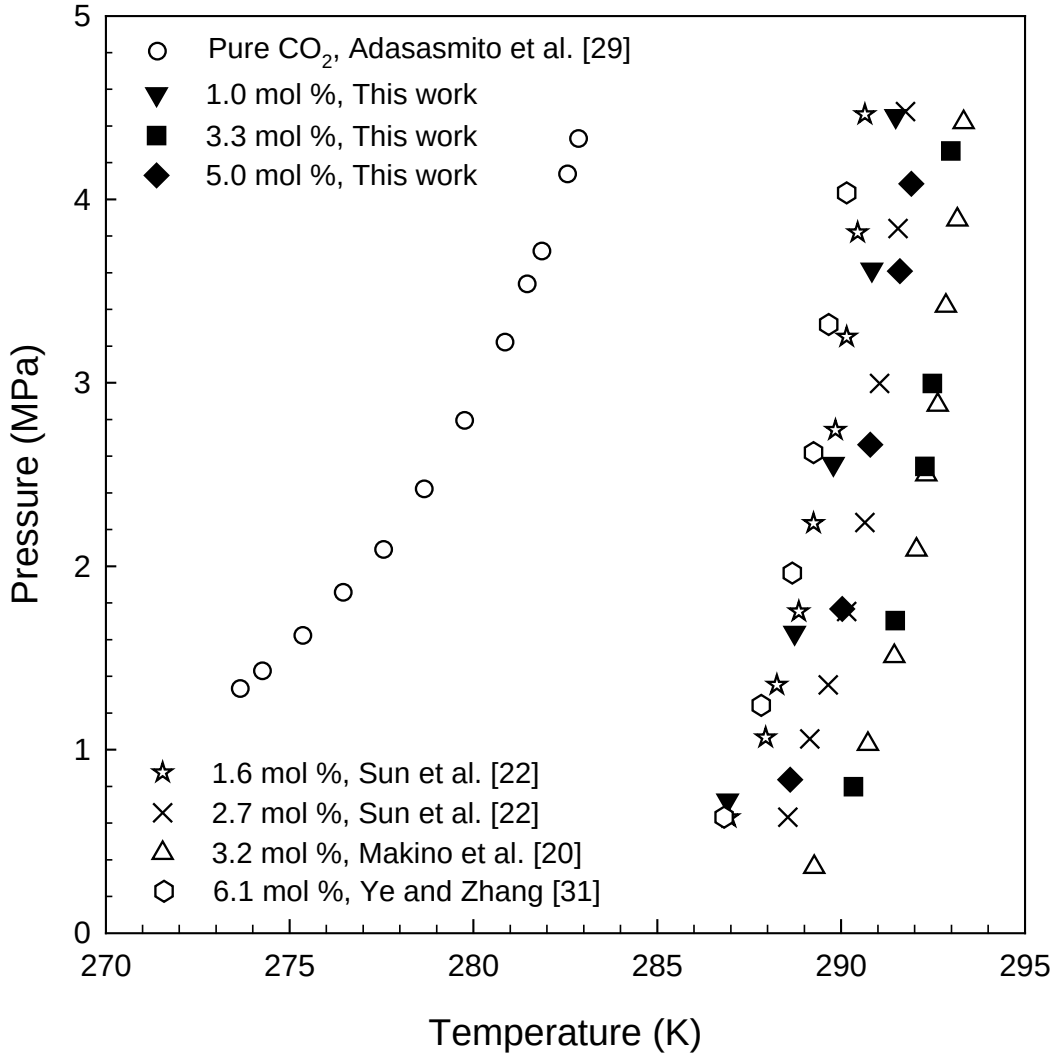

Figure 3.6. Three-phase equilibria of the CO_2 + TBAC (1.0, 3.3 and, 5.0 mol %) + water systems.

The stability conditions of the double CO_2 + TBAC semiclathrates with varying TBAC concentrations of 1.0, 3.3, and 5.0 mol% are shown in (Figure 3.6.). The overall results are also summarized in (Table 3.2.). The double CO_2 + TBAC semiclathrates also demonstrated a significantly increased thermodynamic stability, as shown by their higher temperature at specified pressure or lower pressure at specified temperature when compared with the pure CO_2 hydrate. At 3.0 MPa, the equilibrium temperature of the CO_2 + TBAC semiclathrates with 3.3 mol% was higher by 12 K than the pure CO_2 hydrate.

Table 3.2. Semiclathrate phase equilibrium data for the CO_2 + TBAC + water systems.

1.0 mol %		3.3 mol %		5.0 mol %	
T/K	P/MPa	T/K	P/MPa	T/K	P/MPa
286.9	0.72	290.3	0.80	288.7	0.84
288.7	1.64	291.5	1.70	290.0	1.77
289.8	2.56	292.3	2.55	290.8	2.66
290.8	3.62	292.5	3.00	291.6	3.61
291.5	4.46	293.0	4.26	291.9	4.09

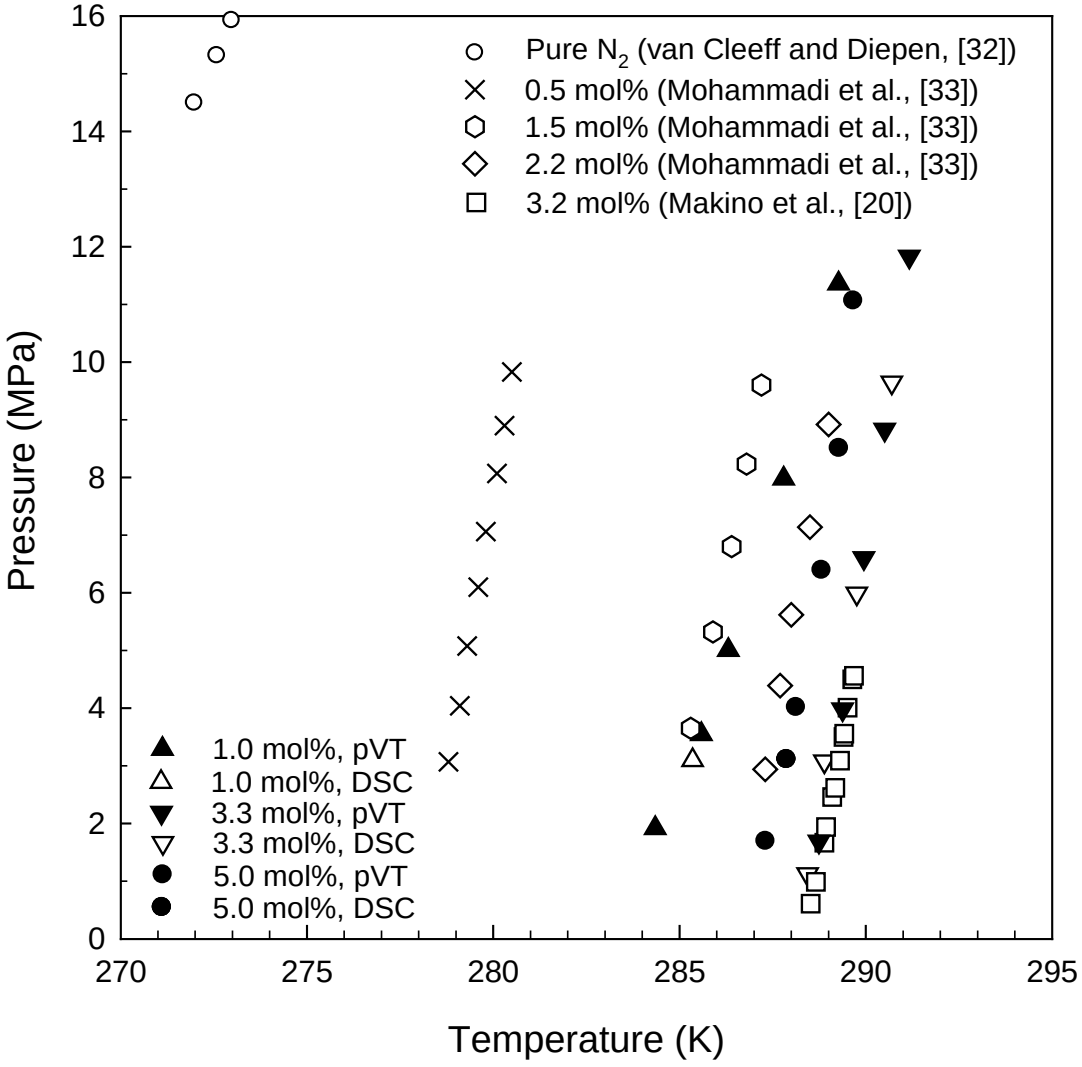

Figure 3.7. Three phase equilibria of the N_2 + TBAC (1.0, 3.3, and 5.0 mol%) + water systems.

The three-phase (H-L_w-V) equilibria of the N_2 + TBAC (1.0, 3.3, and 5.0 mol%) + water systems that were measured using both the conventional isochoric method (pVT) and the HP μ-DSC method is depicted in (Figure 3.7.) and summarized in (Table 3.3.). The semiclathrate equilibrium point measured using the HP μ-DSC was located precisely in each three-phase equilibrium line of the corresponding N_2 + TBAC semiclathrates, which were obtained using the conventional isochoric method (pVT).

Table 3.3. Semiclathrate phase equilibria data of the N_2 + TBAC + water systems.[a]

1.0 mol%				3.3 mol%				5.0 mol%			
pVT		DSC		pVT		DSC		pVT		DSC	
T/K	p/MPa	T/K	p/MPa	T/K	p/MPa	T/K	p/MPa	T/K	p/MPa	T/K	p/MPa
284.3	1.92	285.6	3.08	288.7	1.69	288.9	3.08	287.3	1.68	287.9	3.08
285.6	3.55			289.4	3.98			288.2	4.00		
286.3	5.01			290.0	6.60			288.8	6.38		
287.8	7.98			290.5	8.83			289.3	8.49		
289.3	11.36			291.2	11.83			289.7	11.05		

[a] Standard uncertainties *u* are *u* (T) = 0.1 K and *u* (p) = 0.02 MPa.

The equilibrium lines of the N_2 + TBAC semiclathrate systems shifted significantly to the promoted regions, which are represented by the lowered pressure at any given temperature or elevated temperature at any given pressure, compared with the N_2 gas hydrate. The higher TBAC concentrations resulted in larger equilibrium line shifts of the N_2 + TBAC semiclathrates. The thermodynamic stabilization of the N_2 + TBAC semiclathrate was found to be the highest in the TBAC (3.3 mol%) solution, which corresponds to the stoichiometric concentration of TBAC·29.7H_2O. However, the thermodynamic stability of the N_2 + TBAC (5.0 mol%) semiclathrate was lower than that of the N_2 + TBAC (3.3 mol%) semiclathrate. This was attributed to the excess amount of TBAC in the 5.0 mol% solution. As depicted in (Figure 3.2.)., in the 3.3 mol% solution, ice peaks were not detected during the dissociation of the N_2 + TBAC semiclathrate because all ions of TBA^+ and Cl^-, as well as water molecules were involved in the semiclathrate formation. However, in the 5.0 mol% solution, the TBAC molecules that existed in the excess of the stoichiometric concentration (3.3 mol%) could function as thermodynamic inhibitors that disrupt the hydrogen bonding between the host water molecules, because they were not enclathrated in the semiclathrate structure as either guests or hosts after being ionized into TBA^+ or Cl^-. The experimental results covering the stability condition and dissociation enthalpy measurements indicate that TBAC semiclathrates are expected to be a good candidate material for effective gas storage and CO_2 capture at mild conditions.

Shimada et al. [34] demonstrated that in TBAB semiclathrates, TBA^+ is located in the center of large cages with partially broken bonds while small dodecahedral (5^{12}) cages are left vacant. Lee et al. [18, 35] confirmed using ^{13}C NMR that CH_4 molecules are enclathrated in the small 5^{12} cages of TBAB and TBAF semiclathrates. However, the enclathration of CH_4 molecules in the TBAC semiclathrate has not been analyzed yet. In this study, ^{13}C NMR spectroscopy, which has been recognized as a powerful tool for the structural identification and quantitative determination of gas hydrates or semiclathrates [36], was used for confirming the inclusion of CH_4 molecules in TBAC semiclathrates.

The ^{13}C NMR spectra of a pure CH_4 hydrate, pure TBAC semiclathrate, and double CH_4 + TBAC semiclathrate are shown in (Figure 3.8.). The ^{13}C NMR spectrum of the pure CH_4 hydrate, which is known to form sI hydrate, has two resonance peaks at -4.3 and -6.6 ppm, which indicate the enclathration of CH_4 molecules in the small 5^{12} cages and the large $5^{12}6^2$ cages, respectively. The pure TBAC semiclathrate demonstrated four peaks at 59.3, 24.7, 20.2, and 14.1 ppm, which correspond to the four carbons of the *n*-butyl group of TBA^+ captured in the center of the large cages. In contrast, the double CH_4 + TBAC semiclathrate showed an additional peak at -4.0 ppm, as well as four peaks at 59.3, 24.7, 20.2, and 14.1 ppm. The peak observed at -4.0 ppm can be reasonably assigned to CH_4 molecules captured in the 5^{12} cages of the double TBAC semiclathrate, even though there is a very slight discrepancy in the peak position between the double CH_4 + TBAC semiclathrate and the pure CH_4 hydrate. As observed in the double CH_4 + TBAF semiclathrate [35], the slight downfield shift of the NMR peak for the CH_4 molecules captured in the double CH_4 + TBAC semiclathrate is the result of deshielding caused by the presence of electronegative chloride (Cl).

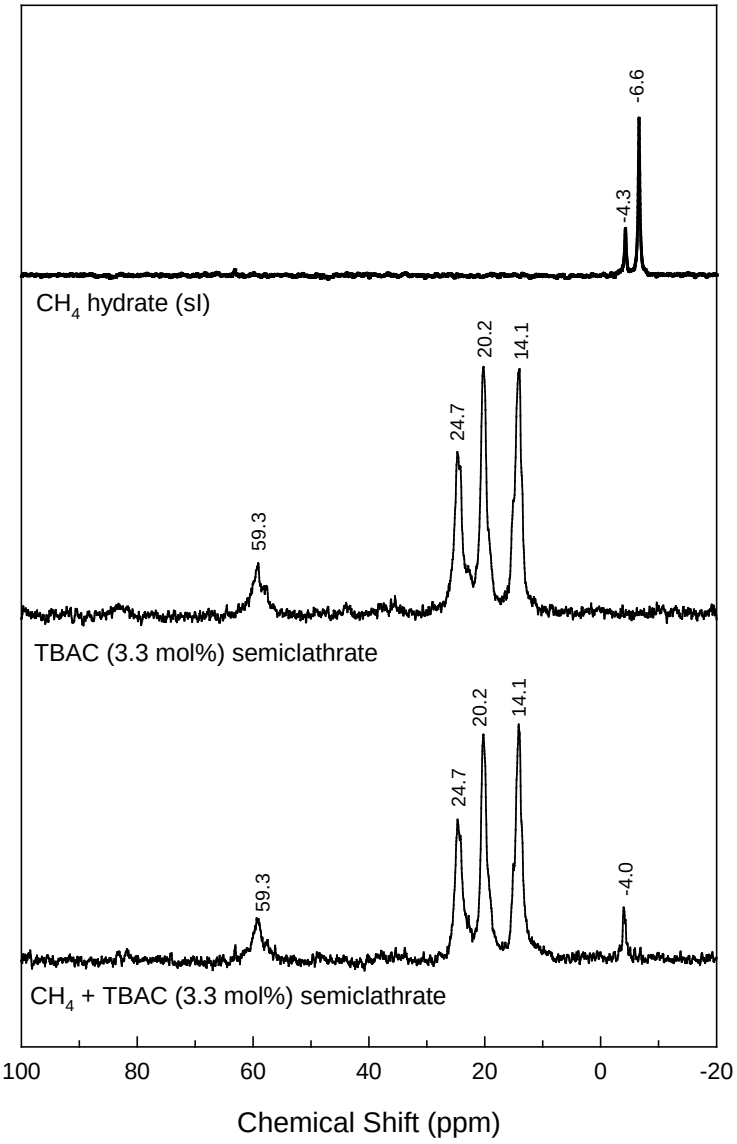

Figure 3.8. ^{13}C NMR spectra of the pure CH_4 hydrates, pure TBAC semiclathrate, and double CH_4 + TBAC semiclathrates.

(Figure 3.9.) shows the Raman spectra of the pure CO_2 hydrate, pure TBAC semiclathrate, and double CO_2 + TBAC semiclathrate. The Raman spectrum of the pure CO_2 hydrate, which is known to form sI hydrate, had two Raman peaks at 1276 and 1380 cm^{-1}. The double CO_2 + TBAC semiclathrate had two Raman peaks at 1273 and 1380 cm^{-1}, which can be assigned to the enclathrated CO_2 molecules. The double CO_2 + TBAC semiclathrate also exhibited many other peaks at a wide range of wavenumbers that can be assigned to an enclathrated TBA^+ in the double TBAC semiclathrate. The slight shift in wavenumbers (1276 → 1273 cm^{-1}) is attributable to the structural transition caused by semiclathrate formation. Even though the CO_2 enclathration in the double TBAC semiclathrate was clearly confirmed via Raman spectroscopy, the detailed distribution of guest molecules cannot be provided because the Raman spectrum of the CO_2 hydrate does not demonstrate peak splitting for guests in different cages.

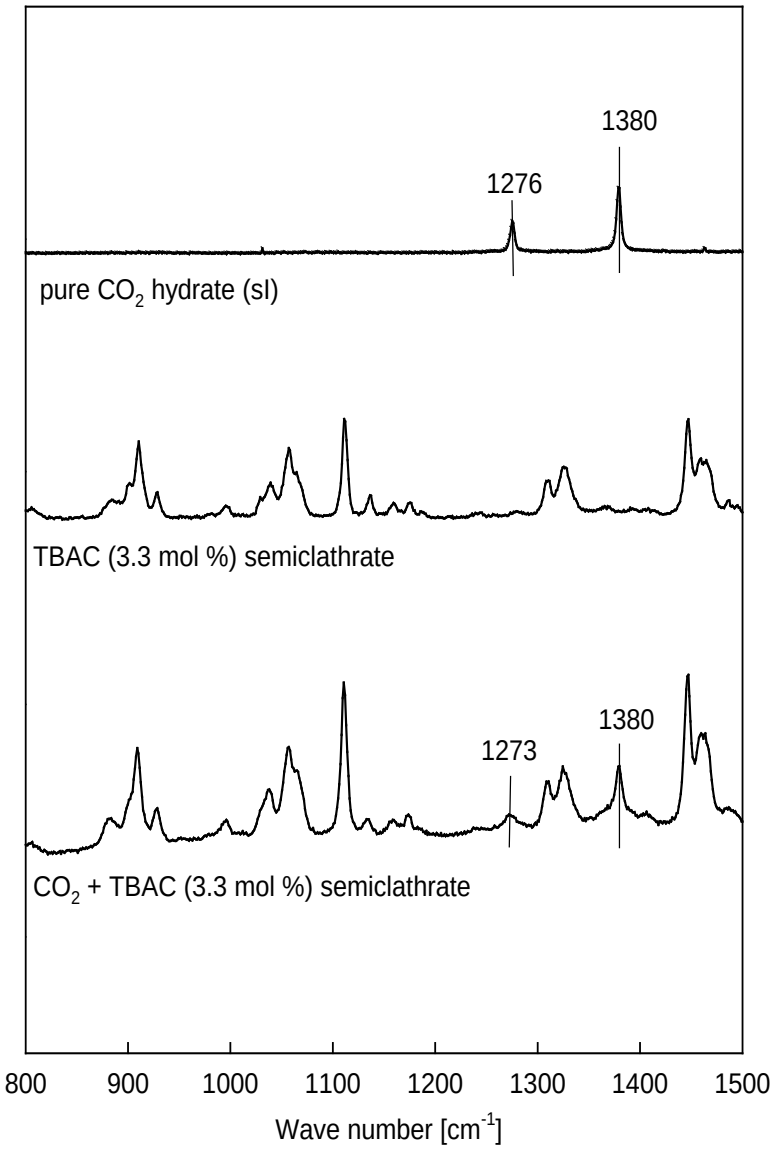

Figure 3.9. Raman spectra of pure CO_2 hydrate, pure TBAC hydrates, and double CO_2 + TBAC hydrates.

The Raman spectra of the N_2 hydrate, pure TBAC (3.3 mol%) semiclathrate, and N_2 + TBAC (3.3 mol%) semiclathrate are presented in (Figure 3.10.). The N_2 gas hydrate is known to be sII hydrate and it exhibits one Raman peak at 2324 cm^{-1}. Even though the N_2 molecules were enclathrated in both the small (5^{12}) and large ($5^{12}6^2$) cages of the sII N_2 hydrate, only one Raman peak appeared because the N_2 molecules are so small in molecular size that the symmetric N-N vibrations of the N_2 molecules are not distinguishable in the small and large cages of the sII hydrates [37, 38]. The N_2 + TBAC (3.3 mol%) semiclathrate also exhibited one Raman peak at 2324 cm^{-1} for the N_2 molecules enclathrated in the small (5^{12}) cages of the semiclathrate, while the pure TBAC semiclathrate did not exhibit Raman peaks around 2324 cm^{-1}. Despite the absence of peak splitting of N_2 molecules enclathrated in different cages, it was clearly confirmed from the Raman spectra that the N_2 molecules are encaged in the TBAC semiclathrate.

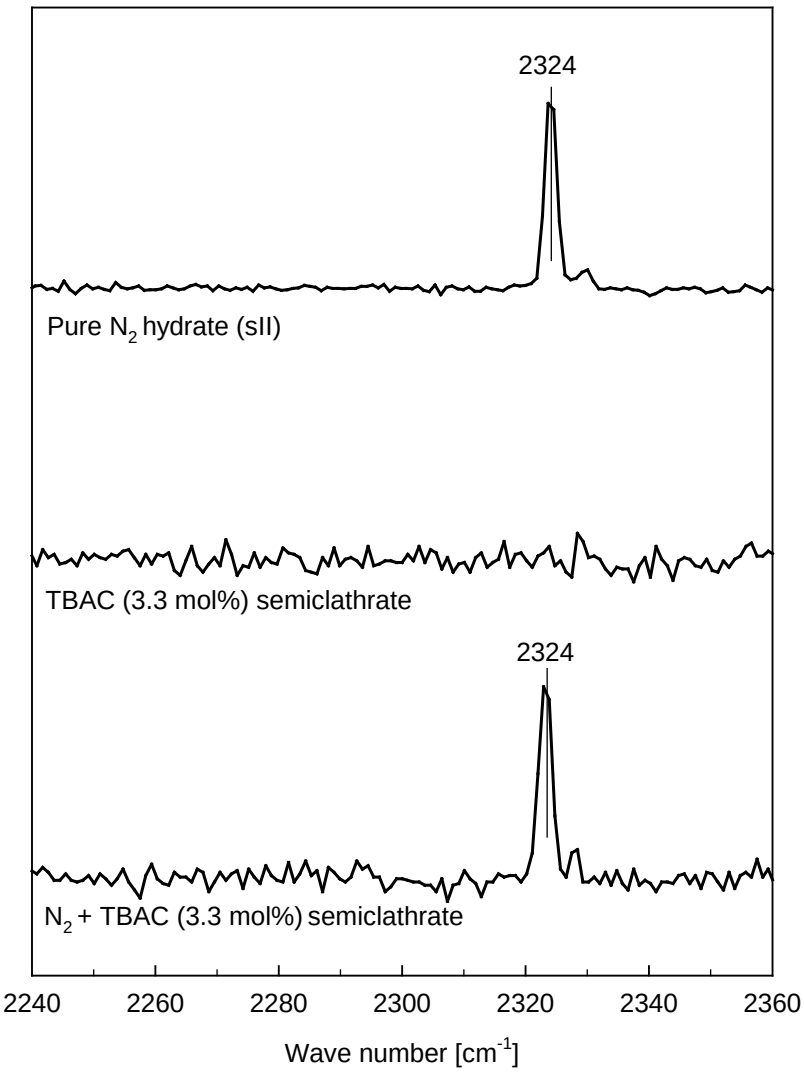

Figure 3.10. Raman spectra of the N_2 hydrate, pure TBAC (3.3 mol%) semiclathrate, and N_2 + TBAC (3.3 mol%) semiclathrate. The small Raman peak located next to 2324 cm^{-1} originated from the N_2 vapor for cooling.

3.2.2. Phase equilibria of TiAAB semiclathrates and spectroscopic analysis

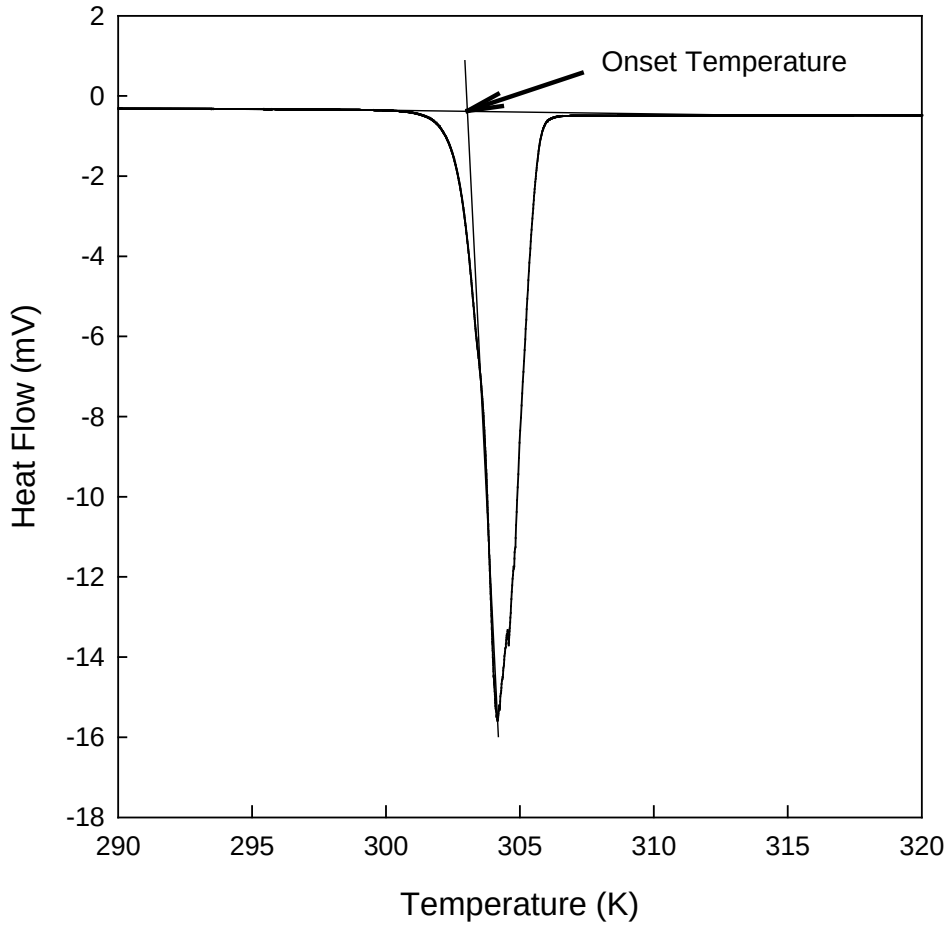

Figure 3.11. Dissociation thermogram of pure TiAAB (3.7 mol%) semiclathrate in DSC under an atmospheric pressure condition.

The phase equilibria and dissociation enthalpies of TiAAB semiclathrates were investigated at 3.7 mol%. The DSC thermograms obtained from the dissociation of pure TiAAB (3.7 mol%) semiclathrates under atmospheric pressure are presented in (Figure 3.11.). The TiAAB (3.7 mol%) semiclathrate exhibited only one endothermic peak without an ice melting peak during the semiclathrate dissociation, which indicates that all water molecules reacted with TiAAB molecules to form the TiAAB semiclathrate (TiAAB·26.0H_2O) at the stoichiometric concentration of 3.7 mol%, where the equilibrium temperature is 303.4 K. The measured dissociation enthalpy value was 214.0±5.5 KJ/mol semiclathrate.

TiAAB semiclathrate, for non-stoichiometric concentrations of semiclathrates, it is very difficult to determine the accurate equilibrium dissociation temperature from the endothermic heat flow curves obtained from the DSC dynamic method due to the appearance of a broad and progressive peak during heating. In order to overcome this inaccuracy of the equilibrium point determination in the dynamic method, the DSC stepwise method was used in this study. The temperature increment and isothermal duration at each step are 0.1 K and 3 h, respectively. The heat flow and temperature profiles during stepwise heating for TiAAB (3.7 mol%) semiclathrate under an atmospheric pressure condition are depicted in (Figure 3.12). The isothermal duration is long enough for the heat flow signal to return to the baseline. For each temperature step, a broad endothermic peak caused by TiAAB dissociation was observed until the semiclathrate dissociation was completely terminated. The point where the endothermic peaks due to the semiclathrate dissociation disappeared and the calorimetric signal change only due to the temperature increment appeared was determined to be the equilibrium dissociation temperature. The dissociation equilibrium temperatures of pure TiAAB semiclathrates were measured and found to be 303.15, 303.45, and 303.25 K at 1.0, 3.7, and 5.0 mol% of TiAAB solutions, respectively, under atmospheric pressure conditions.

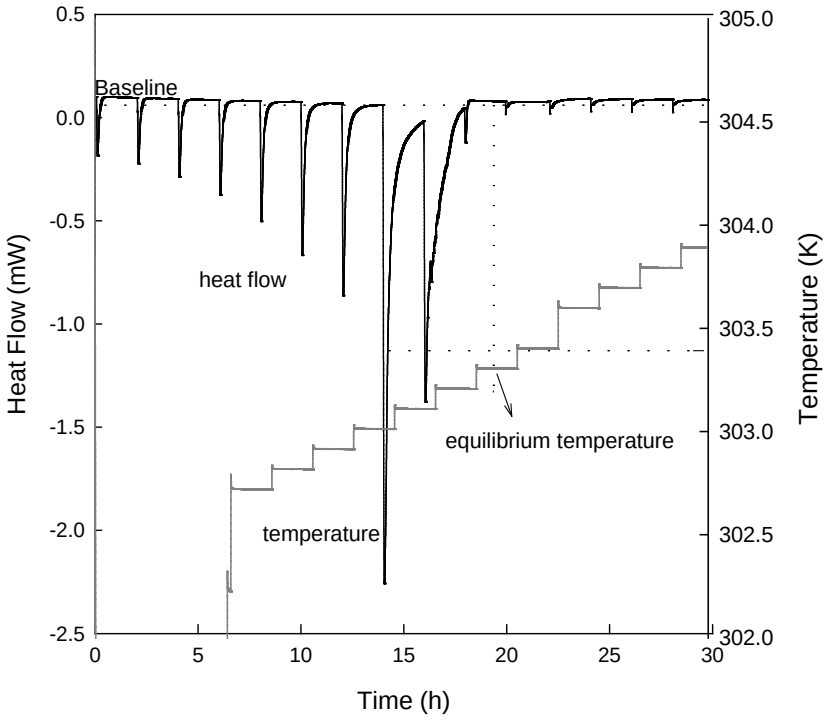

Figure 3.12. Heat flow and temperature profiles during stepwise heating for the TiAAB (3.7 mol%) semiclathrate under atmospheric pressure.

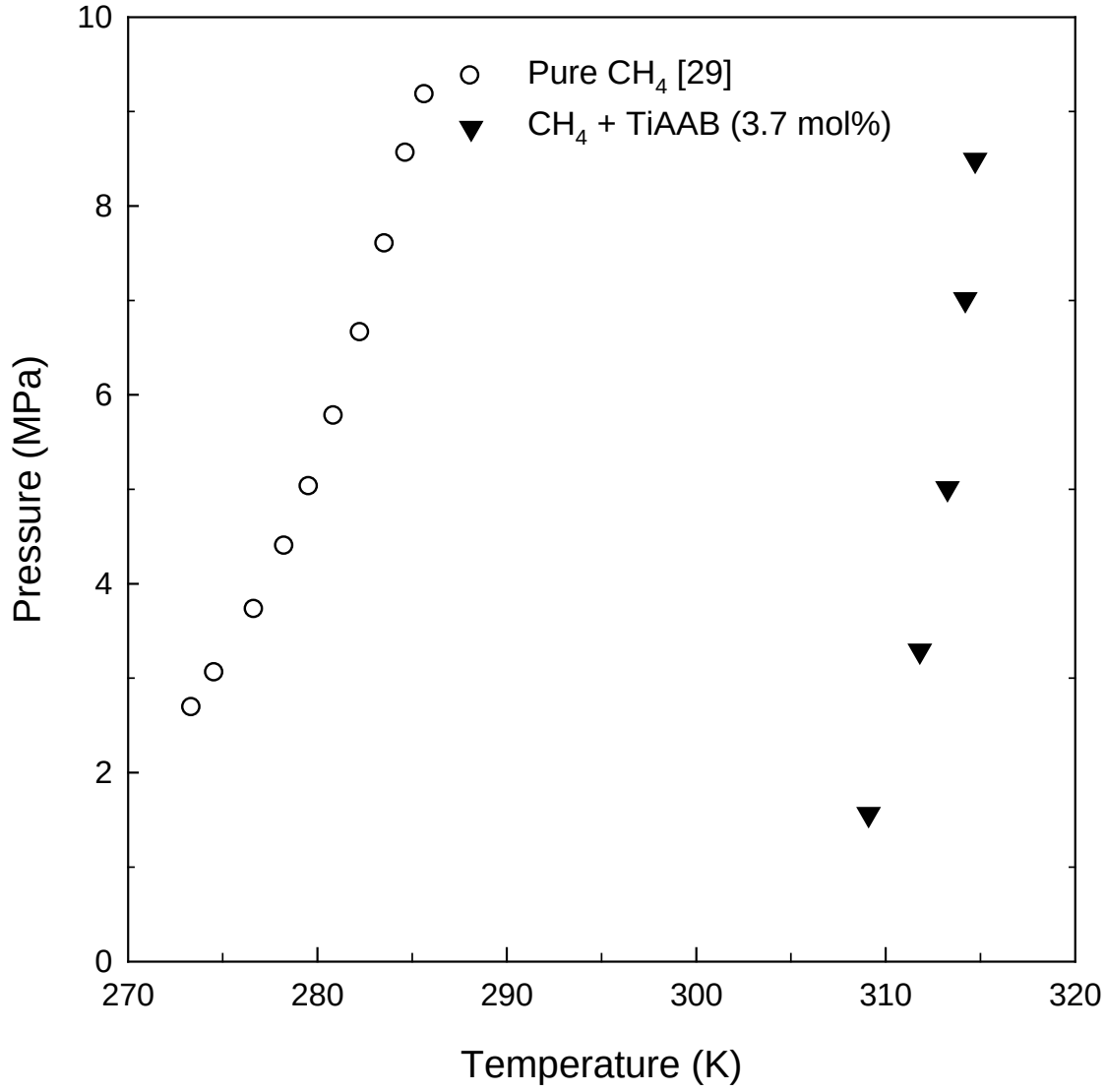

Figure 3.13. Three-phase equilibria of the CH_4 + TiAAB (3.7 mol %) + water systems.

The three-phase equilibria (H - L_W - V) of the CH_4 + TiAAB + water systems were measured at 3.7 mol% of TiAAB. The experimental results were tabulated in (Table 3.4.) and shown in (Figure 3.13.). The double CH_4 + TiAAB semiclathrates showed a significantly enhanced thermodynamic stability compared to pure CH_4 hydrate. As can be seen in (Figure 3.13), at 3.0 MPa the equilibrium temperature of the CH_4 + TiAAB semiclathrate formed from 3.7 mol% solution, which is also the stoichiometric concentration of the TiAAB·$26H_2O$ semiclathrate was higher by 38 K than the pure CH_4 hydrate.

Table 3.4. Semiclathrate phase equilibrium data for the CH_4 + TiAAB + water systems.

3.7 mol %	
T/K	P/MPa
309.1	1.56
311.8	3.29
313.3	5.01
314.2	7.01
314.7	8.49

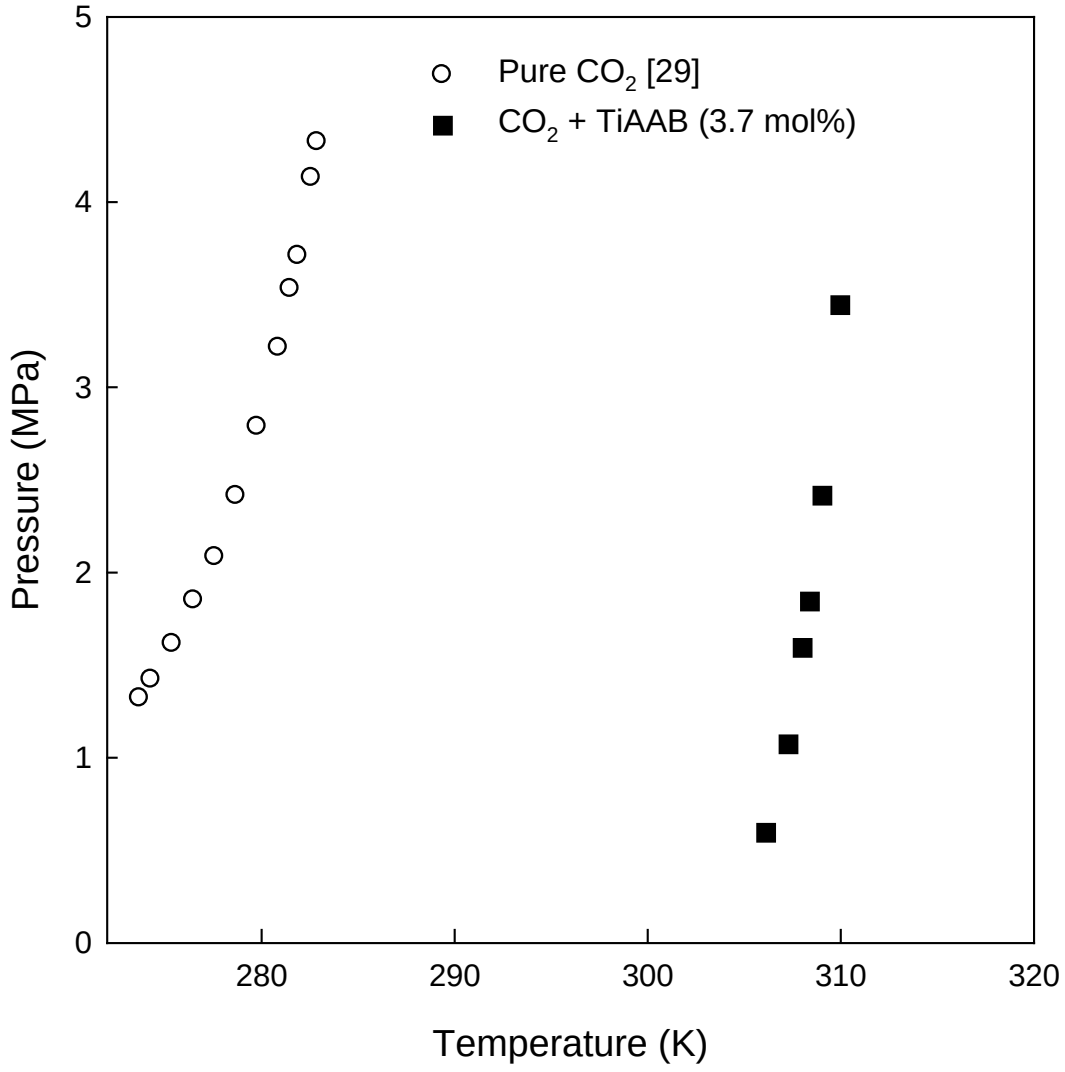

Figure 3.14. Three-phase equilibria of the CO_2 + TiAAB + water systems.

The stability conditions of the double CO_2 + TiAAB semiclathrates with concentration of 3.7 mol% TiAAB are shown in (Figure 3.14.). The overall results are also summarized in (Table 3.5). The double CO_2 + TiAAB semiclathrates also demonstrated a significantly increased thermodynamic stability, as shown by their higher temperature at specified pressure or lower pressure at specified temperature when compared with the pure CO_2 hydrate. At 3.0 MPa, the equilibrium temperature of the CO_2 + TiAAB semiclathrates with 3.7 mol% was higher by 30 K than the pure CO_2 hydrate.

Table 3.5. Semiclathrate phase equilibrium data for the CO_2 + TiAAB + water systems.

3.7 mol %	
T/K	P/MPa
308.4	1.84
308.0	1.59
307.3	1.07
309.9	3.44
309.0	2.41
306.1	0.59

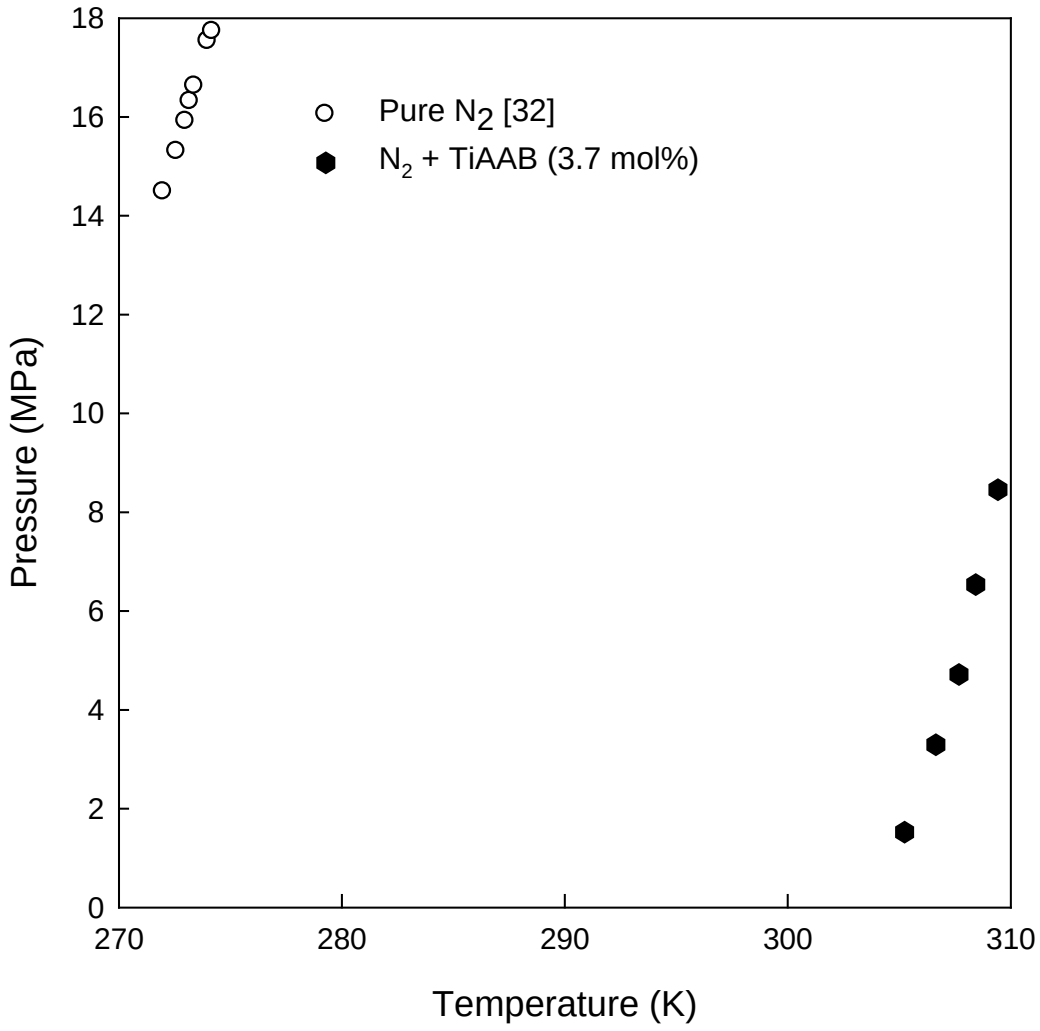

Figure 3.15. Semiclathrate phase equilibria of the N_2 + TiAAB + water systems.

The three-phase (H-L_w-V) equilibria of the N_2 + TiAAB (3.7 mol%) + water systems were depicted in (Figure 3.15.) and summarized in (Table 3.6.). The equilibrium lines of the N_2 + TiAAB semiclathrate systems shifted significantly to the promoted regions, which are represented by the lowered pressure at any given temperature or elevated temperature at any given pressure, compared with the N_2 gas hydrate.

Table 3.6. Semiclathrate phase equilibria data of the N_2 + TiAAB + water systems.

3.7 mol%	
T/K	p/MPa
305.2	1.52
306.6	3.30
307.7	4.71
308.4	6.54
309.4	8.45

The ^{13}C NMR spectra of a pure CH_4 hydrate, pure TiAAB semiclathrate, and double CH_4 + TiAAB semiclathrate are shown in (Figure 3.16.). The ^{13}C NMR spectrum of the pure CH_4 hydrate, which is known to form sI hydrate, has two resonance peaks at -4.3 and -6.6 ppm, which indicate the enclathration of CH_4 molecules in the small 5^{12} cages and the large $5^{12}6^2$ cages, respectively and the double CH_4 + TiAAB semiclathrate showed an additional peak at -4.3 ppm. The peak observed at -4.3 ppm can be reasonably assigned to CH_4 molecules captured in the 5^{12} cages of the double TiAAB semiclathrate.

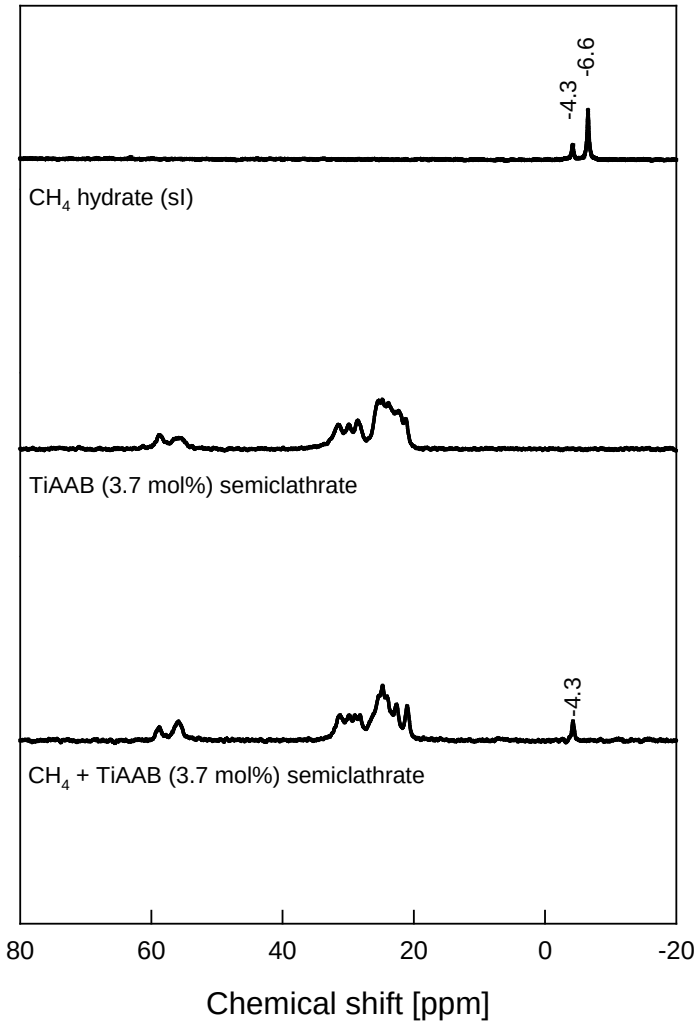

Figure 3.16. ^{13}C NMR spectra of the pure CH_4 hydrates, pure TBAC semiclathrate, and double CH_4 + TiAAB semiclathrates.

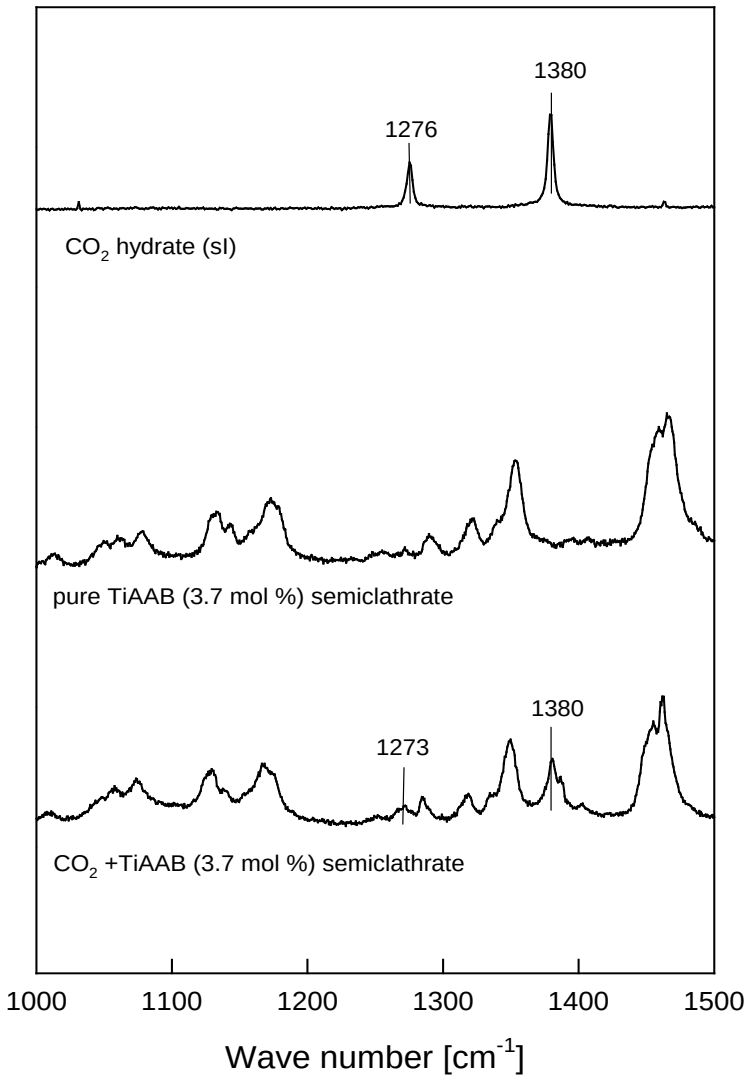

Figure 3.17. Raman spectra of pure CO_2 hydrate, pure TiAAB hydrates, and double CO_2 + TiAAB hydrates.

(Figure 3.17.) shows the Raman spectra of the pure CO_2 hydrate, pure TiAAB semiclathrate, and double CO_2 + TiAAB semiclathrate. The Raman spectrum of the pure CO_2 hydrate, which is known to form sI hydrate, had two Raman peaks at 1276 and 1380 cm^{-1}. The double CO_2 + TiAAB semiclathrate had two Raman peaks at 1273 and 1380 cm^{-1}, which can be assigned to the enclathrated CO_2 molecules. The double CO_2 + TiAAB semiclathrate also exhibited many other peaks at a wide range of wavenumbers that can be assigned to an enclathrated $TiAA^+$ in the double TiAAB semiclath-

rate. The slight shift in wavenumbers (1276 → 1273 cm^{-1}) is attributable to the structural transition caused by semiclathrate formation. Even though the CO_2 enclathration in the double TiAAB semiclathrate was clearly confirmed via Raman spectroscopy, the detailed distribution of guest molecules cannot be provided because the Raman spectrum of the CO_2 hydrate does not demonstrate peak splitting for guests in different cages.

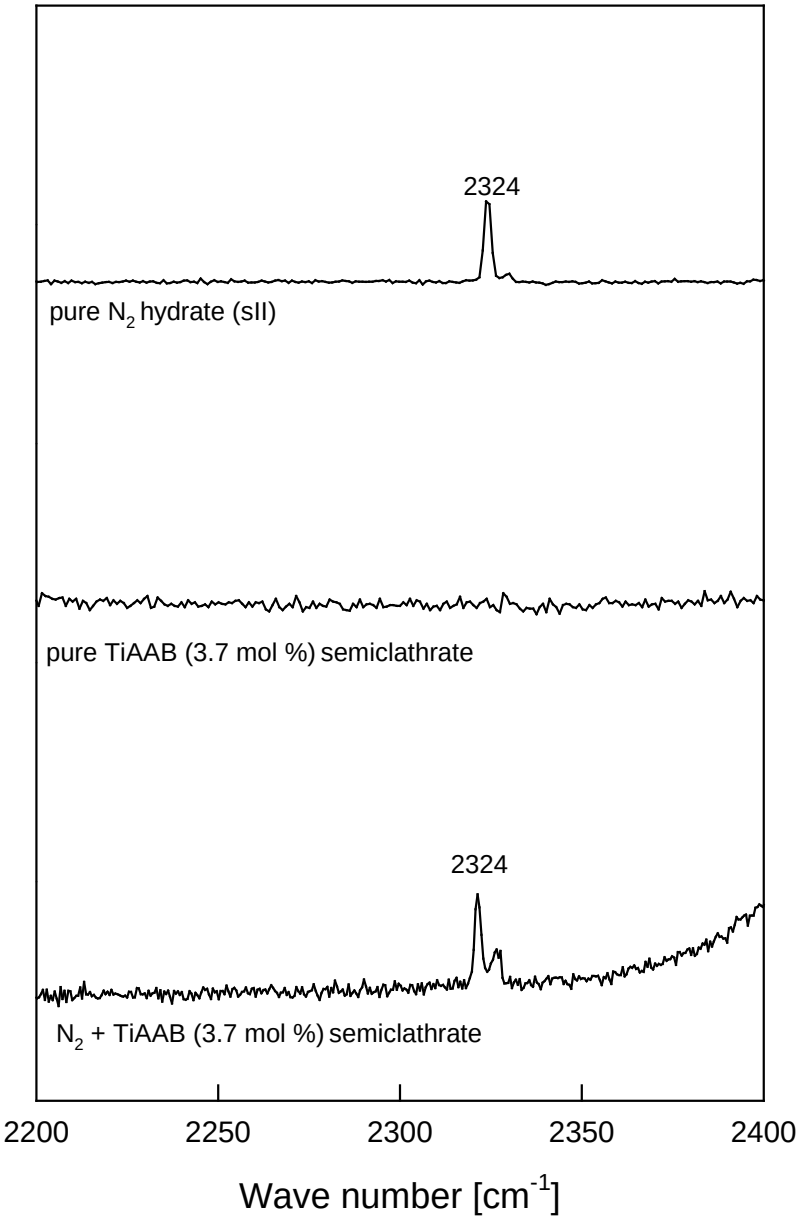

Figure 3.18. Raman spectra of the N_2 hydrate, pure TiAAB (3.7 mol%) semiclathrate, and N_2 + Ti-AAB (3.7 mol%) semiclathrate. The small Raman peak located next to 2324 cm^{-1} originated from the N_2 vapor for cooling.

The Raman spectra of the N_2 hydrate, pure TiAAB (3.7 mol%) semiclathrate, and N_2 + Ti-AAB (3.7 mol%) semiclathrate are presented in (Figure 3.18.). The N_2 gas hydrate is known to be sII hydrate and it exhibits one Raman peak at 2324 cm^{-1}. Even though the N_2 molecules were enclath-

rated in both the small (5^{12}) and large ($5^{12}6^2$) cages of the sII N_2 hydrate, only one Raman peak appeared because the N_2 molecules are so small in molecular size that the symmetric N-N vibrations of the N_2 molecules are not distinguishable in the small and large cages of the sII hydrates [36, 37]. The N_2 + TiAAB (3.7 mol%) semiclathrate also exhibited one Raman peak at 2324 cm^{-1} for the N_2 molecules enclathrated in the small (5^{12}) cages of the semiclathrate, while the pure TiAAB semiclathrate did not exhibit Raman peaks around 2324 cm^{-1}. Despite the absence of peak splitting of N_2 molecules enclathrated in different cages, it was clearly confirmed from the Raman spectra that the N_2 molecules are encaged in the TiAAB semiclathrate.

3.3. Conclusions

The three-phase equilibria of the double TBAC and TiAAB semiclathrates with either CH_4, CO_2, and N_2 as a guest gas were measured to determine thermodynamic stability conditions. The double TBAC and TiAAB semiclathrates showed a significantly enhanced thermodynamic stability when compared with gas hydrate systems. The maximum stabilization was observed at a stoichiometric concentration (3.3 mol%) of the TBAC·29.7H_2O semiclathrate and stoichiometric concentration (3.7 mol%) of the TiAAB·26.0H_2O semiclathrate. In addition, a differential scanning calorimeter (DSC) was used to measure the dissociation enthalpy of the QAS semiclathrate. Furthermore, TBAB and TBAF dissociation enthalpies were measured using u-DSC. The enthalpy (ΔH_d) is a very important thermophysical property of semiclathrates because it is closely related to the amount of heat required for semiclathrate formation or dissociation in the CO_2 capture process. The cage-dependent ^{13}C NMR spectra identified CH_4 molecules being captured in the 5^{12} cages of the double TBAC and TiAAB semiclathrates. The Raman spectroscopic results also confirmed the enclathration of CO_2 and N_2 molecules in the double TBAC and TiAAB semiclathrates. The overall thermodynamic and spectroscopic results provide a better understanding of the thermodynamic stability, phase behavior, guest distribution, and guest-host interaction in the double semiclathrates. Thus, these results can serve as fundamental key information for their actual applications to natural gas storage and CO_2 capture.

3.4. References

[1] Fowler D, Loebenstein W, Pall D, Kraus CA. Some unusual hydrates of quaternary ammonium salts. J Am Chem Soc. 1940;62:1140-2.

[2] Aladko L, Dyadin YA, Rodionova T, Terekhova I. Clathrate hydrates of tetrabutylammonium and tetraisoamylammonium halides. J Struct Chem. 2002;43:990-4.

[3] Shimada W, Ebinuma T, Oyama H, Kamata Y, Takeya S, Uchida T, et al. Separation of gas molecule using tetra-n-butyl ammonium bromide semi-clathrate hydrate crystals. Jpn J Appl Phys Part 2. 2003;42:L129.

[4] Komarov VY, Rodionova TV, Terekhova IS, Kuratieva NV. The cubic superstructure-I of tetrabutylammonium fluoride $(C_4H_9)_4NF•29.7H_2O$ clathrate hydrate. J Inclusion Phenom Macrocyclic Chem. 2007;59:11-5.

[5] Rodionova T, Komarov V, Villevald G, Aladko L, Karpova T, Manakov A. Calorimetric and structural studies of tetrabutylammonium chloride ionic clathrate hydrates. J Phys Chemi B. 2010;114:11838-46.

[6] Lipkowski J, Komarov VY, Rodionova TV, Dyadin YA, Aladko LS. The structure of tetrabutylammonium bromide hydrate $(C_4H_9)_4NBr·2^1/_3H_2O$. J Supramolecular Chemistry. 2002;2:435-9.

[7] Oyama H, Shimada W, Ebinuma T, Kamata Y, Takeya S, Uchida T, et al. Phase diagram, latent heat, and specific heat of TBAB semiclathrate hydrate crystals. Fluid Phase Equilib. 2005;234:131-5.

[8] Shin K, Cha JH, Seo Y, Lee H. Physicochemical properties of ionic clathrate hydrates. Chem Asian J. 2010;5:22-34.

[9] Fan S, Li Q, Nie J, Lang X, Wen Y, Wang Y. Semiclathrate hydrate phase equilibrium for CO_2/CH_4 gas mixtures in the presence of tetrabutylammonium halide (bromide, chloride, or fluoride). J Chem Eng Data. 2013;58:3137-41.

[10] Park S, Lee S, Lee Y, Seo Y. CO_2 capture from simulated fuel gas mixtures using semiclathrate hydrates formed by quaternary ammonium salts. Environ Sci Technol. 2013;47:7571-7.

[11] Deschamps J, Dalmazzone D. Hydrogen storage in semiclathrate hydrates of tetrabutyl ammonium chloride and tetrabutyl phosphonium bromide. J Chem Eng Data. 2010;55:3395-9.

[12] Li S, Fan S, Wang J, Lang X, Wang Y. Semiclathrate hydrate phase equilibria for CO2 in the presence of tetra-n-butyl ammonium halide (bromide, chloride, or fluoride). J Chem Eng Data. 2010;55:3212-5.

[13] Li XS, Xu CG, Chen ZY, Wu HJ. Tetra-n-butyl ammonium bromide semi-clathrate hydrate process for post-combustion capture of carbon dioxide in the presence of dodecyl trimethyl ammonium chloride. Energy. 2010;35:3902-8.

[14] Linga P, Kumar R, Lee JD, Ripmeester J, Englezos P. A new apparatus to enhance the rate of gas hydrate formation: Application to capture of carbon dioxide. Int J Greenhouse Gas Control. 2010;4:630-7.

[15] Lee S, Lee Y, Park S, Kim Y, Lee JD, Seo Y. Thermodynamic and spectroscopic identification of guest gas enclathration in the double tetra-n-butylammonium fluoride semiclathrates. J Phys Chem B. 2012;116:9075-81.

[16] Deschamps J, Dalmazzone D. Dissociation enthalpies and phase equilibrium for TBAB semi-clathrate hydrates of N_2, CO_2, N_2 + CO_2 and CH_4 + CO_2. J Therm Anal Calorim. 2009;98:113-8.

[17] Sfaxi IBA, Durand I, Lugo R, Mohammadi AH, Richon D. Hydrate phase equilibria of CO_2 + N_2 + aqueous solution of THF, TBAB or TBAF system. Int. J. Greenhouse Gas Control. 2014;26:185-92.

[18] Lee S, Park S, Lee Y, Lee J, Lee H, Seo Y. Guest gas enclathration in semiclathrates of tetra-n-butylammonium bromide: stability condition and spectroscopic analysis. Langmuir. 2011;27:10597-603.

[19] Sato K, Tokutomi H, Ohmura R. Phase equilibrium of ionic semiclathrate hydrates formed with tetrabutylammonium bromide and tetrabutylammonium chloride. Fluid Phase Equilib. 2013;337:115-8.

[20] Makino T, Yamamoto T, Nagata K, Sakamoto H, Hashimoto S, Sugahara T, Ohgaki K. Thermodynamic stabilities of tetra-n-butyl ammonium chloride + H_2, N_2, CH_4, CO_2, or C_2H_6 semiclathrate hydrate systems. J Chem Eng Data. 2009;55:839-41.

[21] Nakayama H. Solid-liquid and liquid-liquid phase equilibria in the symmetrical tetraalkylammonium halide-water systems. Bull. Chem. Soc. Jpn. 1981;54:3717-22.

[22] Sun ZG, Liu CG, Zhou B, Xu LZ. Phase equilibrium and latent heat of tetra-n-butylammonium chloride semi-clathrate hydrate. J Chem Eng Data. 2011;56:3416-8.

[23] Aladko LS, Dyadin YA, Rodionova TV, Terekhova IS. Clathrate hydrates of tetrabutylammonium and tetraisoamylammonium halides. J Struct Chem. 2002;43:990-4.

[24] Zhang J, Lee JW. Equilibrium of hydrogen + cyclopentane and carbon dioxide + cyclopentane binary hydrates. J Chem Eng Data. 2008;54:659-61.

[25] Manakov A, Rodionova T, Terekhova I, Komarov V, Burdin A, Sizikov A. Structural and physico-chemical studies of ionic clathrate hydrates of tetrabutyl-and tetraisoamylammonium salts. Proceedings of the 7th International Conference on Gas Hydrates. Edinburgh, Scotland, UK; 2011.

[26] Nakayama H. Hydrates of Organic Compounds. XI. Determination of the melting point and hydration numbers of the clathrate-like hydrate of tetrabutylammonium chloride by differential scanning calorimetry. Bull. Chem. Soc. Jpn. 1987;60:839-43.

[27] S. Kim, I.-H. Baek, J.-K. You, Y. Seo, Guest gas enclathration in tetra-n-butyl ammonium chloride (TBAC) semiclathrates: Potential application to natural gas storage and CO_2 capture, Appl. Energy 140 (2015) 107-112.

[28] Park S, Lee S, Lee Y, Seo Y. CO_2 capture from simulated fuel gas mixtures using semiclathrate hydrates formed by quaternary ammonium salts. Environ Sci Technol 2013;47:7571-7.

[29] Adisasmito S, Frank III RJ, Sloan Jr ED. Hydrates of carbon dioxide and methane mixtures. J Chem Eng Data. 1991;36:68-71.

[30] Kamran-Pirzaman A, Pahlavanzadeh H, Mohammadi AH. Hydrate phase equilibria of furan, acetone, 1, 4-dioxane, TBAC and TBAF. J Chem Thermodyn. 2013;64:151-8.

[31] Ye N, Zhang P. Phase equilibrium and morphology characteristics of hydrates formed by tetra-n-butyl ammonium chloride and tetra-n-butyl phosphonium chloride with and without CO_2. Fluid Phase Equilib. 2014;361:208-14.

[32] A. Van Cleeff, G. Diepen, Gas hydrates of nitrogen and oxygen, Recl. Trav. Chim. Pays-Bas 1060;79:582-6.

[33] A. Mohammadi, M. Manteghian, A.H. Mohammadi, Phase equilibria of semiclathrate hydrates for methane + tetra n-butylammonium chloride (TBAC), carbon dioxide + TBAC, and nitrogen + TBAC aqueous solution systems, Fluid Phase Equilib. 2014;381:102-7.

[34] Shimada W, Ebinuma T, Oyama H, Kamata Y, Takeya S, Uchida T, et al. Separation of gas molecule using tetra-n-butyl ammonium bromide semi-clathrate hydrate crystals. Jpn J Appl Phys 2003;42:L129.

[35] S. Lee, Y. Lee, S. Park, Y. Kim, J.D. Lee, Y. Seo, Thermodynamic and spectroscopic identification of guest gas enclathration in the double tetra-n-butylammonium fluoride semiclathrates, J. Phys. Chem. B 2012;116: 9075-9081.

[36] Ripmeester JA, Ratcliffe CI. On the contributions of NMR spectroscopy to clathrate science. J Struct Chem. 1999;40:654-62.

[37] C.-l. Liu, H.-l. Lu, Y.-g. Ye, Raman spectroscopy of nitrogen clathrate hydrates, Chin. J. Chem. Phys. 29;22:353-8.

[38] K. Sugahara, Y. Tanaka, T. Sugahara, K. Ohgaki, Thermodynamic stability and structure of nitrogen hydrate crystal, J. Supramolecular Chemistry 2002;2:365-8.

Chapter IV

Post-combustion CO_2 capture using QAS semiclathrates formation

4.1. Introduction

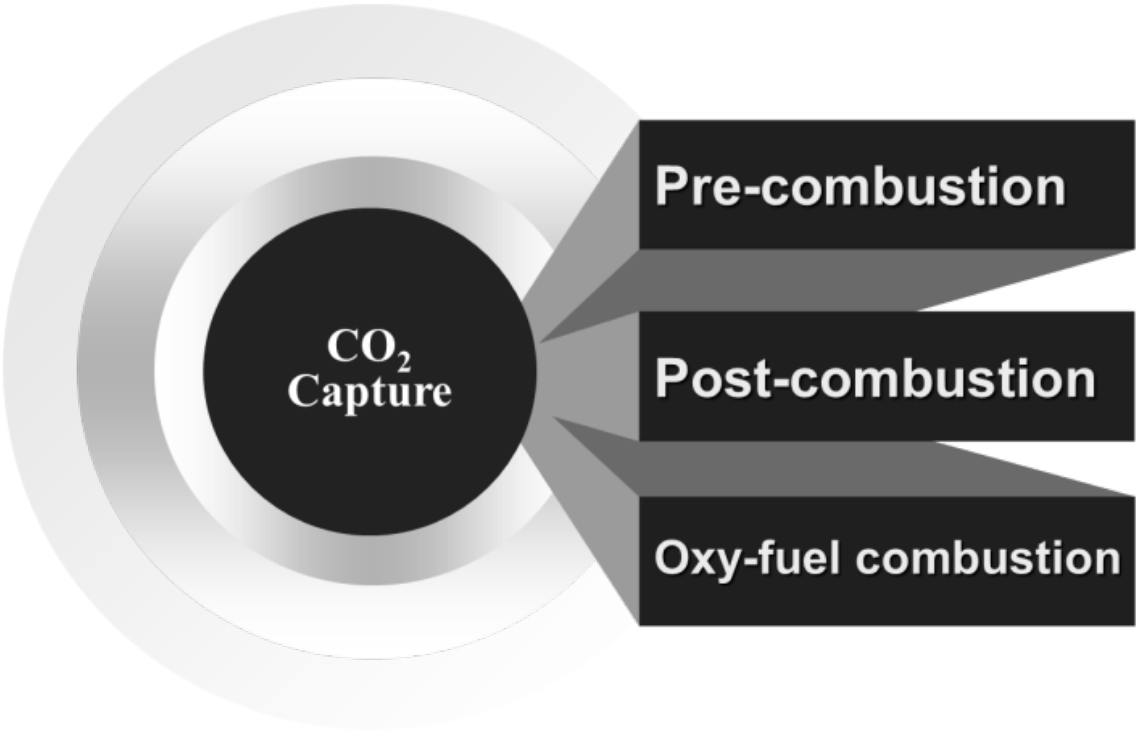

Figure 4.1. Technologies for reducing the CO_2 emission.

Carbon dioxide (CO_2), mainly produced from the combustion of fossil fuels in power plants, is regarded as a primary greenhouse gas. Generally, three main technologies to reduce CO_2 emission from large stationary sources exist: oxy-fuel combustion, post-combustion, and pre-combustion CO_2 capture (Figure 4.1.) [1]. Various methods for CO_2 capture have been developed for each technology. One method that has attracted increasing attention is hydrate-based gas separation, which is based on selective partitioning of CO_2 between hydrate and vapor phases [2, 3].

Semiclathrates, which share many physical and chemical properties with gas hydrates, could be an attractive alternative to gas hydrates because in general, they can maintain their thermodynamic stability under atmospheric pressure conditions [4-9]. In gas hydrates, the guest molecules are not physically bonded to host water lattices, whereas in semiclathrates, guest molecules can both take part

in building the host water frameworks and occupy cages after breaking part of the cage structure. Quaternary ammonium salts (QASs) such as tetra-n-butylammonium bromide (TBAB), tetra-n-butylammonium chloride (TBAC), and tetra-n-butylammonium fluoride (TBAF) form semiclathrates with water molecules under atmospheric pressure.

Most studies on QAS semiclathrates have covered semiclathrate phase equilibria for a single guest gas primarily focusing on TBAB semiclathrates and semiclathrate formation kinetics for pre-combustion CO_2 capture [10-15]. However, preferential partitioning of guest gases, gas storage capacity, and guest gas enclathration behavior in QAS semiclathrates for post-combustion CO_2 capture have not been examined thoroughly. Furthermore, the influences of the three different types of semiclathrate formers on CO_2 capture remain unclear.

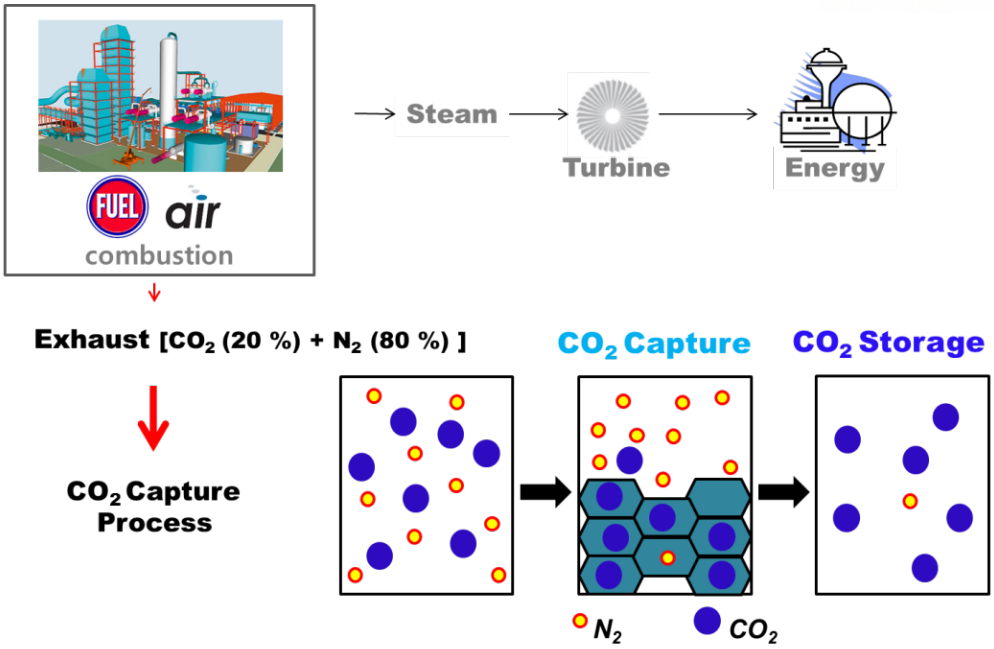

Figure 4.2. The concept of clathrate-based CO_2 capture.

In this study, TBAC semiclathrate-based CO_2 capture from a post-combustion flue gas mixture was investigated with a primary focus on thermodynamic, kinetic, and spectroscopic aspects. The semiclathrate phase equilibria for the CO_2 (20%) + N_2 (80%) + TBAC (1.0, 3.3, and 5.0 mol%) + water mixtures were measured to determine stability conditions of TBAC semiclathrates. The gas uptake in the TBAC semiclathrates and CO_2 composition changes in the vapor phase, were measured according to reaction time in order to investigate selective partitioning of guest molecules, guest distribution, and cage filling characteristics. Furthermore, the guest molecules encaged in the semiclathrate lattices were analyzed via Raman spectroscopy.

Then, semiclathrate-based CO_2 capture from post-combustion flue gas was investigated in the presence of TBAB, TBAC, and TBAF. The thermodynamic stability of the CO_2 (20%) + N_2 (80%) + QAS semiclathrates was examined with an isochoric method using a high pressure reactor as well as with dissociation enthalpy measurement using a high pressure micro-differential scanning calorimeter (HP μ-DSC). The gas uptake and CO_2 concentration changes in the vapor phase during QAS semiclathrate formation were measured to examine the preferential occupation of CO_2 in the semiclathrate phase. CO_2 concentrations in the vapor and semiclathrate phases after the completion of semiclathrate formation were measured to elucidate the CO_2 selectivity based on the types of QAS semiclathrate used. The enclathration of guest molecules in the semiclathrate lattices was confirmed with a micro-Raman spectrometer and time-dependent *in-situ* Raman spectrometer.

4.2. Results and discussion

4.2.1. Stability conditions of the QAS semiclathrates measurements

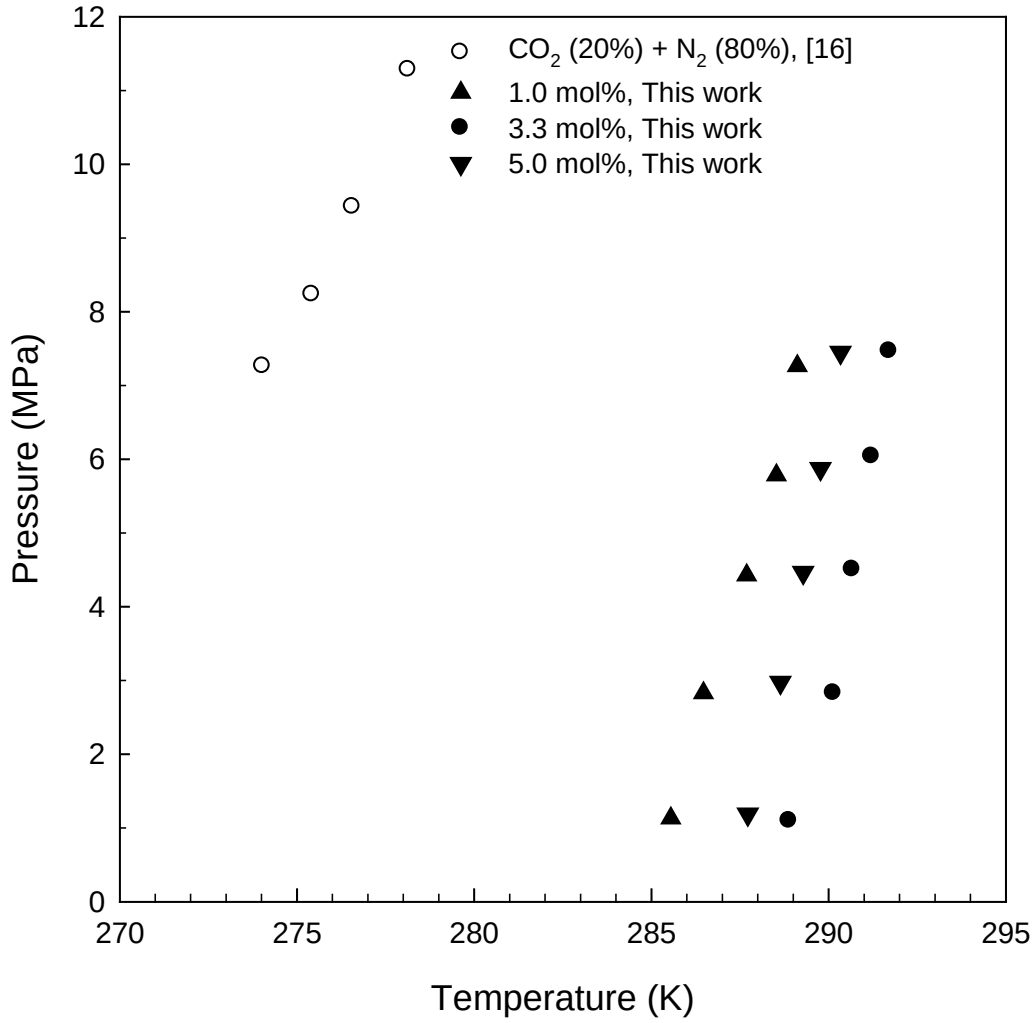

Figure 4.3. Three-phase (H - L_W -V) equilibria for the CO_2 (20%) + N_2 (80%) + TBAC (1.0, 3.3, and 5.0 mol%) + water systems.

(Figure 4.3.) shows three-phase (semiclathrate (H) - liquid water (L_w) - vapor (V)) equilibria for the CO_2 (20%) + N_2 (80%) + TBAC (1.0, 3.3, and 5.0 mol%) + water systems and the results are presented in (Table 4.1.). For the TBAC semiclathrates with CO_2 (20%) + N_2 (80%), the maximum stabilization was observed at 3.3 mol% TBAC solution, which corresponds to the stoichiometric concentration of TBAC•29.7H_2O. The phase equilibrium data clearly demonstrate that when the flue gas

of CO_2 (20%) + N_2 (80%) is used as a feed gas for gas hydrate or semiclathrate formation, TBAC semiclathrate systems are significantly more stable than the gas hydrate system. As can be seen in (Figure 4.3.), the equilibrium temperature of semiclathrate formed from the 3.3 mol % TBAC solution was higher by 15 K than that of gas hydrate at 7.0 MPa.

Table 4.1. Semiclathrate phase equilibrium data for the CO_2 (20%) + N_2 (80%) + TBAC (1.0, 3.3, and 5.0 mol%) + water systems.

1.0 mol% TBAC		3.3 mol% TBAC		5.0 mol% TBAC	
T/K	P/MPa	T/K	P/MPa	T/K	P/MPa
288.9	1.10	285.5	1.13	287.7	1.19
290.1	2.83	286.5	2.83	288.6	2.97
290.7	4.50	287.7	4.43	289.3	4.47
291.2	6.04	288.5	5.78	289.8	5.87
291.7	7.46	289.1	7.27	290.3	7.45

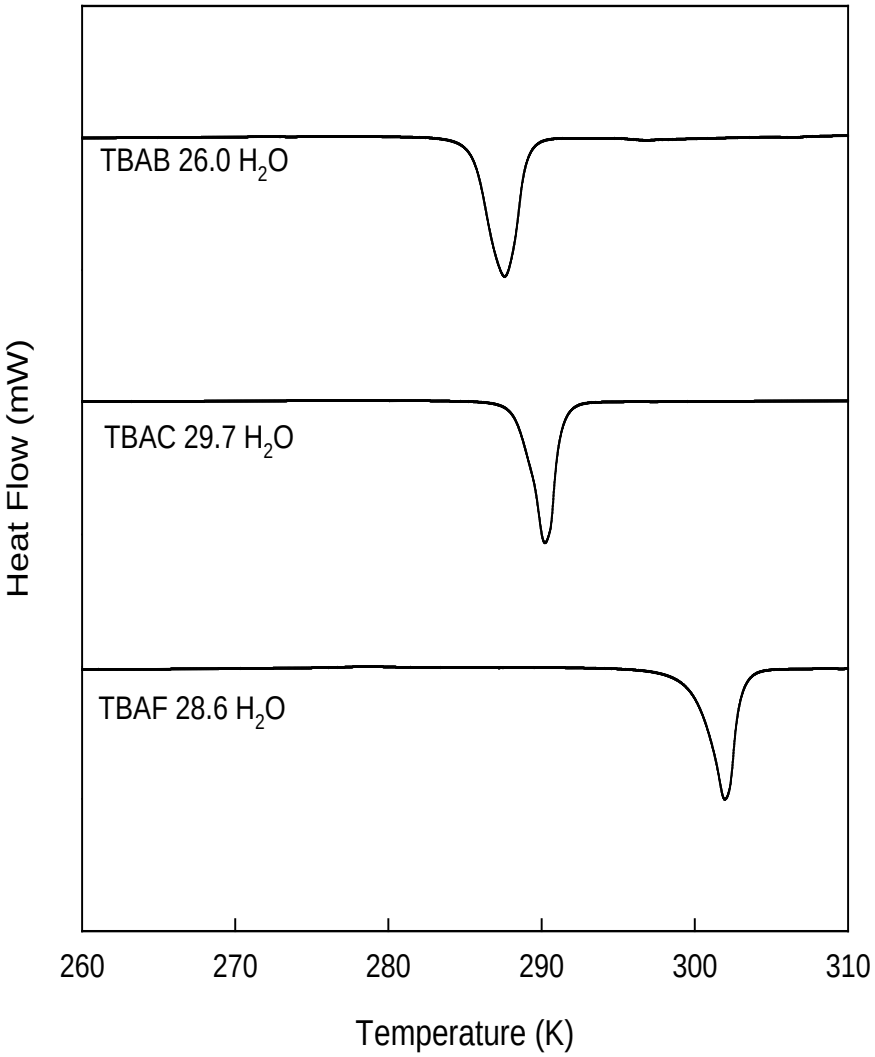

Figure 4.4. Thermograms of the CO_2 (20%) + N_2 (80%) + QAS semiclathrates at 3.1 MPa.

Table 4.2. The onset temperatures and dissociation enthalpies of CO_2 (20%) + N_2 (80%) + QAS semiclathrate at 3.1 MPa.

	T/K	Enthalpy (J/g water)
TBAB	286.9 ± 0.3	342.5 ± 0.8
TBAC	290.3 ± 0.0	344.1 ± 2.0
TBAF	301.2 ± 0.2	350.8 ± 0.9

Semiclathrates of TBAB, TBAC, and TBAF are most stable at 3.7, 3.3, and 3.4 mol% solutions, which correspond to stoichiometric concentrations of TBAB·26.0H_2O, TBAC·29.7H_2O, and TBAF·28.6H_2O, respectively [5-7, 9, 22]. (Figure 4.4.) shows DSC thermograms obtained from melting the CO_2 (20%) + N_2 (80%) + QAS (3.7 mol% TBAB, 3.3 mol% TBAC, and 3.4 mol% TBAF) semiclathrates at 3.1 MPa. As shown in (Figure 3.2.), for each semiclathrate, only one endothermic peak originating from the QAS semiclathrate dissociation was observed without an ice melting peak because all the QAS and water molecules are expected to be consumed in the semiclathrate formation at each stoichiometric concentration, which indicates the complete conversion of the QAS solutions to semiclathrates. (Figure 4.4.) also can offer the information on both the dissociation enthalpies (ΔH_d) of each semiclathrate by integrating an endothermic heat flow curve and the onset temperatures by intersecting a baseline and a tangent line at an inflection point. The overall experimental data for the onset temperature and dissociation enthalpies of each semiclathrate at 3.1 MPa are provided in (Table 4.2.). The dissociation enthalpy of the CO_2 (20%) + N_2 (80%) + TBAB (3.7 mol%) hydrate was in good agreement with a value reported in the literature [23].

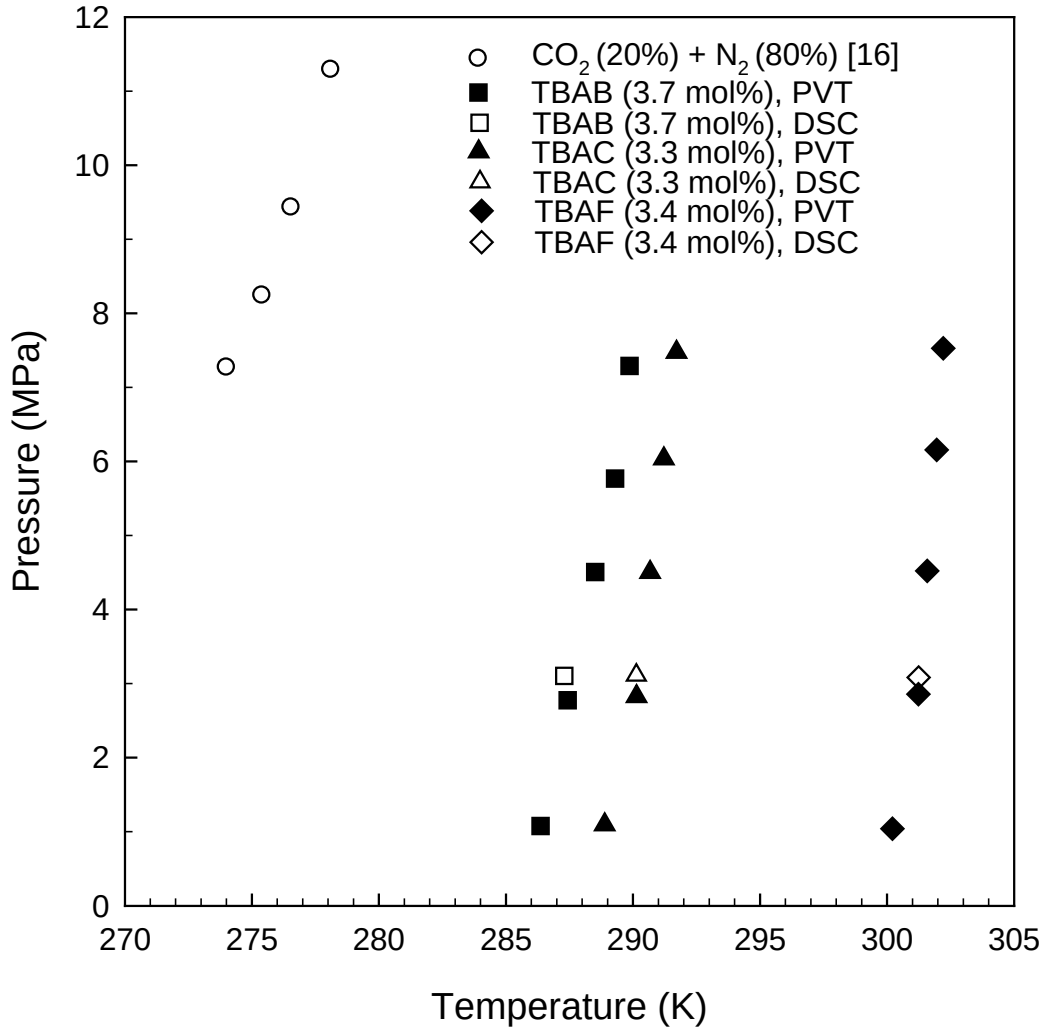

Figure 4.5. Semiclathrate phase equilibria of the CO_2 (20%) + N_2 (80%) + QAS + water systems.

(Figure 4.5.) presents three-phase (semiclathrate (H) - liquid water (L_w) - vapor (V)) equilibria for the CO_2 (20%) + N_2 (80%) + QAS (TBAB 3.7 mol%, TBAC 3.3 mol%, and TBAF 3.4 mol%) + water systems, and the overall experimental data are summarized in (Table 4.3.). In addition, the experimental results obtained from the HP μ-DSC method at 3.1 MPa are also depicted together in (Figure 4.5.). The equilibrium P-T data obtained from the HP μ-DSC were exactly located in the corresponding three-phase equilibrium lines of each semiclathrate which were obtained by the conventional PVT method. The semiclathrate phase equilibrium results indicate that QAS semiclathrates with CO_2 (20%) + N_2 (80%) can offer a significant thermodynamic promotion which represents a pressure reduction at any given temperature or a temperature increase at any given pressure when compared

with gas hydrates with CO_2 (20%) + N_2 (80%). In particular, as seen in (Figure 4.5.), TBAF semiclathrate has a higher thermodynamic stability than that of the TBAB and TBAC semiclathrates, and it is stable at temperatures higher than 300 K for all experimental pressure regions from 1.0 to 7.5 MPa. However, gas hydrate with CO_2 (20%) + N_2 (80%) requires equilibrium pressures as high as 7.0 MPa even at 273.0 K [16]. For this reason, hydrate-based CO_2 capture from a flue gas mixture is difficult to directly apply in the actual process because of its requirement for high pressure and low temperature to form gas hydrates.

Table 4.3. Semiclathrate phase equilibrium data of the CO_2 (20%) + N_2 (80%) + QAS + water systems.

TBAB 3.7 mol%		TBAC 3.3 mol%		TBAF 3.4 mol%	
T/K	P/MPa	T/K	P/MPa	T/K	P/MPa
286.4	1.08	288.9	1.09	300.2	1.04
287.4	2.77	290.1	2.83	301.2	2.86
288.5	4.51	290.7	4.50	301.6	4.52
289.3	5.77	291.2	6.04	302.0	6.16
289.9	7.29	291.7	7.48	302.2	7.53

4.2.2. Gas uptake and composition measurements of QAS semiclathrates

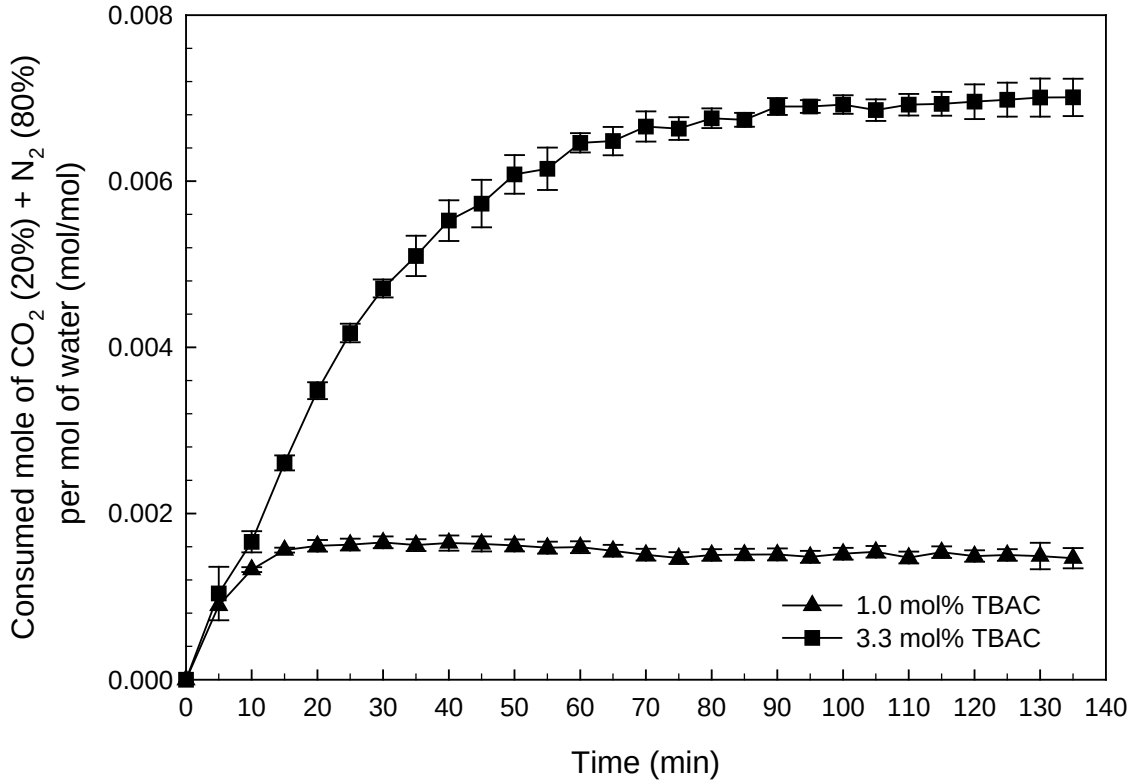

Figure 4.6. Gas uptakes of the CO_2 (20%) + N_2 (80%) + TBAC + water systems at 3.0 MPa and ΔT = 5.0 K.

In the present study, gas uptake and gas composition changes during semiclathrate formation were measured to investigate selective partitioning of CO_2 in the vapor and semiclathrate phases. For these experiments, the driving force, which is defined as the temperature difference (ΔT) between the equilibrium and experimental temperatures, was set to be 5.0 K at 3.0 MPa for semiclathrate formation.

(Figure 4.6.) shows gas uptake curves for the CO_2 (20%) + N_2 (80%) gas mixture during semiclathrate formation in the presence of 1.0 and 3.3 mol % TBAC solutions at 3.0 MPa and ΔT = 5.0 K. The gas consumption was monitored from the beginning of agitation and the effective reaction time was recorded just after the nucleation of semiclathrate crystals. The accumulated amount of gas consumed during the semiclathrate formation reaction corresponds to the total amount of gas captured in the cages of TBAC semiclathrate. The 3.3 mol% TBAC solution exhibited a much larger gas consumption during the semiclathrate formation than the 1.0 mol % TBAC solution.

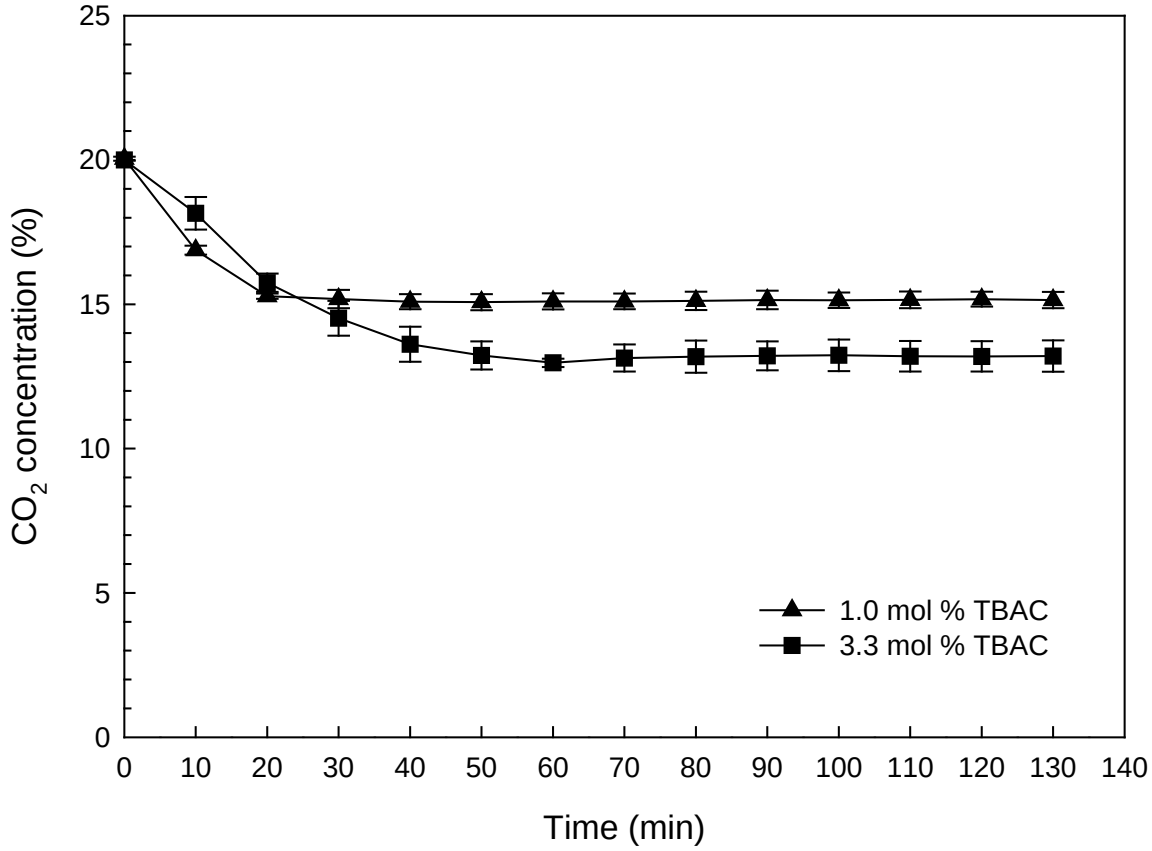

Figure 4.7. CO_2 composition change in the vapor phase during TBAC semiclathrate formation at 3.0 MPa and ΔT = 5.0 K.

The composition change in the vapor phase at 3.0 MPa and ΔT = 5.0 K during TBAC semiclathrate formation is shown in (Figure 4.7.) Due to the selective enclathration of CO_2 in the TBAC semiclathrate lattices, the CO_2 concentration in the vapor phase gradually decreased as semiclathrate formation proceeded. For the 3.3 mol% TBAC solution, the CO_2 concentration in the vapor phase decreased from 20% to 13%, whereas for the 1.0 mol% TBAC solution, the CO_2 concentration was reduced from 20% to 16%. The gas uptake and the composition change during the formation reaction are closely related to the conversion of the TBAC solution to the semiclathrate crystals. In the case of the 3.3 mol% TBAC solution, all of the TBA^+ and Cl^- ions are expected to be used for semiclathrate formation because 3.3 mol% TBAC solution is an equivalent concentration to $TBAC \cdot 29.7H_2O$ semiclathrate. Cl^- ions, together with water molecules, take part in building the polyhedral host framework of the cages where TBA^+ ions are incorporated as guests. However, in the 1.0 mol% TBAC solution, smaller amounts of TBA^+ and Cl^- are available for semiclathrate formation. There must also be an

excess water phase, which is not involved in the semiclathrate formation, resulting in less conversion of water to semiclathrate. As can be seen in (Figures 4.6 and 4.7.), both gas uptake and CO_2 concentration in the vapor phase were rapidly changed in the initial semiclathrate growth period, then slowly stabilized, and almost unchanged after 1 h for each condition, indicating that the semiclathrate formation was completed within 1 h.

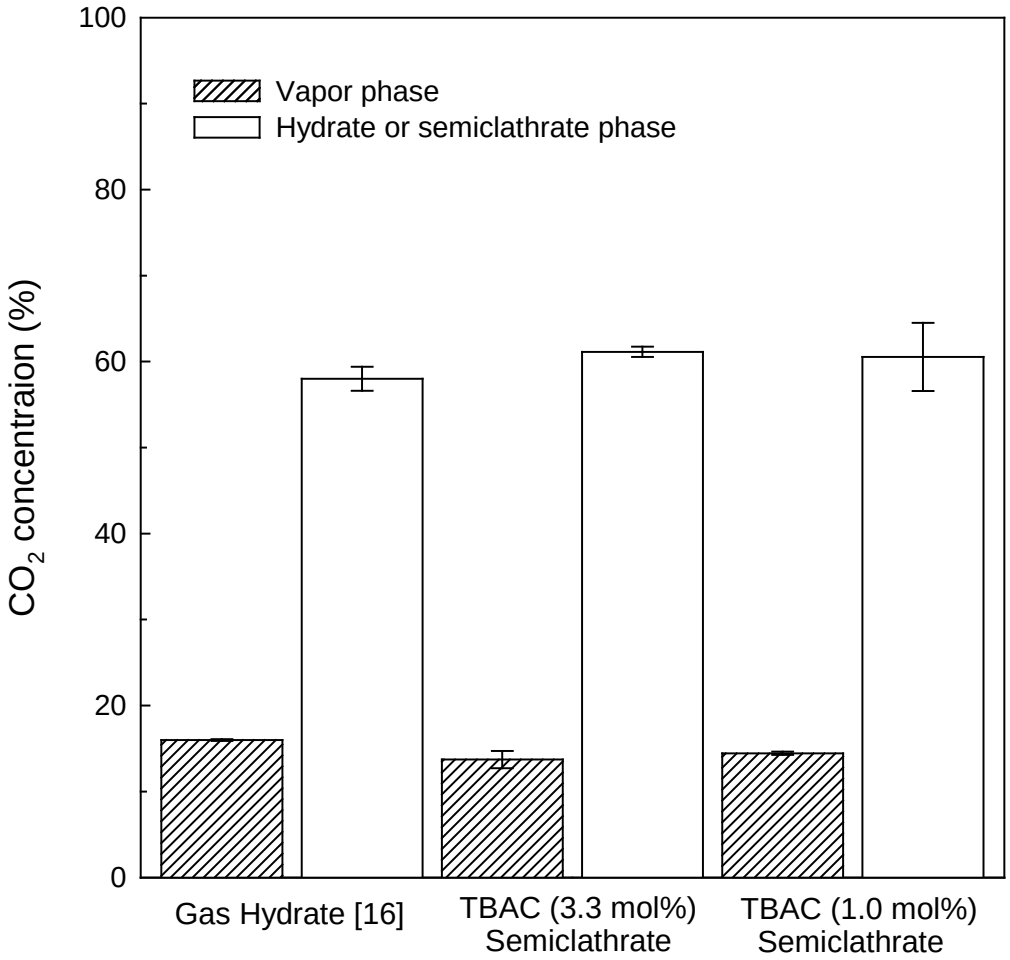

Figure 4.8. CO_2 concentrations in the vapor and semiclathrate phases at 3.0 MPa and ΔT = 5.0 (gas hydrate at 275.15 K and ΔP = 2.0 MPa).

(Figure 4.8.) shows the final CO_2 concentrations in the vapor and semiclathrate phases for the 1.0 and 3.3 mol% TBAC solutions. For comparison, the result for gas hydrate formed at 275.15 K and ΔP = 2.0 MPa was included in (Figure 4.8.). After confirming the completion of the TBAC semiclathrate formation reaction, the CO_2 concentration in the vapor phase was measured, and then the concentration of recovered CO_2 from the semiclathrate phase was analyzed. The result clearly indicates that CO_2 is selectively enriched in the semiclathrate lattices. In TBAC semiclathrates, the large cages with partially broken bonds were occupied by TBA^+ ion, while small cages were left vacant and therefore available for capturing CO_2 molecules. However, it should be noted that the TBAC concentration does not affect the CO_2 composition in the semiclathrate phase even if it does affect the gas

uptake and composition change behavior in the vapor phase. As can be seen in (Figure 4.8.), the CO_2 enrichment in the semiclathrate lattices was almost the same as that in the gas hydrate. However, CO_2 capture using TBAC semiclathrates can occur at significantly lower pressure at a specified temperature or higher temperature at a specified pressure. Based on (Figure 4.8.), it can be reasonably expected that one step of semiclathrate formation enriches 20% CO_2 in the flue gas to approximately 60% CO_2 in the semiclathrate lattices.

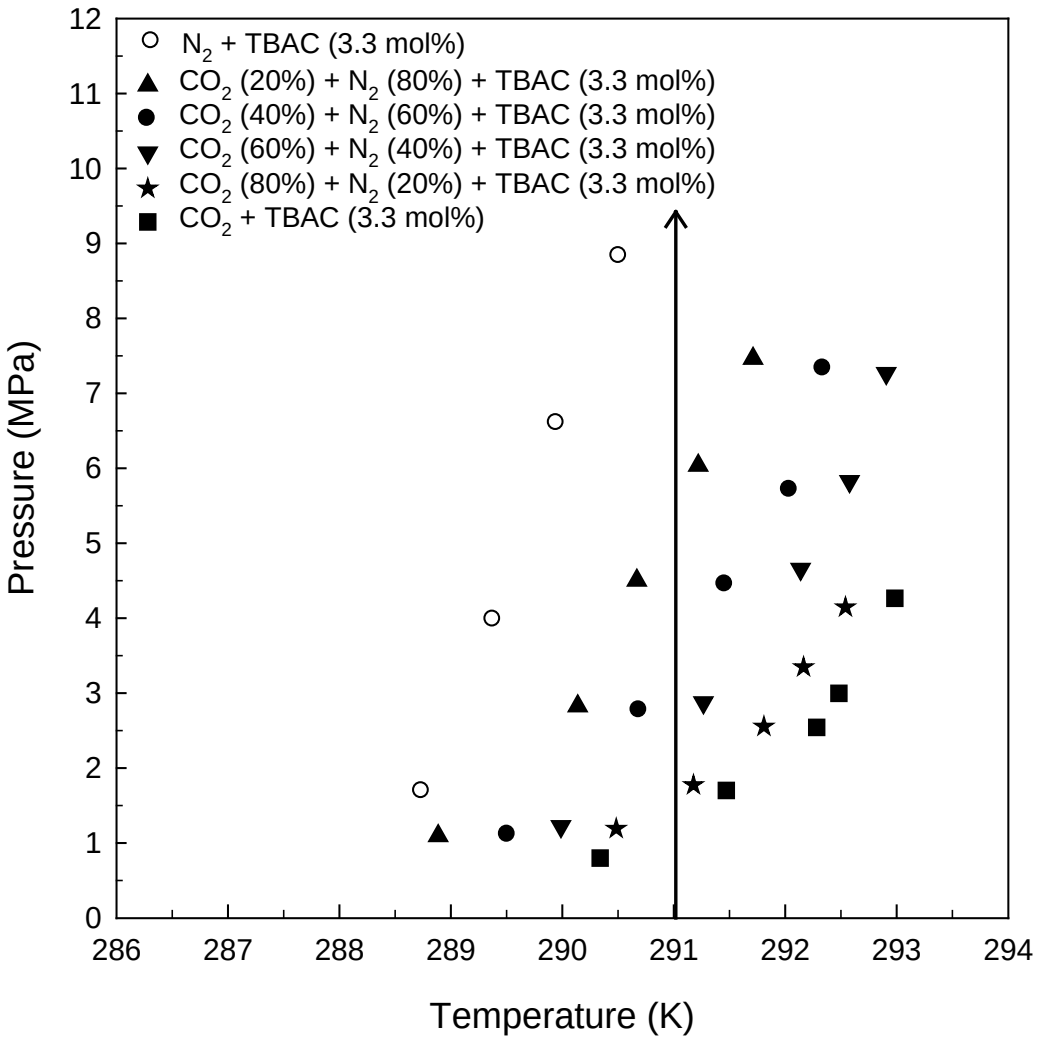

Figure 4.9. Three-phase (H - L_W -V) equilibria of the CO_2 + N_2 + TBAC (3.3 mol%) + water systems.

(Figure 4.9.) shows three-phase semiclathrate equilibria of the CO_2 + N_2 + TBAC (3.3 mol%) + water mixtures with various CO_2 compositions (0, 20, 40, 60, 80, and 100%) and the data as a whole are shown in (Table 4.4.). The entire equilibrium curves of TBAC semiclathrates with CO_2 + N_2 were remarkably shifted to the promoted regions represented by lower pressure and higher temperature conditions. The phase behavior shown in (Figure 4.9.) indicates that for semiclathrate formation from CO_2 + N_2 gas mixtures, the 3.3 mol% TBAC solution requires significantly lowered pressures even at temperature ranges higher than 288 K. The huge equilibrium difference between the TBAC + CO_2 and TBAC + N_2 semiclathrates implies that CO_2 will be selectively captured in the semiclathrate phase when the semiclathrate-based gas separation process is adopted.

Table 4.4. Semiclathrate phase equilibrium data for the CO_2 + N_2 + TBAC (3.3 mol%) + water systems.

CO_2 (40%) + N_2 (60%)		CO_2 (60%) + N_2 (40%)		CO_2 (80%) + N_2 (20%)	
T/K	P/MPa	T/K	P/MPa	T/K	P/MPa
289.5	1.11	290.0	1.22	290.5	1.19
290.7	2.77	291.3	2.87	291.2	1.77
291.5	4.45	292.1	4.66	291.8	2.56
292.0	5.71	292.6	5.82	292.2	3.35
292.3	7.33	292.9	7.30	292.5	4.15

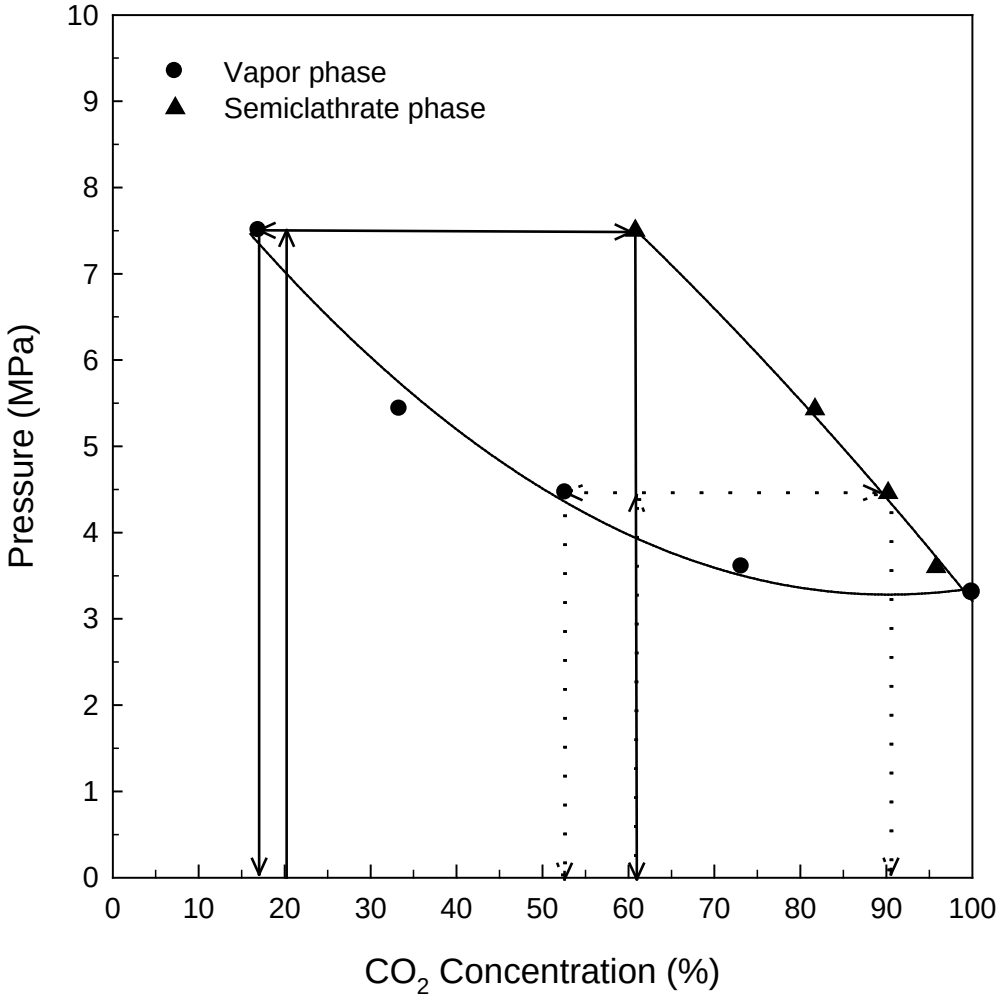

Figure 4.10. CO_2 Compositions in the vapor phase and semiclathrate phases for the 3.3 mol% TBAC solution at 291.0 K and Δ P = 2.0 MPa.

Based on the phase equilibrium data presented in (Figure 4.9.), the pressure-composition diagram, which can provide the CO_2 compositions in the semiclathrate phase corresponding to a given vapor phase composition, is depicted in (Figure 4.10.). The driving force, which is defined here as the pressure difference (ΔP) between the equilibrium and experimental pressure, was set to be 2.0 MPa for semiclathrate formation at 291.0 K. The concentration of retrieved CO_2 from the semiclathrate phase was measured after completing the semiclathrate formation with the 3.3 mol% TBAC solution.

Because consistent experimental conditions of 291.0 K and ΔP = 2.0 MPa were applied for all the CO_2 concentrations in order to draw the complete pressure-composition diagram in (Figure

4.10.), relatively high pressures seem to be required at the lower CO_2 concentration range. However, it should be noted that as shown in (Figure 4.9.), the 3.3 mol% TBAC solution can form semiclathrates with CO_2 + N_2 at a significantly lowered pressure range for the temperature range of 288 - 294 K. In this study, 291.0 K was selected as a reference temperature for the pressure-composition diagram because at 291.0 K, the driving force of 2.0 MPa can be applied for all the equilibrium curves obtained.

In (Figures. 4.8. and 4.10.), when a feed gas of 20% CO_2 and 80% N_2 is introduced into the semiclathrate formation reactor, the corresponding CO_2 concentration in the semiclathrate phase will be approximately 60%. Then, the semiclathrate formed from the retrieved 60% CO_2 is expected to contain more than 90% CO_2. The experimental results indicate that only two consecutive steps of semiclathrate formation and dissociation can enrich 20% CO_2 in flue gas to approximately 90% CO_2 at 291.0 K. The enclathrated CO_2 gas can be easily recovered by either increasing the temperature or decreasing the pressure.

Changes in the gas uptake and CO_2 composition during QAS semiclathrate formation were measured to examine the gas storage capacity and the preferential partitioning of CO_2 in the semiclathrate phase for each QAS semiclathrate. For these experiments, the equilibrium cell was charged with 110 cm^3 of QAS solutions with stoichiometric concentrations of each semiclathrate, and the driving force (ΔT), which is defined as the temperature difference between the equilibrium and experimental temperatures, was set as 5.0 K at 3.0 MPa.

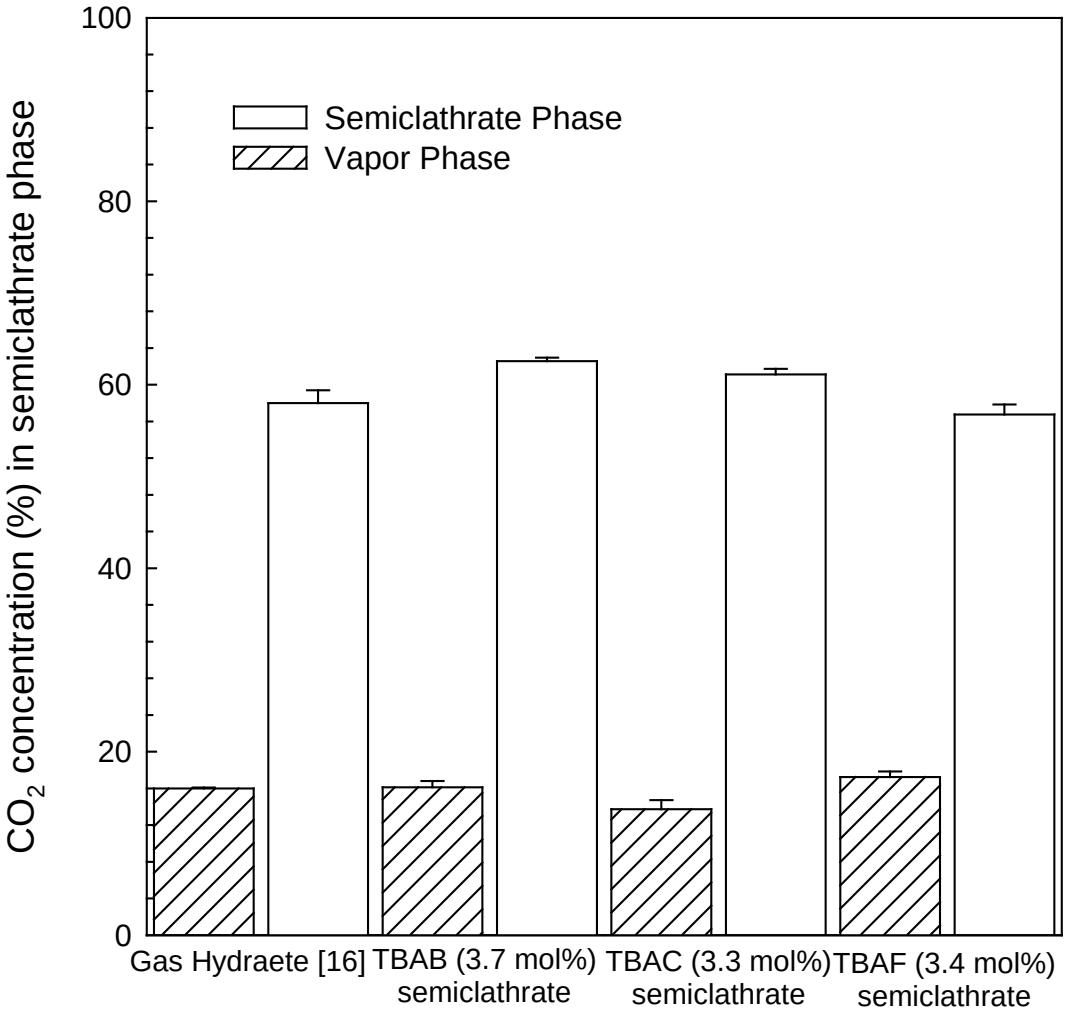

Figure 4.11. CO_2 concentrations in the vapor and semiclathrate phases at ΔT = 5.0 and 3.0 MPa (for gas hydrate at 275.15 K and ΔP = 2.0 MPa).

The final CO_2 compositions in the vapor and semiclathrate phases for the TBAB, TBAC, and TBAF semiclathrates are shown in (Figure 4.11.) and were compared with that of the gas hydrate. After the completion of each QAS semiclathrate formation with CO_2 (20%) + N_2 (80%), the final CO_2 concentration in the vapor phase was first measured, and then, the CO_2 composition of the retrieved gas from the semiclathrate phase was measured. The initial 20% CO_2 from the flue gas mixture was enriched to approximately 60% CO_2 through the semiclathrate formation. The results definitely indicate that CO_2 is selectively enclathrated in the semiclathrate phases. In the structure of the QAS semiclathrates, the large cages are partially broken and occupied by TBA cations, while the small cages are left vacant, which are available for capturing gas molecules of CO_2 + N_2 [4, 24]. Komatsu et al. [25] indicated that for a fuel gas mixture of CO_2 + H_2, CO_2 selectivity in the small cages of QAS semiclathrates could be affected by both the size of the anions in the host frameworks and by the number of distorted small cages in the QAS semiclathrates. However, for a flue gas mixture of CO_2 + N_2, CO_2 selectivity in the semiclathrate phase was not dependent on the types of QAS used, and furthermore, it was almost the same as that in the gas hydrate phase. However, it should be noted that the QAS semiclathrates can capture CO_2 at significantly higher temperature and lower pressure than gas hydrate.

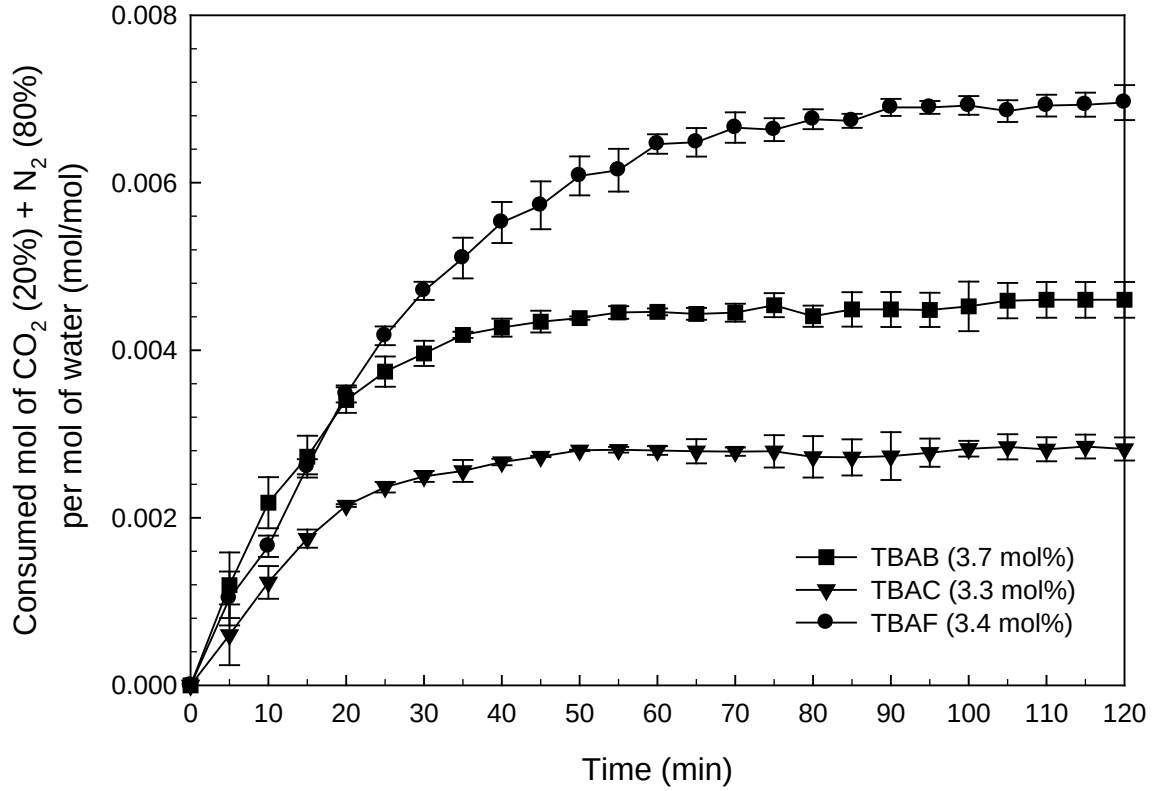

Figure 4.12. Gas uptake curves for the CO_2 (20%) + N_2 (80%) during QAS semiclathrate formation at ΔT =5.0 K and 3.0 MPa.

Table 4.5. Experimental conditions and results of gas uptake measurements for the CO_2 (20%) + N_2 (80%) + QAS + water systems.

QAS	Exp. No.	Conc. (mol%)	T/K	P/MPa	Gas uptake (mol/mol)
TBAB	1	3.7	281.6	3.00	0.00445
	2	3.7	281.6	2.99	0.00475
TBAC	3	3.3	284.8	3.01	0.00685
	4	3.3	284.7	3.04	0.00719
	5	3.3	284.7	2.99	0.00730
TBAF	6	3.4	284.7	3.04	0.00282
	7	3.4	284.7	2.99	0.00292

The gas uptake result for the CO_2 (20%) + N_2 (80%) + QAS semiclathrate formation is shown in (Figure 4.12.), and the experimental conditions and results for the gas uptake measurements are presented in (Table 4.5.). The accumulated amount of gas consumed during semiclathrate formation is expected to be equivalent to the total amount of gas captured in the vacant cages of the QAS semiclathrates. The gas uptakes for each semiclathrate were expressed as the ratio of moles of consumed gas to moles of initially charged water, and are closely related to the number of vacant cages available for capturing CO_2 and N_2 gas molecules. The experimental results clearly show that the TBAC (3.3 mol%) semiclathrate had the largest gas uptake, whereas the TBAF (3.4 mol%) semiclathrate had extremely small gas consumption during semiclathrate formation.

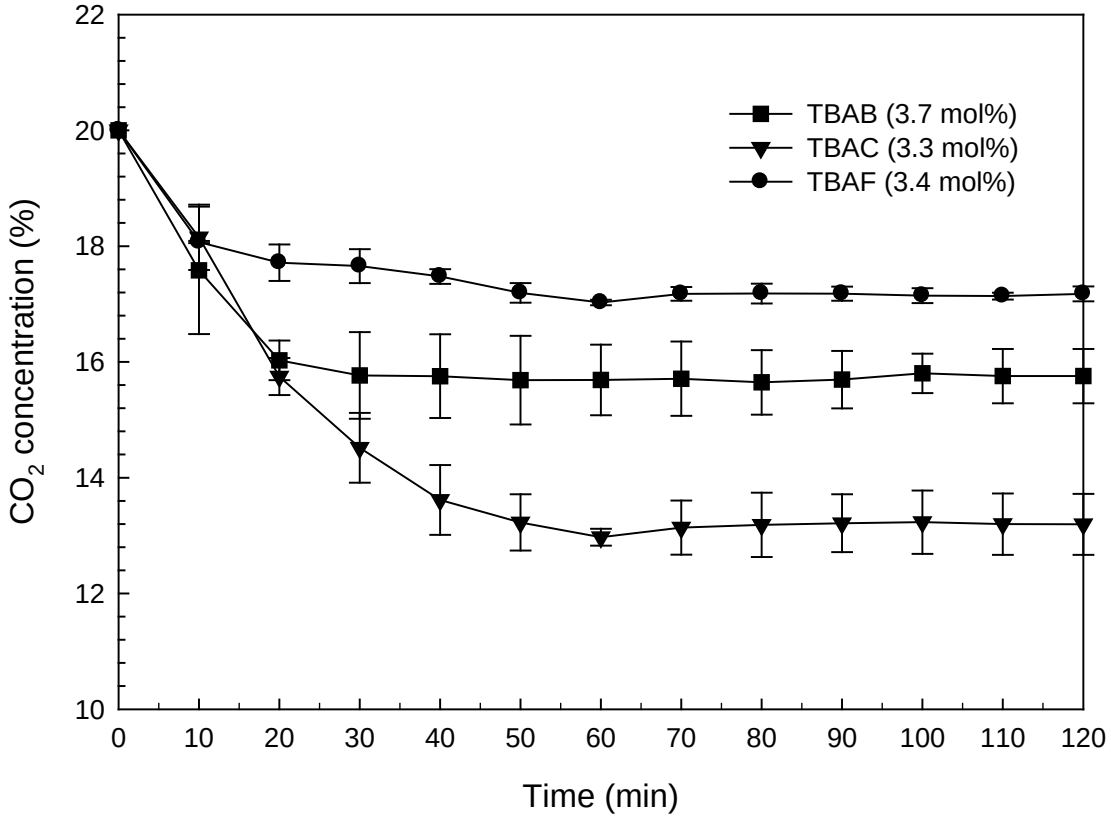

Figure 4.13. Changes in CO_2 composition in the vapor phase at ΔT =5.0 K and 3.0 MPa.

(Figure 4.13.) shows the changes in the CO_2 composition in the vapor phase during semiclathrate formation. The CO_2 concentrations in the vapor phase continued to decline during semiclathrate formation because CO_2 is more selectively captured in the semiclathrate phase than N_2. The CO_2 concentration rapidly dropped just after nucleation, gradually stabilized, and finally became almost constant after 1 h. Even though the change in CO_2 concentration in the vapor phase is a function of the gas uptake and CO_2 selectivity in the semiclathrate phase, in this study, it is strongly affected only by the gas uptake because CO_2 selectivity is almost the same for the TBAB, TBAC, and TBAF semiclathrates shown in (Figure 4.11.). Therefore, the TBAC (3.3 mol%) semiclathrate had a drastic drop in the CO_2 concentration in the vapor phase, whereas the TBAB (3.7 mol%) and TABF (3.4 mol%) semiclathrates had a slight change in the CO_2 concentration: For the TBAC (3.3 mol%) semiclathrate, the CO_2 concentration in the vapor phase was reduced from 20% to 13%, for the TBAB (3.7 mol%) semiclathrate from 20% to 16%, and for the TBAF (3.4 mol%) semiclathrate from 20% to 18%.

The gas uptakes and gas storage capacity of the guest molecules are closely related to the structure details of the QAS semiclathrates. Both TBAB (3.7 mol%) (TBAB·26.0H_2O) and TBAC (3.3 mol%) (TBAC·29.7H_2O) semiclathrates have tetragonal structure-I (TS-I), whereas TBAF (3.4 mol%) (TBAF·28.6H_2O) semiclathrate forms a cubic structure (SCS-I) [1, 5-7, 22, 24, 25]. For the TBAF (3.4 mol%) semiclathrate, 79.5% of the small cages are partially filled with water molecules [7], which indicates that the TBAF semiclathrate possesses fewer numbers of vacant small cages that are available for capturing CO_2 and N_2 gas molecules compared with the TBAB and TBAC semiclathrates. Furthermore, the TBAB (3.7 mol%) semiclathrate has a higher extent of filing of the small cages with TBA cations than that of the TBAC (3.3 mol%) semiclathrate [6, 24, 25], which results in a lower gas storage capacity for the TBAB (3.7 mol%) semiclathrate compared to the TBAC (3.3 mol%) semiclathrate. For these reasons, the TBAC (3.3 mol%) semiclathrate has a larger number of small cages that can be effectively used for capturing CO_2 and N_2 molecules, and therefore, demonstrates a larger gas uptake and steeper changes in the CO_2 concentration than the TBAB and TBAF semiclathrates as shown in (Figures 4.12 and 4.13.).

4.2.3. Raman spectroscopic analysis

(Figure 4.14.) shows the Raman spectra of CO_2 (20%) + N_2 (80%) hydrate, TBAC (3.3 mol%) semiclathrate, CO_2 (20%) + N_2 (80%) + TBAC (3.3 mol%) semiclathrate, TBAC (1.0 mol%) semiclathrate, and CO_2 (20%) + N_2 (80%) + TBAC (1.0 mol%) semiclathrate. The CO_2 (20 %) + N_2 (80%) gas hydrate is known to form sI hydrate [16] and exhibits two peaks for enclathrated CO_2 molecules at 1276 and 1380 cm^{-1} and one peak for enclathrated N_2 molecules at 2324 cm^{-1} [16-19]. CO_2 molecules captured in TBAC semiclathrate lattices were observed at 1273 cm^{-1} and 1380 cm^{-1} and N_2 molecules at 2324 cm^{-1}. A wavenumber shift (1276 cm^{-1} → 1273 cm^{-1}) for CO_2 molecules can be attributed to a slight difference in the size and environment of small 5^{12} cages, where CO_2 molecules are expected to be captured, in both sI gas hydrate and TBAC semiclathrates, even though the small 5^{12} cages are common for both cases. N_2 gas molecules enclathrated in both gas hydrate and semiclathrates, exhibit only one peak at 2324 cm^{-1} because N_2 molecules are so small that the symmetric N-N vibration of N_2 molecules captured in small and large cages of gas hydrates are not distinguishable [19]. Even though Raman spectroscopy cannot provide detailed information on CO_2 distribution in the cages of gas hydrates or semiclathrates due to the impossibility of peak splittings for CO_2 molecules enclathrated in different cages [20, 21], (Figure 4.14.) clearly demonstrates that both CO_2 and N_2 molecules are captured in the lattices of TBAC semiclathrates and that there is no structural transition due to the enclathration of guest gases in the lattices of TBAC semiclathrates.

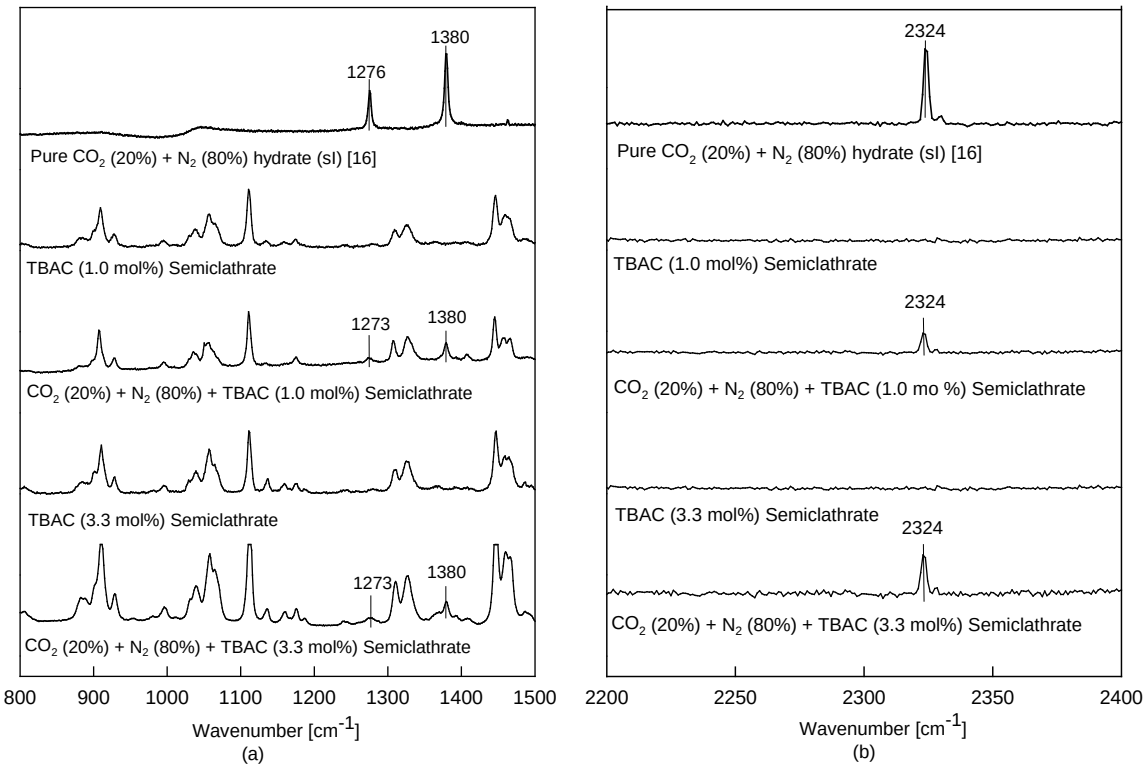

Figure 4.14. Raman spectra of CO_2 (20%) + N_2 (80%) hydrate, TBAC (1.0 mol%) semiclathrate, CO_2 (20%) + N_2 (80%) + TBAC (1.0 mol%) semiclathrate, TBAC (3.3 mol%) semiclathrate, and CO_2 (20%) + N_2 (80%) + TBAC (3.3 mol%) semiclathrate.

To the best of our knowledge, this is the first research into TBAC semiclathrate-based post-combustion CO_2 capture targeting the flue gas mixture of CO_2 (20%) + N_2 (80%) from fossil fuel-fired power plants. The TBAC semiclathrate-based process has many technological advantages over the gas hydrate-based process, mainly because TBAC, with almost no volatility or toxicity, forms semiclathrates with water at significantly stabilized pressure and temperature conditions. Based on the experimental results obtained in this study, it can be reasonably expected that the TBAC semiclathrates have potential for actual application in CO_2 capture from flue gas mixture due to their high selectivity for CO_2 and enhanced thermodynamic stability.

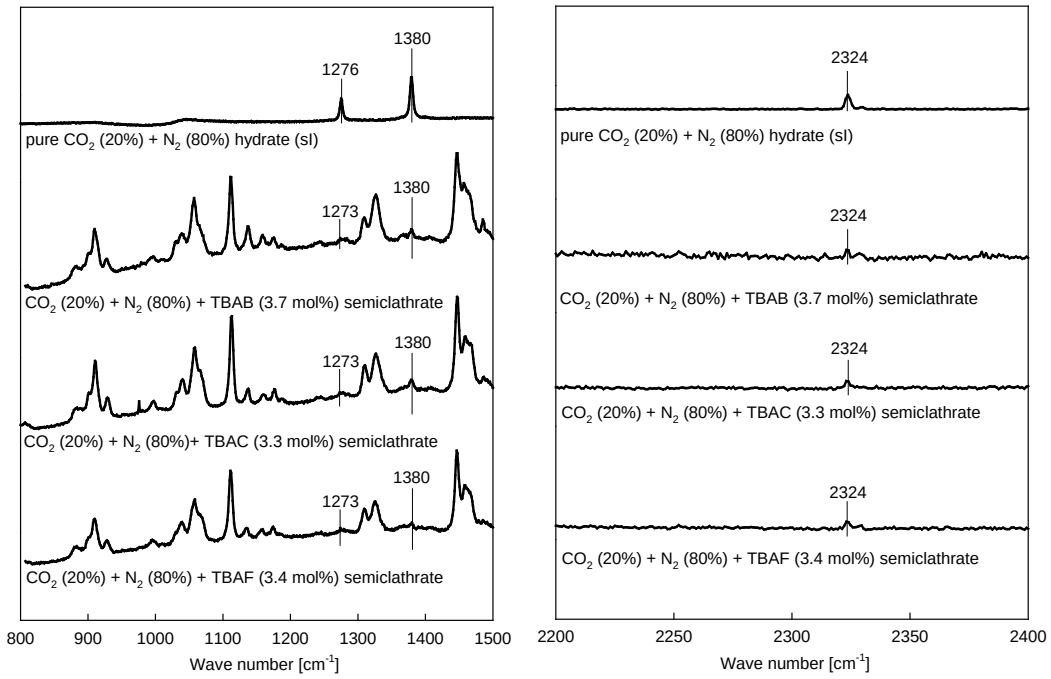

Figure 4.15. Raman spectra of the CO_2 + N_2 hydrate, CO_2 + N_2 + TBAB semiclathrate, CO_2 + N_2 + TBAC semiclathrate, and CO_2 + N_2 + TBAF semiclathrate. The Raman peak located next to 2324 cm^{-1} originated from the N_2 vapor used for cooling.

(Figure 4.15.) shows the Raman spectra of the CO_2 (20%) + N_2 (80%) hydrate, CO_2 (20%) + N_2 (80%) + TBAB (3.7 mol%) semiclathrate, CO_2 (20%) + N_2 (80%) + TBAC (3.3 mol%) semiclathrate, and CO_2 (20%) + N_2 (80%) + TBAF (3.4 mol%) semiclathrate. The CO_2 (20%) + N_2 (80%) gas hydrate, known to form sI hydrate, shows three Raman peaks. Two peaks for the CO_2 molecules were observed at 1276 cm^{-1} and 1380 cm^{-1}, and one peak for the N_2 molecules was observed at 2324 cm^{-1}. However, the Raman spectra of the CO_2 + N_2 + QAS semiclathrates exhibited two Raman peaks for CO_2 molecules at 1273 cm^{-1} and 1380 cm^{-1} and one Raman peak for the N_2 molecules at 2324 cm^{-1}, whereas they had many Raman peaks for the TBA cations enclathrated in the semiclathrate lattices. Even though both CO_2 and N_2 molecules can be enclathrated in both the small 5^{12} cages and large $5^{12}6^2$ cages of sI hydrate, the Raman spectra of the CO_2 + N_2 hydrate cannot offer detailed information about cage occupancy and guest distribution in the hydrate lattices. The Raman spectrum of the CO_2 molecules enclathrated in the sI hydrate provides no peak splittings and accordingly, no one-to-one correspondence between the cages and Raman peaks. Furthermore, N_2 molecules captured in

both small and large cages of the sI hydrate have only one Raman peak at 2324 cm^{-1} because N_2 molecules are so small that the symmetric N-N vibration of the N_2 molecules are not distinguishable in different cages of gas hydrates. However, a wavenumber shift (1276 cm^{-1} to 1273 cm^{-1}) for the enclathrated CO_2 molecules was observed, and this can be attributed to a slight difference in the size and environment of the small 5^{12} cages, which are common for both sI gas hydrate and QAS semiclathrates.

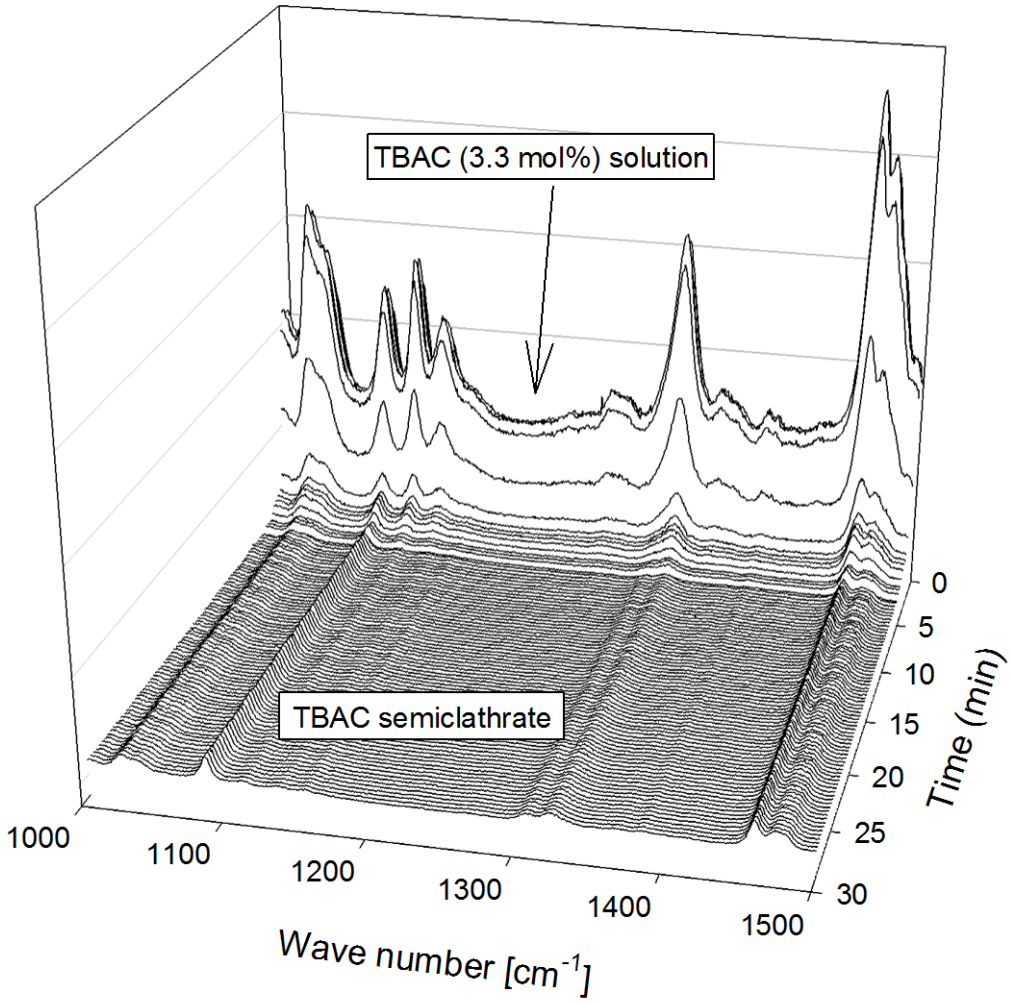

Figure 4.16. Time-dependent *in-situ* Raman spectra during the conversion of TBAC solution to pure TBAC semiclathrate under atmospheric pressure condition.

(Figure 4.16.) shows the time-dependent *in-situ* Raman spectra during the conversion of TBAC solution to pure TBAC semiclathrate under atmospheric pressure condition. The Raman peak intensity of the TBAC solution was abruptly decreased as the pure TBAC semiclathrate formation proceeded. The change in the Raman peak intensity can be used to detect TABC semiclathrate formation. (Figure 4.17.) shows the time-dependent *in-situ* Raman spectra during the conversion of

TBAC solution to the CO_2 (20%) + N_2 (80%) + TBAC (3.3 mol%) semiclathrate at 3.0 MPa and ΔT of 5.0 K. The Raman peak intensity was abruptly decreased with the formation of the TBAC semi-clathrate and then, continuously increased with the enclathration of CO_2 and N_2 into the cages of the TBAC semiclathrate. CO_2 molecules captured in the small cages of the TBAC semiclathrate were also observed at 1273 cm^{-1} and 1380 cm^{-1}, and N_2 molecules were observed at 2324 cm^{-1}, which is in good agreement with the micro-Raman results shown in (Figure 4.15.).

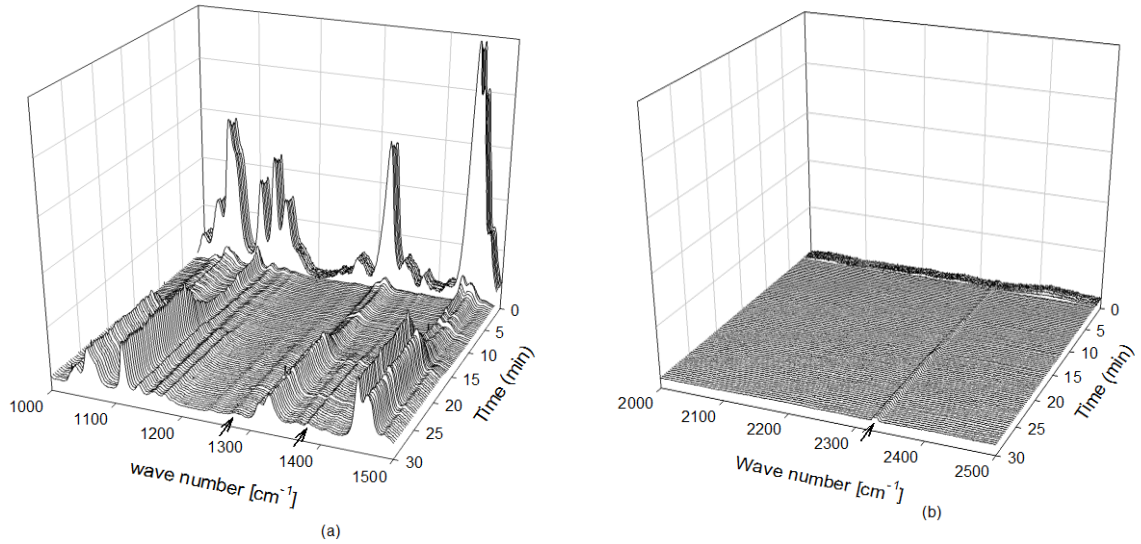

Figure 4.17. Time-dependent *in-situ* Raman spectra during the conversion of TBAC solution to CO_2 (20%) + N_2 (80%) + TBAC semiclathrate at 3.0 MPa and ΔT = 5.0 K.

(Figure 4.18.) shows the Raman spectra of the TBAC (3.3 mol%) solution, TBAC (3.3 mol%) semiclathrate, and CO_2 (20%) + N_2 (80%) + TBAC semiclathrate, which were measured with an *in-situ* Raman spectrometer. The Raman spectra of the TBAC semiclathrate and CO_2 + N_2 + TBAC semiclathrate were obtained after the completion of semiclathrate formation in the experiments shown in (Figures. 4.15 and 4.16.). The Raman spectrum of the TBAC solution was clearly distinguishable from those of both the TBAC semiclathrate and CO_2 + N_2 + TBAC semiclathrate due to its different peak patterns and peak positions. However, the Raman spectrum of the CO_2 + N_2 + TBAC semiclathrate is exactly the same as that of the TBAC semiclathrate except for the peaks that correspond to the enclathrated CO_2 and N_2 molecules, which indicates that the inclusion of CO_2 and N_2 molecules in the TBAC semiclathrate does not change the structure of the semiclathrate. Even though Raman spectroscopy cannot provide accurate information about the cage occupancy of gas molecules and guest distributions in the semiclathrate cages, (Figures. 4.15. and 4.17.) clearly demonstrate that CO_2 and N_2 gas molecules are captured in the small cages of TBAC semiclathrate without any structural transitions.

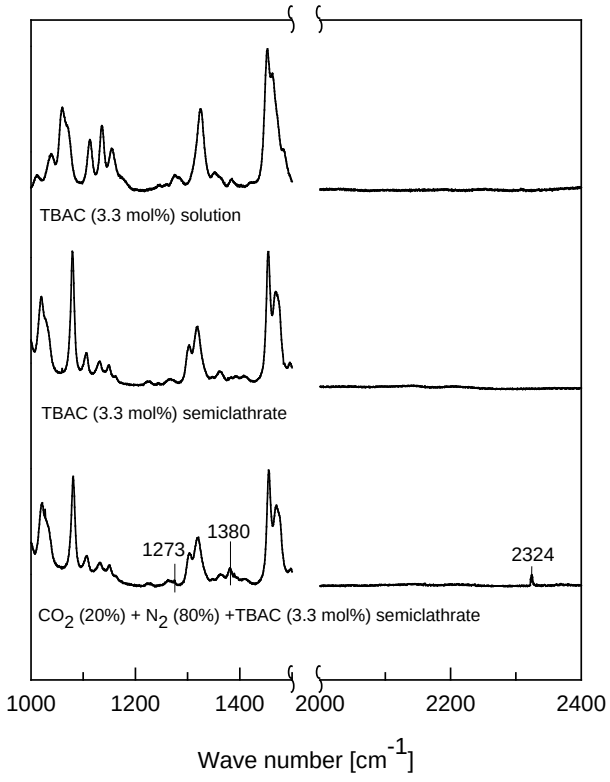

Figure 4.18. Raman spectra of the TBAC (3.3 mol%) solution, TBAC (3.3 mol%) semiclathrate, and CO_2 (20%) + N_2 (80%) + TBAC (3.3 mol%) semiclathrate using an *in-situ* Raman spectrometer.

This study is the first to use thermodynamic and Raman spectroscopic analyses to investigate and compare the thermodynamic stability, gas uptakes, and CO_2 capture performance of QAS semiclathrates formed from TBAB, TBAC, and TBAF targeting post-combustion CO_2 capture from flue gas. QAS semiclathrate-based CO_2 capture has many advantages over the gas hydrate-based process because QASs are non-volatile and non-toxic, and they can form semiclathrates at a significantly lower pressure and higher temperature conditions. Among the three QAS semiclathrates considered in this study, the TBAC semiclathrate is more thermodynamically stable than the TBAB semiclathrate and can store the largest amount of gas molecules in the small cages, even though the three QAS semiclathrates have almost the same CO_2 selectivity in the semiclathrate phase. Therefore, it can be reasonably expected that the TBAC semiclathrate is a good candidate material for post-combustion CO_2 capture from flue gas.

4.3. Conclusions

The TBAC semiclathrate formation was investigated for its application in post-combustion CO_2 capture from the flue gas mixture, primarily focusing on thermodynamic stability, gas uptake, and guest distributions. The CO_2 (20%) + N_2 (80%) + TBAC semiclathrate systems showed significant thermodynamic stabilization when compared with the CO_2 (20%) + N_2 (80%) gas hydrate system. The gas uptake and CO_2 composition change in the vapor phase were closely related to the conversion of TBAC solution to semiclathrate. A higher gas uptake and lower CO_2 concentration in the vapor phase during the semiclathrate formation reaction were observed for the 3.3 mol% TBAC solution, which corresponds to TBAC·29.7H_2O semiclathrate. The CO_2 concentration in the semiclathrate phase after completion of semiclathrate formation was found to be approximately 60% for both 1.0 and 3.3 mol% TBAC solutions. The pressure-composition diagram demonstrated that when a flue gas mixture with 20% CO_2 is introduced, with two consecutive steps of TBAC semiclathrate formation dissociation, more than 90% CO_2 can be enriched in the semiclathrate phase at 291.0 K. It was confirmed from the Raman spectra that both CO_2 and N_2 molecules are enclathrated in the cages of TBAC semiclathrates.

QAS semiclathrates formed from TBAB, TBAC, and TBAF solutions were investigated for their application to post-combustion CO_2 capture, primarily focusing on the thermodynamic stability, gas uptakes, and CO_2 selectivity. The CO_2 (20%) + N_2 (80%) + QAS semiclathrate systems showed significantly stabilized equilibrium conditions when compared with the CO_2 (20%) + N_2 (80%) gas hydrate system. Even though the TBAF (3.4 mol%) semiclathrate had the most significant thermodynamic stability among the QASs used in this study, the TBAC (3.3 mol%) semiclathrate had the highest gas uptake and the steepest changes in CO_2 concentration in the vapor phase. However, CO_2 selectivity in the semiclathrate phase was not dependent on the type of QASs. For all the cases, the CO_2 concentration in the semiclathrate phase after the completion of semiclathrate formation was found to be approximately 60% at 3.0 MPa and ΔT of 5.0 K. It was confirmed from the Raman spectra that both CO_2 and N_2 molecules are enclathrated in the cages of the TBAC semiclathrates and that guest gas enclathration does not affect the semiclathrate structure. The experimental results obtained in this study provide fundamental information required to design and develop a QAS semiclathrate-based CO_2 capture process from post-combustion flue gas.

4.4. References

[1] Spigarelli BP, Kawatra SK. Opportunities and challenges in carbon dioxide capture. J CO2 Util 2013;1:69-87.

[2] Eslamimanesh A, Mohammadi AH, Richon D, Naidoo P, Ramjugernath D. Application of gas hydrate formation in separation precesses: A review of experimental studies. J Chem Thermodyn 2012;46:62-72.

[3] Dashti H, Zhehao Yew L, Lou X. Recent advances in gas hydrate-based CO_2 capture. J Nat Gas Sci Eng 2015;23:195-207.

[4] Kim S, Baek I-H, You J-K, Seo Y. Guest gas enclathration in tetra-n-butyl ammonium chloride (TBAC) semiclathrates: Potential application to natural gas storage and CO_2 capture. Appl Energy 2015;140:107-12.

[5] Aladko L, Dyadin YA, Rodionova T, Terekhova I. Clathrate hydrates of tetrabutylammonium and tetraisoamylammonium halides. J Struct Chem 2002;43:990-4.

[6] Lipkowski J, Komarov VY, Rodionova TV, Dyadin YA, Aladko LS. The Structure of Tetrabutylammonium Bromide Hydrate $(C_4H_9)_4NBr^{\cdot 2}1/3\ H_2O$. J Supramolecular Chemistry 2002;2:435-9.

[7] Komarov VY, Rodionova T, Terekhova I, Kuratieva N. The cubic superstructure-I of tetrabutylammonium fluoride $(C_4H_9)_4F^{\cdot 2}9.7H_2O$ clathrate hydrate. J Inclusion Phenom Macrocyclic Chem 2007;59:11-5.

[8] Fowler D, Loebenstein W, Pall D, Kraus CA. Some unusual hydrates of quaternary ammonium salts. J Am Chem Soc 1940;62:1140-2.

[9] Shimada W, Ebinuma T, Oyama H, Kamata Y, Takeya S, Uchida T, et al. Separation of gas molecule using tetra-n-butyl ammonium bromide semi-clathrate hydrate crystals. Jpn J Appl Phys 2003;42:L129.

[10] Deschamps J, Dalmazzone D. Dissociation enthalpies and phase equilibrium for TBAB semi-clathrate hydrates of N_2, CO_2, $N_2 + CO_2$ and $CH_4 + CO_2$. J Therm Anal Calorim 2009;98:113-8.

[11] Gholinezhad J, Chapoy A, Tohidi B. Separation and capture of carbon dioxide from CO_2/H_2 syngas mixture using semi-clathrate hydrates. Chem Eng Res Des 2011;89:1747–51.

[12] Li X-S, Xu C-G, Chen Z-Y, Cai J. Synergic effect of cyclopentane and tetra-nbutyl ammonium bromide on hydrate-based carbon dioxide separation from fuel gas mixture by measurements of gas uptake and X-ray diffraction patterns. Int J Hydrogen Energy 2012;37:720–7.

[13] Park S, Lee S, Lee Y, Lee Y, Seo Y. Hydrate-based pre-combustion capture of carbon dioxide in the presence of a thermodynamic promoter and porous silica gels. Int J Greenhouse Gas Control 2013;14:193–9.

[14] Komatsu H, Ota M, Sato Y, Watanabe M, Smith RL. Hydrogen and carbon dioxide adsorption with tetra-n-butyl ammonium semi-clathrate hydrates for gas separations. AIChE J 2014.

[15] Park S, Lee S, Lee Y, Seo Y. CO_2 capture from simulated fuel gas mixtures using semiclathrate hydrates formed by quaternary ammonium salts. Environ Sci Technol 2013;47:7571–7.

[16] Lee Y, Lee S, Lee J, Seo Y. Structure identification and dissociation enthalpy measurements of the CO_2 + N_2 hydrates for their application to CO_2 capture and storage. Chem Eng J 2014;246:20-6.

[17] Liu CL, Lu HL, Ye YG. Raman spectroscopy of nitrogen clathrate hydrates. Chin. J. Chem. Phys 2009;22:353-8.

[18] Cha I, Lee S, Lee JD, Lee GW, Seo Y. Separation of SF_6 from gas mixtures using gas hydrate formation. Environ. Sci. Technol 2010;44:6117-22.

[19] Sugahara K, Tanaka Y, Sugahara T, Ohgaki K. Thermodynamic stability and structure of nitrogen hydrate crystal. J. Supramolecular Chemistry 2002;2:365-8.

[20] Kumar R, Englezos P, Moudrakovski I, Ripmeester JA. Structure and composition of CO_2/H_2 and $CO_2/H_2/C_3H_8$ hydrate in relation to simultaneous CO_2 capture and H_2 production. AIChE J 2009;55:1584-94.

[21] Lee S, Park S, Lee Y, Lee J, Lee H, Seo Y. Guest gas enclathration in semiclathrates of tetra-n-butylammonium bromide: stability condition and spectroscopic analysis. Langmuir 2011;27:10597-603.

[22] Rodionova T, Komarov V, Villevald G, Aladko L, Karpova T, Manakov A. Calorimetric and structural studies of tetrabutylammonium chloride ionic clathrate hydrates. J Phys Chem B2010;114:11838-46.

[23] Sun Z-G, Liu C-G, Zhou B, Xu L-Z. Phase equilibrium and latent heat of tetra-n-butylammonium chloride semi-clathrate hydrate. J Chem Eng Data 2011;56:3416-8.

[24] Sfaxi IBA, Durand I, Lugo R, Mohammadi AH, Richon D. Hydrate phase equilibria of CO_2 + N_2 + aqueous solution of THF, TBAB or TBAF system. Int J Greenhouse Gas Control 2014;26:185-92.

[25] Komatsu H, Ota M, Sato Y, Watanabe M, Smith RL. Hydrogen and carbon dioxide adsorption with tetra-n-butyl ammonium semi-clathrate hydrates for gas separations. AIChE J 2014.

Chapter V

Post-combustion CO_2 capture using THF, CP, and TBAC clathrates formation

5.1. Introduction

Carbon dioxide (CO_2) is suspected as a major source of global warming. Much effort has been conducted to cut CO_2 emissions from the combustion of fossil fuels in power stations [1, 2]. One possible way to lowering the CO_2 emissions in power plants is post-combustion CO_2 capture before the exhausted flue gas is released to the atmosphere. These clathrate-based CO_2 capture technologies are easier than others because this can be done without other facilities for mitigating global warming gas release. A novel effort to clathrate-based gas separation technology is interested as an alternative to the existing post-combustion gas separation technologies [3-15].

Gas hydrates are inclusion compounds formed by hydrogen bonding of water molecules at high pressure and low temperature conditions [16]. The host water molecules form frameworks of gas hydrates while the small guest molecules are trapped in empty cages. The suggested clathrate-based CO_2 capture process consists of two process units of flue gas capture and release [17]. When CO_2 from flue gas is selectively captured in the clathrate phase, the clathrate slurry is transferred to the dissociation unit. Then, the clathrate is dissociated by either heating or pressure release. Released heat during clathrate formation can be recovered and reused in the dissociation unit. The dissociated solution can be recycled to the gas capture unit. This indicates that the clathrate-based CO_2 capture is eco-friendly through solution recycle and heat recovery between the clathrate formation and dissociation units [18].

However, this technology has the limitation of requiring high pressure and low temperatures for hydrate formation. To improve this disadvantage gas hydrate formation needs to be performed at a much milder pressure and temperature conditions. It has been found that the addition of sII hydrate and semiclathrate former may lower the pressure required [3-15, 19-21]. These former stabilize a clathrate structure at low pressure or high temperature conditions, although the gas storage capacity when compares the gas hydrate is lower by adding these promoters, since the clathrate former occupied in the lattice cavities. In addition, the clathrate former are operated in the liquid phase, it means that the final gas product does not pollute since it will remain with the liquid phase when the clathrate are dissociated.

In this study, clathrate-based CO_2 capture from post-combustion flue gas was investigated in

the presence of THF, TBAC, and CP. The thermodynamic stability of the CO_2 (20%) + N_2 (80%) + clathrate was examined with an isochoric method using a high pressure reactor. The gas uptake and CO_2 concentration changes in the vapor phase during clathrate formation were measured to analyze the preferential gas occupation in the clathrate phase. CO_2 concentrations in the vapor and clathrate phases after the completion of clathrate formation were measured to provide the CO_2 selectivity based on the types of hydrate former used. The enclathration of guest molecules in the clathrate lattices was confirmed with a micro-Raman spectrometer.

5.2. Results and discussion

5.2.1. Stability conditions of clathrates

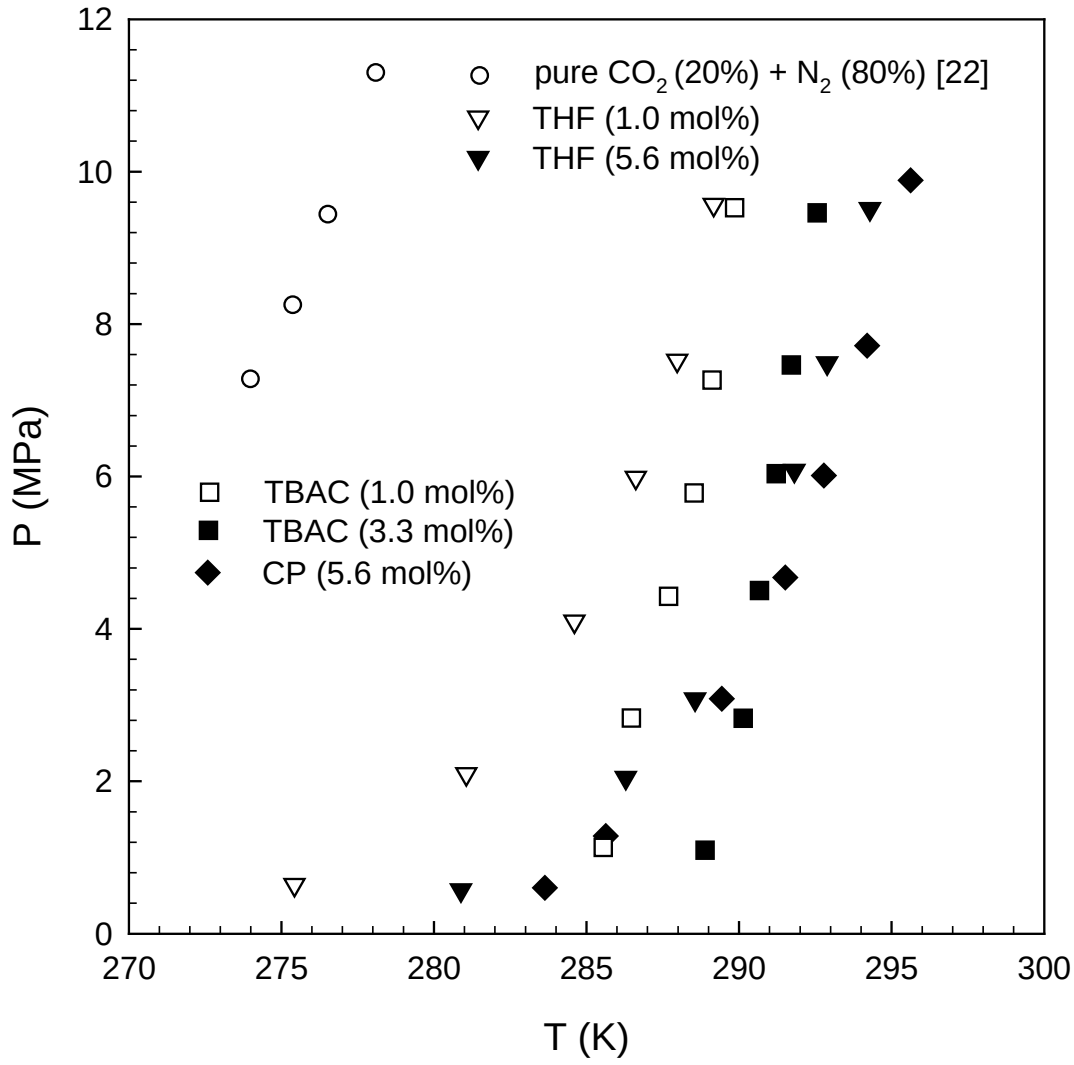

Figure 5.1. Clathrate phase equilibria of the CO_2 (20%) + N_2 (80%) + THF, TBAC, and CP + water systems.

(Figure 5.1.) presents three-phase (clathrate (H) - liquid water (L_w) - vapor (V)) equilibria for the CO_2 (20%) + N_2 (80%) + THF (1.0 and 5.6 mol%), TBAC (1.0 and 3.3 mol%), and CP (5.6 mol%) + water systems, and the overall experimental data are summarized in (Table 5.1.). In case of CP hy-

drate, there are three components and four phases of hydrate formation; components (gas, water, and cyclopentane) and phase (vapor, water, liquid hydrocarbon, and hydrate). According to the degree of freedom, only one intensive variable is needed to define the CP hydrate system. Therefore, the phase equilibrium does not depend on the composition of the CP concentration at a given temperature on that system. In this study, the phase equilibria for the CP hydrate are conducted at only 5.6 mol% conditions. Clathrate of THF, TBAC, and CP are most stable at 5.6, 3.3, and 5.6 mol% solutions, which correspond to stoichiometrics concentrations of THF·16.0H_2O, TBAC·29.7H_2O, and CP·16.0H_2O, respectively. The phase equilibrium results indicate that clathrate formed from clathrate formers can offer a significant thermodynamic promotion which represents a pressure reduction at any given temperature or a temperature increase at any given pressure when compared with gas hydrates. In particular, as seen in (Figure 5.1.), TBAC (3.3 mol%) semiclathrate has a higher thermodynamic stability than that of the THF and CP hydrates below 4.5 MPa, and it is stable at temperatures higher than 288.0 K for all experimental pressure regions from 1.0 to 9.5 MPa. However, gas hydrate with CO_2 (20%) + N_2 (80%) requires equilibrium pressures as high as 7.0 MPa even at 273.0 K. Since gas hydrate formation requires high pressure and low temperature, clathrate-based CO_2 capture from a flue gas is difficult to apply in the actual process. However, in the presence of clathrate former, the gas hydrate equilibrium pressure can significantly decrease at a given temperature.

Table 5.1. Three phase equilibrium data with CO_2 (20%) + N_2 (80%) gas mixture.

THF (1.0 mol%)		THF (5.6 mol%)		TBAC (1.0 mol%)		TBAC (3.3 mol%)		CP (5.6 mol%)	
T/K	P/MPa	T/K	P/MPa	T/K	P/MPa	T/K	P/MPa	T/K	P/MPa
275.4	0.64	280.9	0.57	285.5	1.13	288.9	1.10	283.6	0.60
281.1	2.10	286.3	2.05	286.5	2.83	290.1	2.83	285.6	1.28
284.6	4.10	288.6	3.08	287.7	4.43	290.7	4.50	289.4	3.08
286.6	5.99	291.8	6.08	288.5	5.78	291.2	6.04	291.5	4.67
288.0	7.52	292.9	7.49	289.1	7.27	291.7	7.46	292.8	6.01
289.2	9.57	294.3	9.51	289.9	9.53	292.6	9.46	294.2	7.72
								295.6	9.89

5.2.2. Gas uptake and composition measurements of clathrates

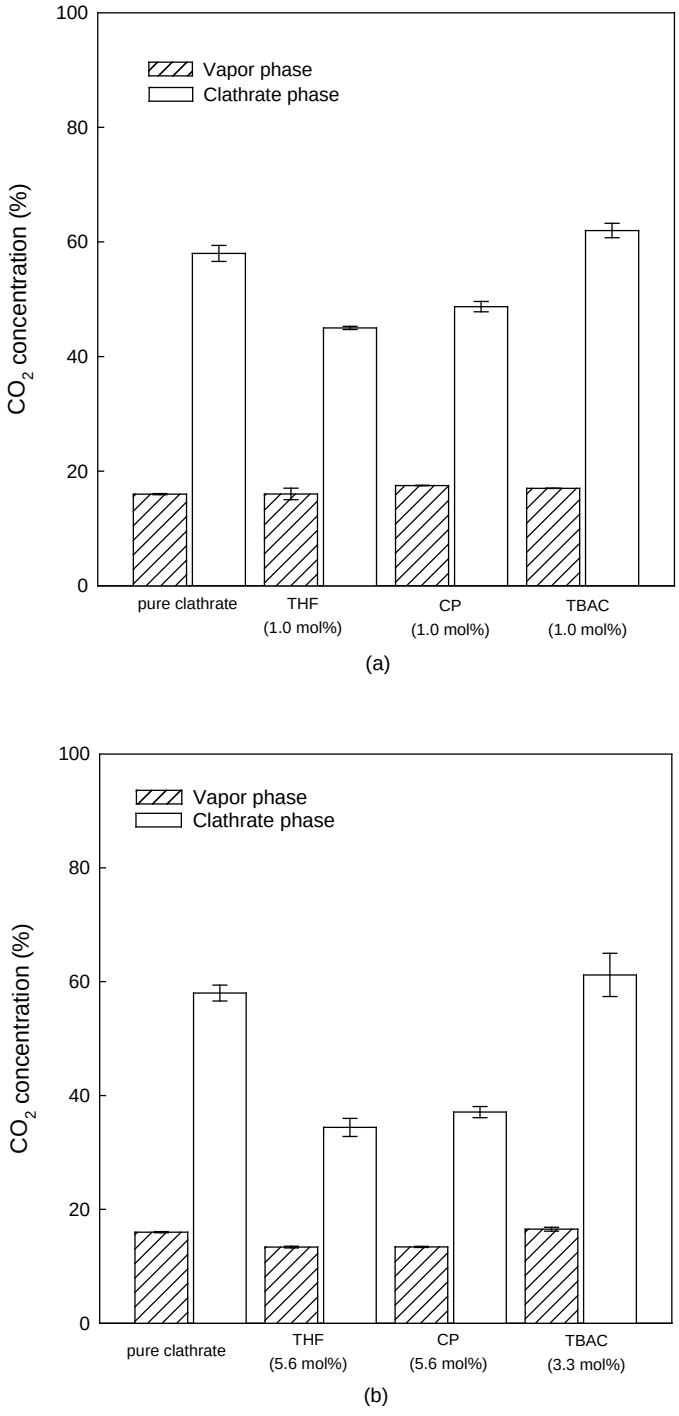

Figure 5.2. CO_2 concentrations in the vapor and clathrate phases at ΔT = 5.0 and 3.1 MPa (for the pure clathrate at 275.15 K and ΔP = 2.0 MPa) (a) for the 1.0 mol% solutions (b) for the solutions with stoichiometric concentrations of each clathrate structure.

Table 5.2. CO_2 concentration data in the vapor and clathrate phases at ΔT = 5.0 and 3.1 MPa.

		CO_2 concentration	
	Concentration (mol %)	Vapor Phase	Clathrate Phase
THF	1.0	16.0 ± 1.00	45.0 ± 0.29
TBAC	1.0	17.0 ± 0.03	62.0 ± 1.25
CP	1.0	17.5 ± 0.03	59.2 ± 2.25
THF	5.6	13.4 ± 0.15	37.1 ± 1.58
TBAC	3.3	16.5 ± 0.34	61.2 ± 3.80
CP	5.6	13.4 ± 0.11	34.4 ± 0.98

The gas uptake in clathrates and the CO_2 composition changes during clathrate formation were measured to examine the gas storage capacity and CO_2 selectivity in the clathrate phase. The final CO_2 compositions in the vapor and clathrate phases for the CO_2 (20%) + N_2 (80%) clathrates with thermodynamic promoters were compared at ΔT = 5.0 and 3.1 MPa, and the result is depicted in (Figure 5.2.). After the completion of each clathrate formation with CO_2 (20%) + N_2 (80%), the final CO_2 concentration in the vapor phase was first measured, followed by the CO_2 composition of the retrieved gas from the clathrate phase when clathrate formation with CO_2 (20%) + N_2 (80%) was complete. For the 1.0 mol% solutions, the initial 20% CO_2 from the simulated flue gas mixture was enriched to 45 ± 0.3% CO_2 in the THF (1.0 mol%) clathrate phase, 49 ± 0.9% CO_2 in the CP (1.0 mol%) clathrate phase, and 62 ± 1.3% CO_2 in the TBAC (1.0 mol%) semiclathrate phase. For the solutions with stoichiometric concentrations of each structure, the initial 20% CO_2 from the simulated flue gas mixture was enriched to 34 ± 1.6% CO_2 in the THF (5.6 mol%) clathrate phase, 37 ± 1.0% CO_2 in the CP (5.6 mol%) clathrate phase, and 61 ± 3.8% CO_2 in the TBAC (3.3 mol%) semiclathrate phase.

As shown in (Figure 5.2.), both the THF and CP solutions exhibited higher CO_2 concentrations in the clathrate phase at 1.0 mol% than at 5.6 mol%. For the 5.6 mol% THF or CP solutions, the THF or CP molecules occupy the large $5^{12}6^4$ cages of the sII clathrates, whereas the CO_2 and N_2 molecules occupy the vacant small 5^{12} cages. However, for the 1.0 mol% THF or CP solutions, some portion of the large $5^{12}6^4$ cages of sII clathrates remain vacant. Thus, the large cages are also available for capturing CO_2 molecules, which have a strong preference for the large $5^{12}6^4$ cages over the small 5^{12} cages, resulting in a relatively higher CO_2 selectivity compared to the 5.6 mol% THF or CP solutions [32, 33, 48-50]. The TBAC solutions demonstrated the highest CO_2 selectivity in the clathrate phase for both the 1.0 mol% and the stoichiometric (3.3 mol%) concentrations. Additionally, the CO_2 selec-

tivity was not significantly affected by the TBAC concentration, as reported in a previous paper [46]. The CO_2 selectivity in the TBAC semiclathrate phase was comparable to that in the pure clathrate. At the stoichiometric concentration of each clathrate structure in the presence of thermodynamic promoters, only small 5^{12} cages are vacant and thus, available for capturing CO_2 molecules. THF and CP clathrates have only regular 5^{12} cages whereas TBAC semiclathrate has regular 5^{12} cages as well as distorted 5^{12} cages, which have higher cage occupancy of CO_2 molecules [51, 52]. Therefore, TBAC semiclathrate showed relatively higher CO_2 selectivity than THF and CP clathrates.

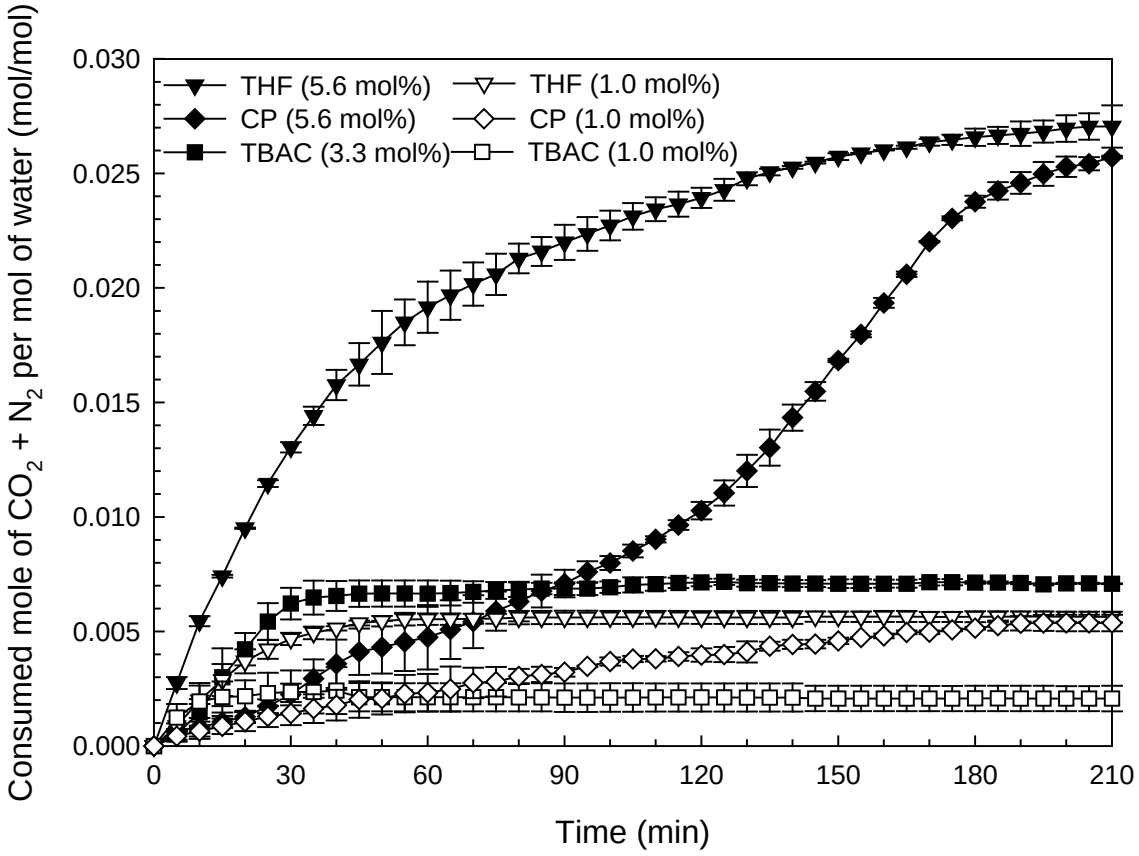

Figure 5.3. Gas uptake curves for the CO_2 (20%) + N_2 (80%) during clathrate formation at ΔT =5.0 K and 3.0 MPa.

Table 5.3. Experimental conditions and results of gas uptake measurements for the CO_2 (20%) + N_2 (80%) + THF, TBAC, and CP + water systems.

Addictive	Exp. No.	Conc. (mol%)	T/K	P/MPa	Gas uptake (mol/mol)
THF	1	1.0	278.7	3.05	0.00579
	2	1.0	278.6	3.05	0.00548
	3	5.6	283.2	3.05	0.02770
	4	5.6	283.1	3.03	0.03117
TBAC	5	1.0	281.4	3.05	0.00168
	6	1.0	281.7	3.03	0.00247
	7	3.3	284.8	3.01	0.00790
	8	3.3	284.7	3.04	0.00629
CP	9	1.0	284.4	3.03	0.00562
	10	1.0	284.5	3.03	0.00512
	11	5.6	284.8	3.01	0.02575
	12	5.6	284.5	3.04	0.02567

The gas uptake result of the CO_2 (20%) + N_2 (80%) + THF, TBAC, and CP clathrate formation is shown in (Figure 5.3.), and the experimental conditions and results of the gas uptake measurements are presented in (Table 5.3.). The accumulated amount of gas consumed during clathrate formation is expected to be equivalent to the total amount of gas captured in the vacant cages of the clathrate. The gas uptakes for each clathrate were expressed as the ratio of moles of consumed gas to moles of initially charged water, and are closely related to the number of vacant cages available for capturing CO_2 and N_2 gas molecules. The experimental results clearly show that the THF (5.6 mol%) and CP (5.6 mol%) hydrate had the largest gas uptake, whereas the TBAC (3.3 mol%) semiclathrate had small gas consumption during clathrate formation.

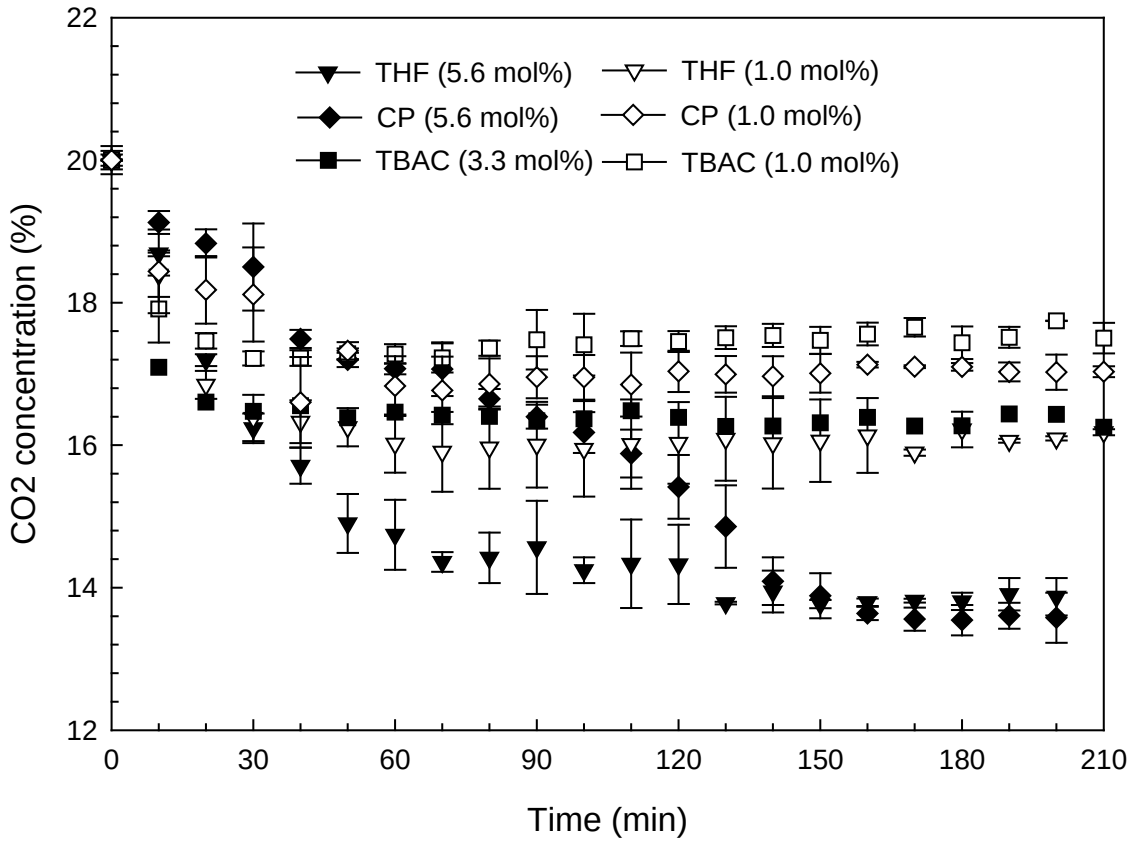

Figure 5.4. Changes in CO_2 composition in the vapor phase at ΔT =5.0 K and 3.1 MPa.

(Figure 5.4.) shows the changes in the CO_2 composition in the vapor phase during clathrate formation. The CO_2 concentrations in the vapor phase continued to decline during clathrate formation, because CO_2 is more selective captured in the clathrate phase than N_2. The CO_2 concentration rapidly dropped just after nucleation, gradually stabilized, and finally became almost constant after 1h, excepting CP hydrate formation. The decrease of CO_2 concentrations during the CP hydrate is lagged becuase the CP is a water immiscible promotor. For this reason, it took longer time for the CP hydrate formation than THF hydrate and TBAC semiclathrate which are the water miscible promotor. The change of CO_2 concentration in the vapor phase is strongly affected by the sort and concentration of promotor. The THF (5.6 mol%) hydrate, TBAC (3.3 mol%) semiclathrates, and CP (5.6 mol%) hydrates had a drastic drop in the CO_2 concentration in the vapor phase, whereas the THF (1.0 mol%) hydrate, TBAC (1.0 mol%) semiclathrates, and CP (1.0 mol%) hydrates had a slight slow change in the CO_2 concentration; for the THF (5.6 mol%) hydrate, the CO_2 concentration in the vapor phase

was reduced from 20.0% to 13.5%, for the TBAC (3.3 mol%) semiclathrate from 20.0% to 16.0%, for the CP (5.6 mol%) hydrate from 20.0% to 13.5%, for the THF (1.0 mol%) hydrate from 20.0% to 16.0%, for the TBAC (1.0 mol%) semiclathrate from 20.0% to 17.0%, and for the CP (1.0 mol%) hydrate from 20.0% to 17.5%.

As shown in (Figures. 5.2., 5.3., and 5.4.), the gas uptake of THF (5.6 mol%) and CP (5.6 mol%) hydrate is noticeably higher than TBAC (3.3 mol%) semiclathrate. However, CO_2 selectivity is much higher in TBAC semiclathrate dissociation. In addition, TBAC concentration are not affect CO_2 composition in the semiclathrate phase even the gas uptake and composition change behavior are affected in the vapor phase. Adding THF and CP to the CO_2 (20%) + N_2 (80%) + water system can cause the gas hydrate equilibrium pressure to significantly decrease at a given temperature because they are enclathrated in large cages of sII hydrates, which results in significant thermodynamic promotion. The gas uptakes and gas storage capacity of the guest molecules are closely related to the structure details of the sII hydrate and TBAC semiclathrates.

However, these sII hydrate former have several disadvantages to their use in actual processes. They are highly volatile and toxic, indicating that an additional process for further purification of the gas phase and complete recovery from the liquid phase is required after use. A significant loss after repeated use can also be expected because of their high volatility. In addition, when compared with water-miscible promoters, the liquid phase of CP needs more vigorous agitation to enhance the gas - liquid contact area for gas hydrate formation because of its immiscibility in water, which suggests a larger energy requirement for the actual application. In addition, the CO_2 enrichment in THF (5.6 mole%) hydrate formation has low gas separation, approximately 36 % CO_2. CP (5.6 mole%) hydrate dissociation has expected to have similar behavior in the gas separation process. Unlike THF and CP, TBAC is non-volatile and far from toxic, but their thermodynamic promotion capability is comparable to or more significant than THF and CP. In addition, they are completely soluble in water and the gas separation rate is higher than THF and CP hydrate. Due to their significant thermodynamic stability and guest gas enclathration ability, TBAC semiclathrates have been investigated as an alternative to gas hydrates for gas storage and separation.

5.2.3. Raman spectroscopic analysis

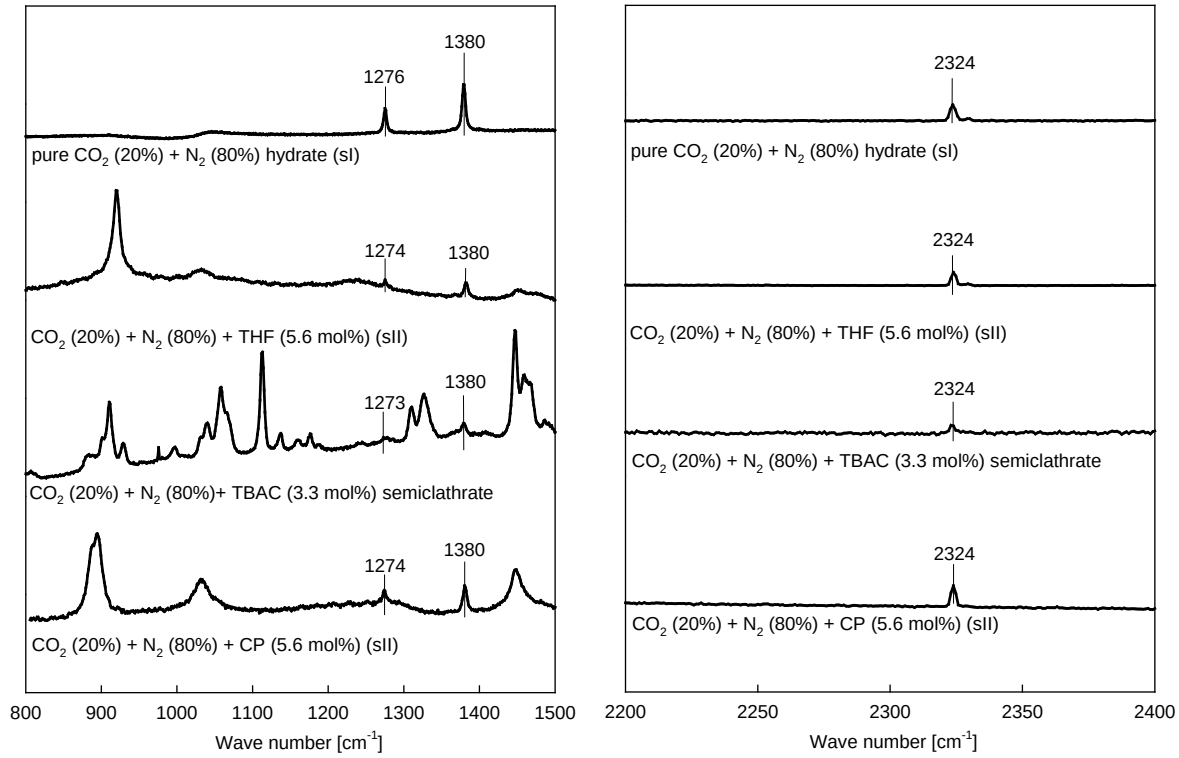

Figure 5.5. Raman spectra of the CO_2 + N_2 hydrate, CO_2 + N_2 + THF hydrate, CO_2 + N_2 + TBAC semiclathrate, and CO_2 + N_2 + CP hydrate. The Raman peak located next to 2324 cm^{-1} originated from the N_2 vapor used for cooling.

(Figure 5.5.) shows the Raman spectra of the CO_2 (20%) + N_2 (80%) hydrate, CO_2 (20%) + N_2 (80%) + THF (5.6 mol%) hydrate, CO_2 (20%) + N_2 (80%) + TBAC (3.3 mol%) semiclathrate, and CO_2 (20%) + N_2 (80%) + CP (5.6 mol%) hydrate. The CO_2 (20%) + N_2 (80%) gas hydrate, known to form sI hydrate, shows three Raman peaks. Two peaks for the CO_2 molecules were observed at 1276 cm^{-1} and 1380 cm^{-1}, and one peak for the N_2 molecules was observed at 2324 cm^{-1}. However, the Raman spectra of the CO_2 + N_2 + THF and CP hydrates, known to form sII hydrate, exhibited two Raman peaks for CO_2 molecules at 1274 cm^{-1} and 1380 cm^{-1} and one Raman peak for the N_2 molecules at 2324 cm^{-1}, whereas they had several Raman peaks for the THF and CP molecules enclathrated in the hydrate lattices. In addition, the Raman spectra of the CO_2 + N_2 + TBAC semiclathrate exhibited two Raman peaks for CO_2 molecules at 1273 cm^{-1} and 1380 cm^{-1} and one Raman peak for the N_2 molecules at 2324 cm^{-1}, whereas they had many Raman peaks for the TBA^+ enclathrated in the semi-

clathrate lattices. The CO_2 and N_2 molecules can be enclathrated in both small 5^{12} cages and large $5^{12}6^2$ cages of sI hydrate. However, Raman spectra cannot offer detailed information about cage occupancy and guest distribution in the clathrate lattices. The Raman spectrum of the CO_2 molecules enclathrated in the sI hydrate provides no peak splittings and accordingly, no one-to-one correspondence between the cages and Raman peaks. Furthermore, N_2 molecules captured in both small and large cages of the sI hydrate have only one Raman peak at 2324 cm^{-1} because N_2 molecules are so small that the symmetric N-N vibration of the N_2 molecules are not distinguishable in different cages of gas hydrates. However, a wavenumber shift (1276 cm^{-1} to 1274 cm^{-1}) indicating the sII hydrate or (1276 cm^{-1} to 1273 cm^{-1}) indicating the semiclathrate for the enclathrated CO_2 molecules was observed, and this can be attributed to a slight difference in the size and environment of the small 5^{12} cages, which are common for sI and sII gas hydrate and TBAC semiclathrates.

This study is the first to use thermodynamic and Raman spectroscopic analyses to investigate and compare the thermodynamic stability, gas uptakes, and CO_2 capture performance of clathrates formed from THF, TBAC, and CP targeting post-combustion CO_2 capture from flue gas. TBAC semiclathrate-based CO_2 capture has many advantages over the gas hydrate-based process because TBAC is non-volatile and non-toxic, and this can form semiclathrates at a significantly lower pressure and higher temperature conditions. The TBAC semiclathrate is a good candidate material for post-combustion CO_2 capture from flue gas.

5.3. Conclusions

The thermodynamic stability, gas uptakes, and CO_2 distributions in empty cages were investigated formed from post-combustion gas mixture + aqueous solutions of THF, TBAC, and CP. The CO_2 (20%) + N_2 (80%) + clathrate systems showed noticeably stabilized equilibrium conditions when compared with the CO_2 (20%) + N_2 (80%) gas hydrate system. TBAC (3.3 mol%) semiclathrate had the most significant thermodynamic stability among the THF and CP in this study at 3.1 MPa. Even though the CP (5.6 mol%) semiclathrate had the highest gas uptake and the steepest changes in CO_2 concentration in the vapor phase, CO_2 selectivity in the THF and CP hydrate phase was lower than TBAC (3.3 mol%) semiclathrate. In all the cases, the CO_2 concentration in the semiclathrate phase after the completion of semiclathrate formation was found to be approximately 60% at 3.1 MPa and ΔT of 5.0 K, whereas the CO_2 concentration in the THF and CP hydrate phase were found to be approximately 34.0%. This gas composition analysis was indicated that the TBAC had higher enrichment of CO_2 in the semiclathrate phase than THF and CP hydrate phase at stoichiometric concentration, respectively. A further comparison between TBAC and another promoter THF and CP also found that TBAC performed better in reducing the semiclathrate formation pressure requirement, increasing CO_2 enrichment. The results provided that the semiclathrate formation with TBAC as a promoter is promising for separating CO_2 from post-combustion gas. Both CO_2 and N_2 molecules are enclathrated in the cages of the clathrate was confirmed from the Raman spectra. The experimental results obtained in this study provide fundamental information required to design and develop a clathrate-based CO_2 capture process from post-combustion flue gas.

5.4. References

[1] Aaron D, Tsouris C. Separation of CO_2 from flue gas: a review. Separ Sci Technol, 40 (1–3) (2005), pp. 321–348

[2] Freund P, Ormerod W.G.. Progress toward storage of carbon dioxide. Energ Convers Manage 1997;38:199-204

[3] Eslamimanesh A, Mohammadi AH, Richon D. Thermodynamic modeling of phase equilibria of semi-clathrate hydrates of CO_2, CH_4, or N_2 + tetra-n-butylammonium bromide aqueous solution. Chem. Eng. Sci 2012;81:319-2.

[4] Li XS, Xu CG, Chen ZY, Wu HJ. Tetra-n-butyl ammonium bromide semi-clathrate hydrate process for post-combustion capture of carbon dioxide in the presence of dodecyl trimethyl ammonium chloride. Energy 2010;35:3902-8.

[5] Shimada W, Ebinuma T, Oyama H, Kamata Y, Takeya S, Uchida T, et al. Separation of gas molecule using tetra-n-butyl ammonium bromide semi-clathrate hydrate crystals. Jpn. J. Appl. Phys., Part 2 2003;42:L129.

[6] Oyama H, Shimada W, Ebinuma T, Kamata Y, Takeya S, Uchida T, et al. Phase diagram, latent heat, and specific heat of TBAB semiclathrate hydrate crystals. Fluid Phase Equilib 2005;234:131-5.

[7] Lee S, Lee Y, Park S, Kim Y, Lee JD, Seo Y. Thermodynamic and spectroscopic identification of guest gas enclathration in the double tetra-n-butylammonium fluoride semiclathrates. J. Phys. Chem. B 2012;116:9075-81.

[8] Chapoy A, Anderson R, Tohidi B. Low-pressure molecular hydrogen storage in semi-clathrate hydrates of quaternary ammonium compounds. J. Am. Chem. Soc 2007;129:746-7.

[9] Mohammadi A, Manteghian M, Mohammadi AH. Dissociation data of semiclathrate hydrates for the systems of tetra-n-butylammonium fluoride (TBAF) + methane + water, TBAF + carbon dioxide + water, and TBAF + nitrogen + water. J. Chem. Eng. Data 2013;58:3545-50.

[10] Lee S, Park S, Lee Y, Lee J, Lee H, Seo Y. Guest gas enclathration in semiclathrates of tetra-n-butylammonium bromide: stability condition and spectroscopic analysis. Langmuir 2011;27:10597-603.

[11] Gholinezhad J, Chapoy A, Tohidi B. Separation and capture of carbon dioxide from CO_2/H_2 syngas mixture using semi-clathrate hydrates. Chem. Eng. Res. Des 2011;89:1747-51.

[12] Park S, Lee S, Lee Y, Seo Y. CO_2 capture from simulated fuel gas mixtures using semiclathrate hydrates formed by quaternary ammonium salts. Environ. Sci. Technol 2013;47:7571-7.

[13] Sfaxi IBA, Durand I, Lugo R, Mohammadi AH, Richon D. Hydrate phase equilibria of CO_2 + N_2 + aqueous solution of THF, TBAB or TBAF system. Int. J. Greenhouse Gas Control 2014;26:185-92.

[14] Li XS, Xu CG, Chen ZY, Wu HJ. Hydrate-based pre-combustion carbon dioxide capture process in the system with tetra-n-butyl ammonium bromide solution in the presence of cyclopentane. Energy 2011;36:1394-403.

[15] Li XS, Xu CG, Chen ZY, Cai J. Synergic effect of cyclopentane and tetra-n-butyl ammonium bromide on hydrate-based carbon dioxide separation from fuel gas mixture by measurements of gas uptake and X-ray diffraction patterns. Int. J. Hydrogen Energy 2012;37:720-7.

[16] Sloan ED, Koh C. Clathrate Hydrates of Natural Gases, 3th ed. Boca Raton: Taylor &Francis; 2007.

[17] Herslund PJ, Thomsen K, Abildskov J, Solms N. Modelling of cyclopentane promoted gas hydrate systems for carbon dioxide capture processes. Fluid Phase Equilib 2014;375:89-103

[18] Babu P, Linga P, Kumar R, Englezos P. A review of the hydrate based gas separation (HBGS) process for carbon dioxide pre-combustion captue. Energy 2015;85:261-79

[19] Seo Y, Kang SP, Lee S, Lee H. Experimental measurements of hydrate phase equilibria for carbon dioxide in the presence of THF, propylene oxide, and 1,4-dioxane. J. Chem. Eng. Data 2008;53:2833-7.

[20] Kang SP, Lee H, Lee CS, Sung WM. Hydrate phase equilibria of the guest mixtures containing CO_2, N_2 and tetrahydrofuran. Fluid Phase Equilib 2001;185:101-9.

[21] Delahaye A, Fournaison L, Marinhas S, Chatti I, Petitet JP, Dalmazzone D, et al. Effect of THF on equilibrium pressure and dissociation enthalpy of CO_2 hydrates applied to secondary refrigeration. Ind. Eng. Chem. Res 2005;45:391-7.

[22] Lee Y, Lee S, Lee J, Seo Y. Structure identification and dissociation enthalpy measurements of the CO_2 + N_2 hydrates for their application to CO_2 capture and storage. Chem Eng J 2014;246:20-6.

Chapter VI

Pre-combustion CO_2 capture using TBAC semiclathrates

6.1. Introduction

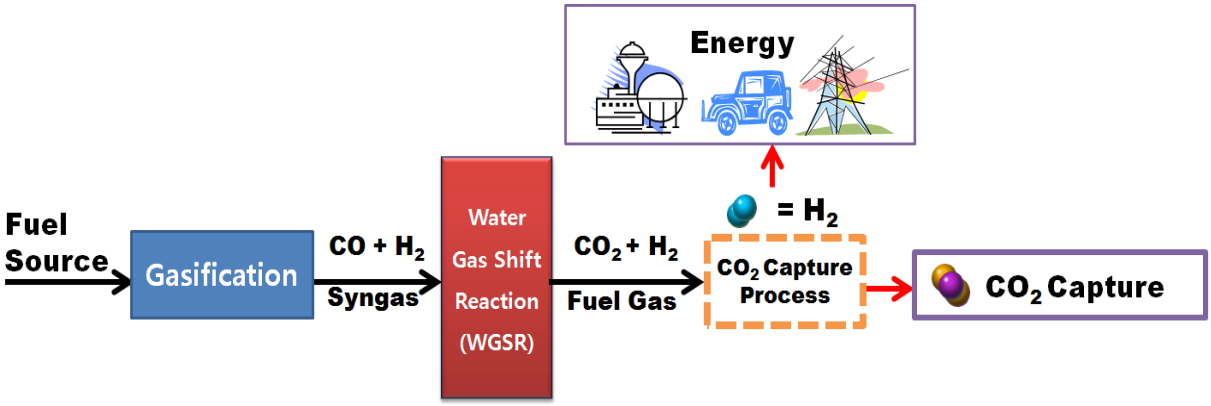

Figure 6.1. The Concept of clathrate-based CO_2 capture from fuel gas.

(Figure 6.1) depicted the concept of clathrate-based CO_2 capture form fuel gas. The pre-combustion CO_2 capture is mainly applicable to coal-based gasification plants. The fuel source reacts with oxygen in the gasifier to create syngas. This syngas is added to a WGSR for converting carbon monoxide (CO) to carbon dioxide (CO_2). With the entire pre-combustion process, the fossil fuel is chemically converted into two pure gas streams of CO_2 and H_2. From this gas cleanup process, low-grade fuels can be turned into high-grade fuels which can be burned to make electricity or be used for other industrial applications. Pre-combustion CO_2 capture processes and their applications (Figure 6.2). Ultimately, the CO_2 should be captured by the most eco-friendly and efficiency way. The future investigation will be conducted for CO_2 capture and H_2 separation by clathrates formation process.

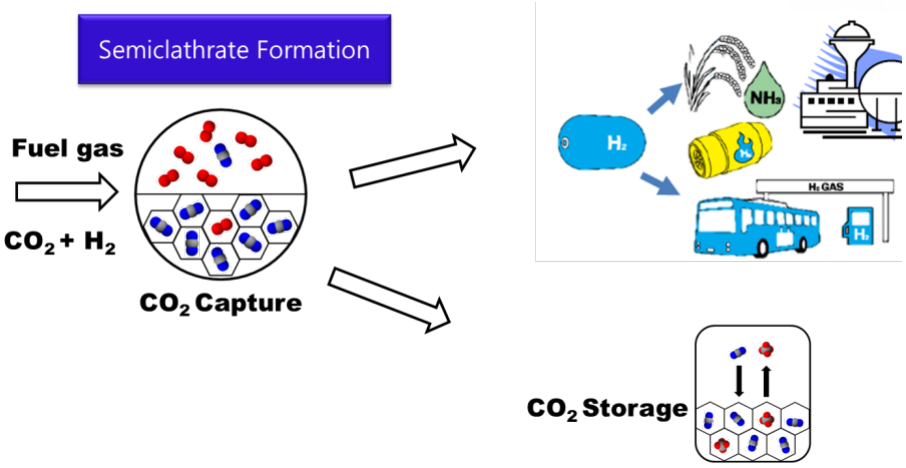

Figure 6.2. Pre-combustion CO_2 capture processes and their applications.

The most promising options of clathrate-based CO_2 capture from the fuel gas mixture is clathrate formation, because CO_2, whose hydrate equilibrium condition is remarkably milder than H_2, is expected to be enriched in the clathrate phase, resulting in the high selectivity of CO_2 in the clathrate phase. In this study, TBAC, semiclathrate former, was taken as clathrate-based CO_2 capture process from fuel gas for achieving a wider study than previous studies. Clathrate phase equilibria in the presence of semiclathrate former would be greater than that of CO_2 and H_2 hydrate, since CO_2 and H_2 hydrate form at higher pressure and lower temperature conditions. In general, treated synthesis gas coming out of fuel gas in an IGCC power station consists of approximately 40% CO_2 and 60% H_2 mixture at a total pressure of 2.5–8.0 MPa approximately. According to preliminary experimental results, the TBAC semiclathrate systems are significantly more stable than the gas hydrate system. Clathrate-based CO_2 capture from pre-combustion fuel gas was investigated in the presence of TBAC. The thermodynamic stability of the CO_2 (40%) + H_2 (60%) + clathrate was examined with an isochoric method using a high pressure reactor. The gas uptake and CO_2 concentration changes in the vapor phase during clathrate formation were measured to analyze the preferential gas occupation in the clathrate phase. CO_2 concentrations in the vapor and clathrate phases after the completion of clathrate formation were measured to provide the CO_2 selectivity. The enclathration of guest molecules in the clathrate lattices was confirmed with a micro-Raman spectrometer. In addition, the semiclathrate stability conditions and heat of dissociation values in the presence of TBAC with fuel gas are will be provided using a high pressure micro-differential scanning calorimeter (HP μ-DSC).

6.2. Results and discussion

6.2.1. Stability conditions of TBAC semiclathrates

Table 6.1. Three phase equilibrium data with CO_2 (40%) + H_2 (60%) gas mixture.

1.0 mol%		3.3 mol%		5.0 mol%	
T/K	P/MPa	T/K	P/MPa	T/K	P/MPa
285.9	1.32	289.6	1.38	288.6	1.35
287.3	2.68	290.9	2.94	289.6	2.80
288.2	4.09	291.6	4.33	290.3	4.08
289.2	6.04	292.1	5.79	291.0	5.78
289.8	7.93	292.7	7.90	291.5	7.89

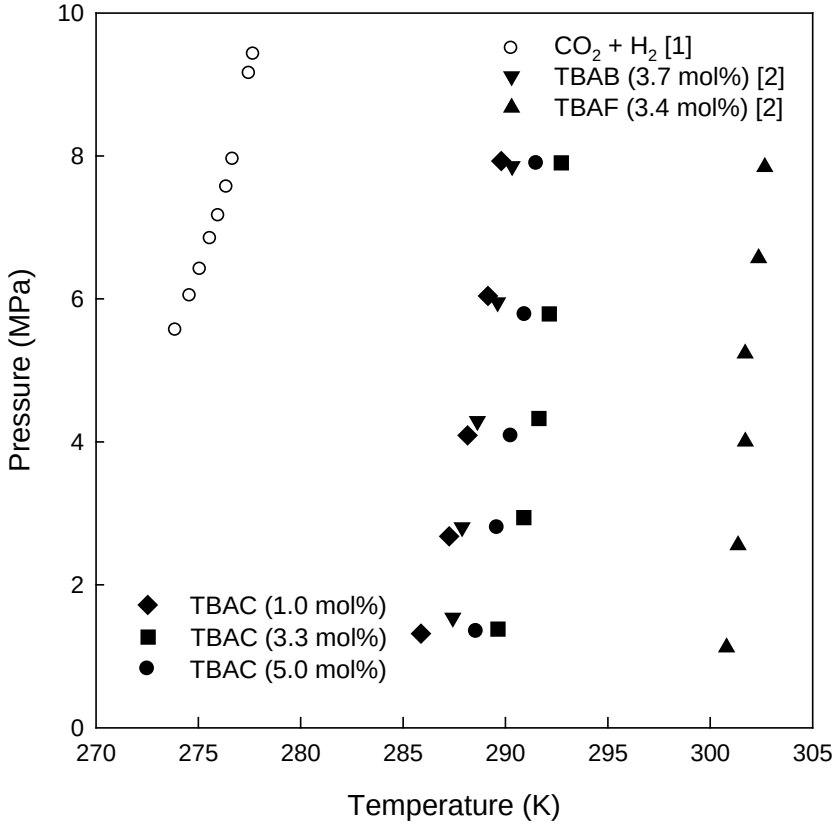

Figure 6.3. Three-phase equilibria of the CO_2 + H_2 + TBAB, TBAC, and TBAF + water systems.

(Figure 6.3.) presents three-phase (clathrate (H) - liquid water (L_w) - vapor (V)) equilibria for the CO_2 (40%) + H_2 (60%) + TBAB (3.7 mol%), TBAC (1.0, 3.3, and 5.0 mol%), and TBAF (3.4 mol%) + water systems, and the overall experimental data are summarized in (Table 6.1.). TBAC clathrate is most stable at 3.3 mol% solutions, which correspond to stoichiometrics concentrations of TBAC·29.7H_2O. The phase equilibrium results indicate that clathrate formed from clathrate formers can offer a significant thermodynamic promotion which represents a pressure reduction at any given temperature or a temperature increase at any given pressure when compared with gas hydrates. In particular, as seen in (Figure 6.3.), gas hydrate with CO_2 (40%) + H_2 (60%) requires equilibrium pressures as high as 5.0 MPa even at 273.0 K. Since gas hydrate formation requires high pressure and low temperature, clathrate-based CO_2 capture from a flue gas is difficult to apply in the actual process. However, in the presence of TBAC clathrate former, the gas hydrate equilibrium pressure can significantly decrease at a given temperature.

6.2.2. Gas uptake and composition measurements of QAS semiclathrates

In this study, changes in the gas uptake and CO_2 composition during semiclathrate formation were measured to examine the gas storage capacity and the preferential separation of CO_2 in the clathrate phase. The final CO_2 compositions in the vapor and clathrate phases for the TBAB, TBAC, and TBAF clathrate are compared in (Figure 6.4.). For these experiments, the equilibrium cell was charged with 50 cm^3 of aqueous solutions, respectively, and the driving force (ΔT), which is defined as the temperature difference between the equilibrium and experimental temperatures, was set as 5.0 K at 4.0 MPa for TBAB (3.7 mol%), TBAC (1.0 and 3.3 mol%), and TBAF (3.4 mol%) semiclathrate and 8.0 MPa for TBAC (1.0 and 3.3 mol%). After the completion of each clathrate formation with CO_2 (40%) + H_2 (60%), the final CO_2 concentration in the vapor phase was first measured, and then, the CO_2 composition of the retrieved gas from the clathrate phase was measured. The initial 40.0% CO_2 from the fuel gas mixture was introduced, more than 93.0% CO_2 was enriched in semiclathrate phase.

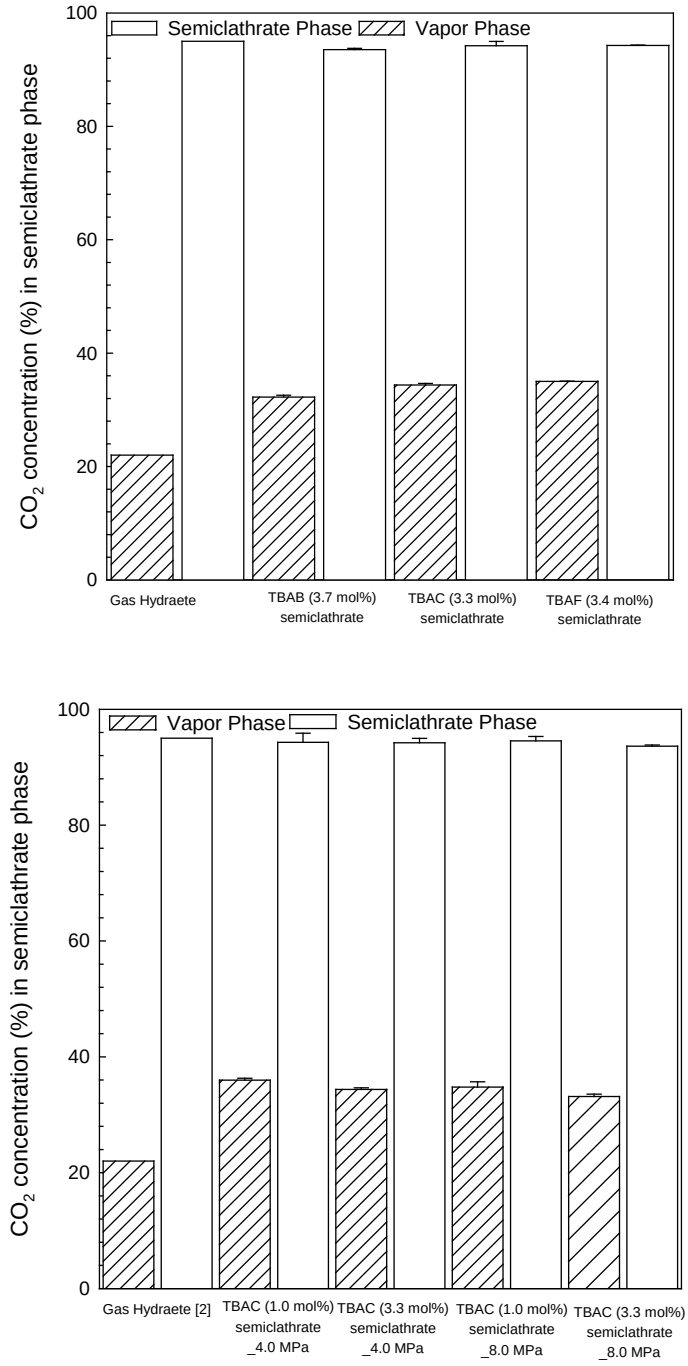

Figure 6.4. CO_2 concentrations in the vapor and clathrate phases at ΔT = 5.0 (for gas hydrate at 275.15 K and ΔP = 8.0 MPa) (a) for the solutions with stoichiometric concentrations of each clathrate structure at 4.0 MPa (b) for TBAC 1.0 and 3.3 mol%) solutions at 4.0 and 8.0 MPa.

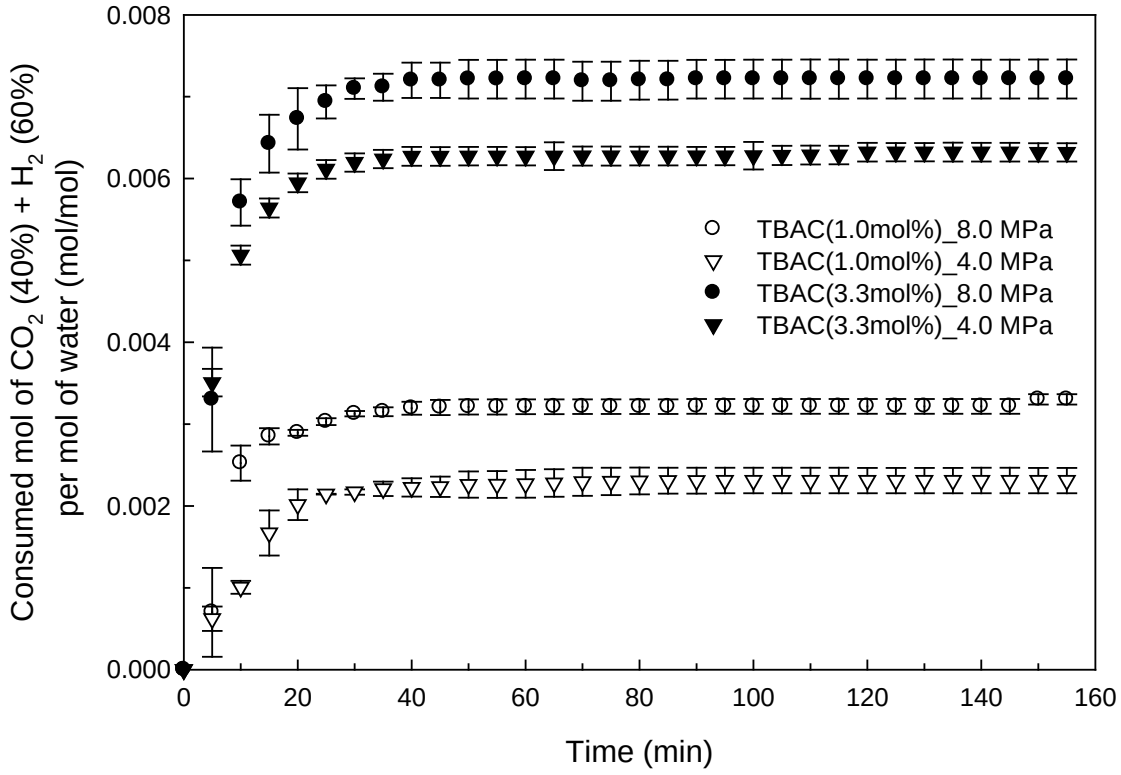

Figure 6.5. Gas uptake curves for the CO_2 (40%) + H_2 (60%) during clathrate formation at ΔT =5.0 K and (4.0 and 8.0 MPa).

The gas uptake result of the CO_2 (40%) + H_2 (60%) + TBAC (1.0 and 3.3 mol%) semiclathrate formation is shown in (Figure 6.5.). The accumulated amount of gas consumed during semiclathrate formation is expected to be equivalent to the total amount of gas captured in the vacant cages of the clathrate. The gas uptakes for each semiclathrate were expressed as the ratio of moles of consumed gas to moles of initially charged water, and are closely related to the number of vacant cages available for capturing CO_2 and H_2 gas molecules. The experimental results clearly show that the TBAC (3.3 mol%) clathrate had the larger gas uptake than the TBAC (1.0 mol%) semiclathrate formation.

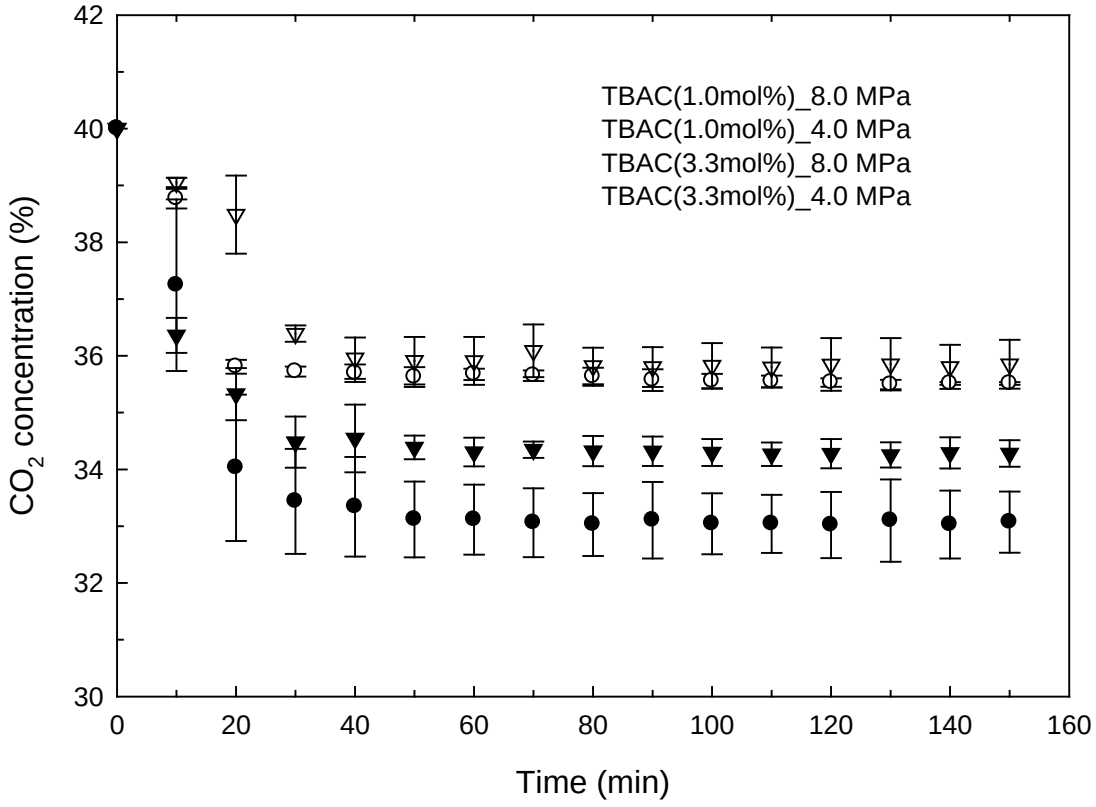

Figure 6.6. Changes in CO_2 composition in the vapor phase at ΔT =5.0 K and (4.0 and 8.0 MPa).

(Figure 6.6.) shows the changes in the CO_2 composition in the vapor phase during clathrate formation. The CO_2 concentrations in the vapor phase continued to decline during clathrate formation, because CO_2 is more selective captured in the clathrate phase than H_2. The CO_2 concentration rapidly dropped just after nucleation, gradually stabilized, and finally became almost constant after 1h. The change of CO_2 concentration in the vapor phase is strongly affected by the sort and concentration of promotor. The TBAC (3.3 mol%) semiclathrates had a drastic drop in the CO_2 concentration in the vapor phase, whereas the TBAC (1.0 mol%) semiclathrates had a slight slow change in the CO_2 concentration; for the TBAC (3.3 mol%) semiclathrate from 40.0% to 34.0%, for the TBAC (1.0 mol%) semiclathrate from 40.0% to 36.0% at 4.0 MPa, and for the TBAC (3.3 mol%) semiclathrate from 40.0% to 32.0%, for the TBAC (1.0 mol%) semiclathrate from 40.0% to 35.0% at 8.0 MPa.

6.2.3. Raman spectroscopic analysis

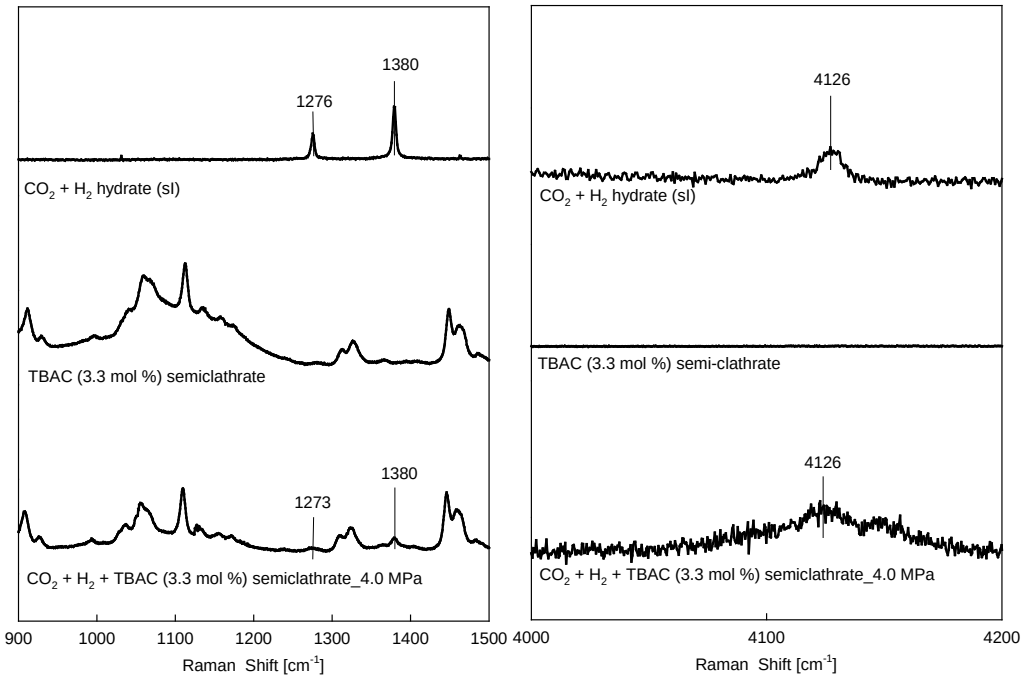

Figure 6.7. Raman spectra of the CO_2 + H_2 hydrate, pure TBAC semiclathrate, and CO_2 + H_2 + TBAC semiclathrate.

(Figure 6.7.) shows the Raman spectra of the CO_2 (40%) + H_2 (60%) hydrate, the pure TBAC (3.3 mol%) semiclathrate, and the CO_2 (40%) + H_2 (60%) + TBAC (3.3 mol%) semiclathrate. The the CO_2 (40%) + H_2 (60%) gas hydrate, known to form sI hydrate, shows three Raman peaks. Two peaks for the CO_2 molecules were observed at 1276 cm^{-1} and 1380 cm^{-1}, and one peak for the H_2 molecules was observed at 4126 cm^{-1}. The Raman spectra of the CO_2 (40%) + H_2 (60%) + TBAC semiclathrate exhibited two Raman peaks for CO_2 molecules at 1273 cm^{-1} and 1380 cm^{-1} and one Raman peak for the H_2 molecules at 4126 cm^{-1}, whereas they had many Raman peaks for the TBA^+ enclathrated in the semiclathrate lattices. The CO_2 and H_2 molecules can be enclathrated in both small 5^{12} cages and large $5^{12}6^2$ cages of sI hydrate. However, Raman spectra cannot offer detailed information about cage occupancy and guest distribution in the clathrate lattices. The Raman spectrum of the CO_2 molecules enclathrated in the sI hydrate provides no peak splittings and accordingly, no one-to-one correspondence between the cages and Raman peaks. A wavenumber shift (1276 cm^{-1} to 1273 cm^{-1}) indicating the semiclathrate for the enclathrated CO_2 molecules was observed, and this can be attributed to a slight difference in the size and environment of the small 5^{12} cages, which are common for sI gas hydrate and TBAC semiclathrates.

6.2.4. Differential scanning calorimeter (DSC) measurements

The three-phase (H-L_w-V) equilibria of the CO_2 + H_2 + TBAC (3.3 mol%) + water systems and the CO_2 + TBAC (3.3 mol%) + water systems that were measured using both the conventional isochoric method (pVT) and the DSC method are depicted in (Figure. 6.8.). The semiclathrate equilibrium point measured using the HP μ-DSC was located precisely in each three-phase equilibrium line of the corresponding the CO_2 + H_2 + TBAC (3.3 mol%) + water systems and the CO_2 + TBAC (3.3 mol%) + water systems semiclathrate, which were obtained using the conventional isochoric method (pVT). In addition, (Figure 6.8.) presents the dissociation enthalpies (ΔH_d) of the CO_2 + H_2 + TBAC (3.3 mol%) + water systems and the CO_2 + TBAC (3.3 mol%) semiclathrate as a function of pressure. In the pressure range from 0.1 to 10 MPa, the dissociation enthalpies of the CO_2 + TBAC (3.3 mol%) semiclathrate were higher than that of the CO_2 + H_2 + TBAC (3.3 mol%) semiclathrate and increased with increases in the pressure of H_2. The dissociation enthalpy (ΔH_d) is a very important thermophysical property of semiclathrates because it is closely related to the amount of heat required for the semiclathrate formation/dissociation in real semiclathrate-based gas storage and capture processes.

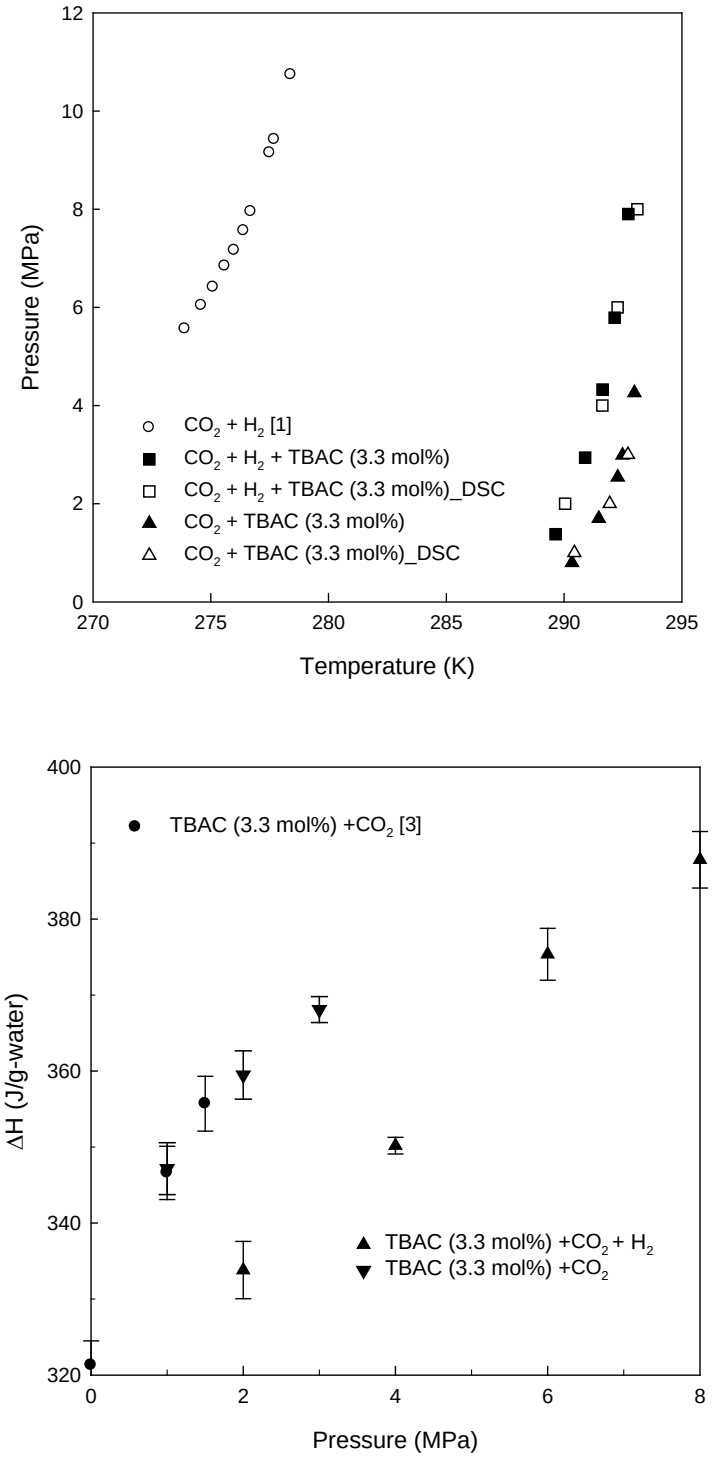

Figure 6.8. (a) Semiclathrate phase equilibria of the CO_2 + H_2 + TBAC (3.3 mol%) + water systems and the CO_2 + TBAC (3.3 mol%) + water systems. (b) Dissociation enthalpies (ΔH_d) of the CO_2 + H_2 + TBAC (3.3 mol%) semiclathrates as a function of pressure.

6.3. Conclusions

The thermodynamic stability, gas uptakes, and CO_2 distributions in empty cages were investigated formed from post-combustion gas mixture + aqueous solutions of TBAC. The CO_2 (40%) + H_2 (60%) + clathrate systems showed noticeably stabilized equilibrium conditions when compared with the CO_2 (40%) + H_2 (60%) gas hydrate system. The TBAC (3.3 mol%) semiclathrate at 8.0 MPa had the highest gas uptake and the steepest changes in CO_2 concentration in the vapor phase. In all the cases, the CO_2 concentration in the semiclathrate phase after the completion of semiclathrate formation was found to be more than 93% at all experiments. This gas composition analysis was indicated that the TBAC had highly enrichment of CO_2 in the semiclathrate phase. Both CO_2 and H_2 molecules are enclathrated in the cages of the clathrate was confirmed from the Raman spectra. The experimental results obtained in this study provide fundamental information required to design and develop a clathrate-based CO_2 capture process from pre-combustion fuel gas. This study is the first to use thermodynamic and Raman spectroscopic analyses to investigate and compare the thermodynamic stability, gas uptakes, and CO_2 capture performance of clathrates formed from TBAC targeting pre-combustion CO_2 capture. TBAC semiclathrate-based CO_2 capture has many advantages over the gas hydrate-based process because TBAC is non-volatile and non-toxic, and this can form semiclathrates at a significantly lower pressure and higher temperature conditions. The TBAC semiclathrate is a good candidate material for pre-combustion CO_2 capture from fuel gas.

6.4 References

[1] R. Kumar, H.J. Wu, P. Englezos, Incipient hydrate phase equilibrium for gas mixtures containing hydrogen, carbon dioxide and propane, Fluid Phase Equilibria, 244 (2) (2006), 167–171

[2] Park S, Lee S, Lee Y, Seo Y. CO_2 capture from simulated fuel gas mixtures using semiclathrate hydrates formed by quaternary ammonium salts. Environ Sci Technol. 2013;47:7571-7.

[3] N. Mayoufi, D. Dalmazzone, W. Fürst, A. Delahaye, L. Fournaison, CO_2 enclathration in hydrates of peralkyl-(ammonium/phosphonium) salts: stability conditions and dissociation enthalpies, J. Eng. Data 55 (2009) 1271-1275.

[4] J. Deschamps, D. Dalmazzone, Hydrogen storage in semiclathrate hydrates of tetrabutyl ammonium chloride and tetrabutyl phosphonium bromide, J. Chem. Eng. Data 55 (2010) 3395-3399.

Chapter VII

Conclusion

Clathrate hydrates have many potential applications such as CO_2 capture/sequestration, natural gas storage/transportation, hydrogen storage, and desalination. However, the major limitation of gas hydrate-based applications is that they require high pressure and low temperature conditions for gas hydrate formation. To overcome this concern, gas hydrate formation needs to be performed at a much milder pressure and temperature conditions. Semiclathrates, which share many physical and chemical properties with gas hydrates, could be an attractive alternative to gas hydrates. This is because in general, they can maintain their thermodynamic stability under atmospheric pressure conditions. In this study, I'm focusing on the clathrate-based CO_2 capture with thermodynamic promoters from flue and fuel gas mixtures.

Clathrate-based CO_2 capture from flue gas was investigated in the presence of thermodynamic promoters such as TBAB, TBAC, TBAF, THF, and CP. The thermodynamic stability of the CO_2 (20%) + N_2 (80%) + promoter was examined with an isochoric method. The gas uptake and CO_2 concentration changes in the vapor phase during clathrate formation were measured to analyze the preferential gas occupation in clathrate phase. CO_2 concentrations in the vapor and clathrate phases after the completion of clathrate formation, were measured to provide the CO_2 selectivity based on the types of promoters used. The enclathration of guest molecules in the semiclathrate lattices was confirmed with a micro-Raman spectrometer.

In chapter 3, QASs were investigated as a thermodynamic promoters. The enclathration of guest gases such as CH_4, CO_2, and N_2 in QAS semiclathrates and their potential application to natural gas storage and CO_2 capture were examined with a primary focus on stability condition measurements and cage filling characteristics.

(1) Maximum promotion effect at TBAC concentration was 3.3 mol%, Less promotion effect over TBAC concentration was 1 mol%.
(2) The dissociation enthalpy of TBAC·29.7H_2O was found to be 166.53 kJ/mol·semi-clathrate.
(3) The phase behaviors clearly demonstrated that the double CH_4 (or CO_2, N_2) + QAS semiclathrates yielded a significantly enhanced thermodynamic stability.
(4) The cage-dependent ^{13}C NMR chemical shift identified CH_4 molecules enclathrated in the

small 5^{12} cages of the double QAS semiclathrates. CO_2 and N_2 inclusion in the double QAS semiclathrate was also confirmed using Raman spectroscopy.

In chapter 4, I investigated semiclathrate-based CO_2 capture from the flue gas mixture of fossil fuel-fired power plants in the presence of in the presence of various quaternary ammonium salts (QASs). This includes tetra-n-butyl ammonium bromide (TBAB), tetra-n-butyl ammonium chloride (TBAC), and tetra-n-butyl ammonium fluoride (TBAF) with a primary focus on the thermodynamic, kinetic, and spectroscopic aspects.

(1) The semiclathrate phase equilibria of the quaternary CO_2 (20%) + N_2 (80%) + QAS semiclathrates + water mixtures showed that TBAC solutions form semiclathrates with guest gases at significantly stabilized pressure and temperature conditions.
(2) The TBAF semiclathrate with CO_2 (20%) + N_2 (80%) showed the most significant equilibrium pressure reduction at a specified temperature. However, the TBAC semiclathrate had the highest gas uptake and steepest CO_2 concentration change in the vapor phase, which indicates the largest gas storage capacity for CO_2 capture.
(3) CO_2 was found to be selectively captured and thus enriched to approximately 60% in the semiclathrate phase.
(4) CO_2 selectivity was independent of the type of QASs used.
(5) Raman spectroscopic results demonstrated that both CO_2 and N_2 are captured in the TBAC semiclathrate lattices and that there is no structural transition due to the enclathration of guest gases.

In chapter 5, clathrate-based CO_2 capture from the simulated flue gas mixture was investigated in the presence of tetrahydrofuran (THF) as a water-soluble sII hydrate former, cyclopentane (CP) as a water-insoluble sII hydrate former, and tetra-butyl ammonium chloride (TBAC) as a semiclathrate former.

(1) The clathrate stabilities of the CO_2 (20%) + N_2 (80%) + promoters + THF (1.0 and 5.6mol%), TBAC (1.0 and 3.3mol%), and CP (1.0 and 5.6mol%)) systems were measured using an isochoric method. Thermodynamic stability : THF < CP < TBAC below 4.5 MPa
(2) The gas consumption was TBAC < CP < THF at stoichiometric concentration.
(3) The 5.6 mol% THF solution showed the largest gas uptake during the clathrate formation, but it demonstrated the lowest CO_2 concentration (35 %) in the clathrate phase after the completion of clathrate formation.

(4) TBAC solutions exhibited approximately 60% CO_2 concentrations in the clathrate phases regardless of TBAC concentration.
(5) The inclusion of CO_2 in the clathrate phase was confirmed via Raman spectroscopy.

In In chapter 6, TBAC semiclathrate-based CO_2 capture from the simulated fuel gas mixture was investigated. This chapter is primarily focused on the thermodynamic, kinetic, and spectroscopic aspects at difference pressure and concentration condition.

(1) The phase equilibria showed that the TBAC (3.3 mol%) semiclathrate with CO_2 (40 %) + H_2 (60 %) was significantly stabilized when compared with pure gas hydrate.
(2) The enclathration of guest molecules in the small cages was confirmed via in-situ Raman spectroscopy.
(3) The gas uptake of TBAC (1.0 and 3.3 mol%) semiclathrate was investigated at 4.0 and 8.0 MPa pressure conditions.
(4) The CO_2 concentration in the semiclathrate phase was found to be approximately 93 %.

In this work, I suggested post- and pre- combustion CO_2 capture using QAS semiclathrate formation. This study is the first attempt to investigate the thermodynamic stability and gas uptakes of the CO_2 + N_2 + promoter clathrates and CO_2 + H_2 + promoter clathrates for post-and pre-combustion CO_2 capture from flue and fuel gas. It was found from the experimental results that the semiclathrate-based CO_2 capture can be feasible due to their high thermodynamic stability and favorable enclathration characteristics of guest gases when compared with hydrate-based CO_2 capture.

The suggested semiclathrate-based CO_2 capture process consists of two process units of gas capture and release. When CO_2 from flue gas is selectively captured in the semiclathrate phase, the clathrate slurry is transferred to the dissociation unit. Then, the semiclathrate is dissociated by either heating or pressure decrease. Released heat during clathrate formation can be recovered and reused in the dissociation unit. The dissociated solution can be recycled to the gas capture unit. This indicates that the semiclathrate-based capture is eco-friendly through solution recycle and heat recovery between the semiclathrate formation and dissociation units.

Various methods such as membrane separation, cryogenic separation, and solvent absorption have been developed for CO_2 capture. However, these methods have several drawbacks such as the high energy requirement for regeneration, high solvent toxicity, low selectivity, and high corrosion. One method increasing attention is clathrate-based gas separation, which is formed only from water molecules and thus, is less energy intensive and environment-friendly. In addition, the separated CO_2 can recover thought the temperature increasing or pressure release. These simple processes required

lower energy consumption than other CO_2 capture methods, such as adsorption and absorption method, which required high energy consumption and high material cost. It should be noted that clathrate-based CO_2 capture method still has limitations since there is a low storage capacity of the semiclathrate. This caused the increasing of gas capture unit size and handling flow rates, which is increasing the energy penalty. Moreover, it will be conducted for further investigation to increase the conversion of water to clathrate for application to the actual process. However, the obtained results can be a fundamental key and expanded into the potential applications of clathrates such as CO_2 sequestration, natural gas storage/transportation, hydrogen storage, and desalination.

REFERENCES

Chapter 1. References

[1] Spigarelli BP, Kawatra SK. Opportunities and challenges in carbon dioxide capture. J CO_2 Util 2013;1:69-87.

[2] Khokhar AA, Gudmundsson JS, Sloan ED. Gas storage in structure H hydrates. Fluid Phase Equilib 1998;150-151:383-92.

[3] Eslamimanesh A, Mohammadi AH, Richon D. Thermodynamic modeling of phase equilibria of semi-clathrate hydrates of CO_2, CH_4, or N_2 + tetra-n-butylammonium bromide aqueous solution. Chem. Eng. Sci 2012;81:319-2.

[4] Linga P, Kumar R, Lee JD, Ripmeester J, Englezos P. A new apparatus to enhance the rate of gas hydrate formation: Application to capture of carbon dioxide. Int. J. Greenhouse Gas Control 2010;4:630-7.

[5] Tajima H, Yamasaki A, Kiyono F. Process design of a new injection method of liquid CO_2 at the intermediate depths in the ocean using a static mixer. Fuel Process. Technol 2005;86:1667-78.

[6] Lee H, Seo Y, Seo YT, Moudrakovski IL, Ripmeester JA. Recovering methane from solid methane hydrate with carbon dioxide. Angew. Chem. Int. Ed 2003;42:5048-51.

[7] Kang S-P, Lee H. Recovery of CO_2 from flue gas using gas hydrate: thermodynamic verification through phase equilibrium measurements. Environ. Sci. Technol 2000;34:4397-400.

[8] Linga P, Kumar R, Englezos P. The clathrate hydrate process for post and pre-combustion capture of carbon dioxide. J. Hazard. Mater 2007;149:625-9.

[9] Lee Y, Lee S, Lee J, Seo Y. Structure identification and dissociation enthalpy measurements of the CO_2 + N_2 hydrates for their application to CO_2 capture and storage. Chem. Eng. J 2014;246:20-6.

[10] Li XS, Xu CG, Chen ZY, Wu HJ. Tetra-n-butyl ammonium bromide semi-clathrate hydrate process for post-combustion capture of carbon dioxide in the presence of dodecyl trimethyl ammonium chloride. Energy 2010;35:3902-8.

[11] Lee Y, Lee S, Jin YK, Seo Y. 1-Propanol as a co-guest of gas hydrates and its potential role in gas storage and CO_2 sequestration. Chem. Eng. J 2014;258:427-32.

[12] Kang KC, Linga P, Park K-n, Choi S-J, Lee JD. Seawater desalination by gas hydrate process and removal characteristics of dissolved ions (Na^+, K^+, Mg^{2+}, Ca^{2+}, B^{3+}, Cl^-, SO_4^{2-}). Desalination 2014;353:84-90.

[13] Cha J-H, Seol Y. Increasing Gas Hydrate Formation Temperature for Desalination of High Salinity Produced Water with Secondary Guests. ACS Sustainable Chem. Eng. 2013;1:1218-24.

[14] Sloan ED, Koh C. Clathrate hydrates of natural gases, 3th ed. Boca Raton. Taylor & Fr

ancis; 2007.

[15] Koh CA. Towards a fundamental understanding of natural gas hydrates. Chem Soc Rev. 2002;31:157-67.

[16] Torré J-P, Ricaurte M, Dicharry C, Broseta D. CO_2 enclathration in the presence of water-soluble hydrate promoters: Hydrate phase equilibria and kinetic studies in quiescent conditions. Chem Eng Sci 2012;82:1-13.

[17] Yang M, Song Y, Jiang L, Zhao Y, Ruan X, Zhang Y, et al. Hydrate-based technology for CO_2 capture from fossil fuel power plants. Appl Energy 2014;116:26-40.

[18] Kang S-P, Lee H, Lee C-S, Sung W-M. Hydrate phase equilibria of the guest mixtures containing CO_2, N_2 and tetrahydrofuran. Fluid Phase Equilib 2001;185:101-9.

[19] Delahaye A, Fournaison L, Marinhas S, Chatti I, Petitet J-P, Dalmazzone D, et al. Effect of THF on equilibrium pressure and dissociation enthalpy of CO_2 hydrates applied to secondary refrigeration. Ind Eng Chem Res 2005;45:391-7.

[20] Hashimoto S, Murayama S, Sugahara T, Ohgaki K. Phase equilibria for H_2 + CO_2 + tetrahydrofuran + water mixtures containing gas hydrates. J Chem Eng Data 2006;51:1884-6.

[21] Kang S-P, Lee H. Recovery of CO_2 from flue gas using gas hydrate: thermodynamic verification through phase equilibrium measurements. Env Sci Technol 2000;34:4397-400.

[22] Park S, Lee S, Lee Y, Seo Y. CO_2 capture from simulated fuel gas mixtures using semiclathrate hydrates formed by quaternary ammonium salts. Environ Sci Technol. 2013;47:7571-7.

[23] Seo Y, Kang S-P, Lee S, Lee H. Experimental measurements of hydrate phase equilibria for carbon dioxide in the presence of THF, propylene oxide, and 1,4-dioxane. J Chem Eng Data 2008;53:2833-7.

[24] Hashimoto S, Sugahara T, Sato H, Ohgaki K. Thermodynamic stability of H_2 + tetrahydrofuran mixed gas hydrate in nonstoichiometric aqueous solutions. J Chem Eng Data 2007;52:517-20.

[25] Sfaxi IBA, Durand I, Lugo R, Mohammadi AH, Richon D. Hydrate phase equilibria of CO_2 + N_2 + aqueous solution of THF, TBAB or TBAF system. Int J Greenhouse Gas Control 2014;26:185-92.

[26] Mayoufi N, Dalmazzone D, Fürst W, Delahaye A, Fournaison L. CO_2 enclathration in hydrates of peralkyl-(ammonium/phosphonium) salts: stability conditions and dissociation enthalpies. J Chem Eng Data 2009;55:1271-5.

[27] Mohammadi A, Manteghian M, Mohammadi AH. Dissociation data of semiclathrate hydrates for the systems of tetra-n-butylammonium fluoride (TBAF) + methane + water, TBAF + carbon dioxide + water, and TBAF + nitrogen + water. J Chem Eng Data 2013;58:3545-50.

[28] http://www.uwgb.edu/dutchs/petrology/Clathrate-0.HTM

[29] https://miktechnology.wordpress.com/2010/05/22/hydrates-a-novel-concept-for-plugging-deep-sea-severed-pipeline-proposed-scenario-for-bp-gulf-of-mexico-spill/

[30] http://pubs.rsc.org/en/content/articlehtml/2013/cs/c2cs35340g

[31] http://hubpages.com/education/Water-Desalination-Process-Using-Hydrates#

Chapter 2. References

[1] Kim, S., Baek I., You, J., Seo, Y. "Guest gas enclathration in tetra-n-butyl ammonium chloride (TBAC) semiclathrates: Potential application to natural gas storage and CO_2 capture" Applied Energy, 2015;140, 107-112.

[2] Kim, S., Kang, S., Seo, Y. "Semiclathrate-based CO_2 capture from flue gas in the presence of tetra-n-butyl ammonium chloride (TBAC)", Chemical Engineering Journal, 2015;276, 205–212.

[3] Kim, S., Seo, Y. "Semiclathrate-based CO_2 capture from flue gas mixtures: An experimental approach with thermodynamic and Raman spectroscopic analyses", Applied Energy, 2015;154, 987-994.

[4] Kim, S., Baek I., You, J., Seo, Y. “Phase equilibria, dissociation enthalpies, and Raman spectroscopic analyses of N_2 + tetra-n-butyl ammonium chloride (TBAC) semiclathrates”, Fluid Phase Equilibria, 2016;413, 86-91.

[5] Kim, S., Choi S-D., Seo, Y., “CO_2 capture from flue gas using clathrate formation in the presence of thermodynamic promoters”, Energy (In press).

Chapter 3. References

[1] Fowler D, Loebenstein W, Pall D, Kraus CA. Some unusual hydrates of quaternary ammonium salts. J Am Chem Soc. 1940;62:1140-2.

[2] Aladko L, Dyadin YA, Rodionova T, Terekhova I. Clathrate hydrates of tetrabutylammonium and tetraisoamylammonium halides. J Struct Chem. 2002;43:990-4.

[3] Shimada W, Ebinuma T, Oyama H, Kamata Y, Takeya S, Uchida T, et al. Separation of gas molecule using tetra-n-butyl ammonium bromide semi-clathrate hydrate crystals. Jpn J Appl Phys Part 2. 2003;42:L129.

[4] Komarov VY, Rodionova TV, Terekhova IS, Kuratieva NV. The cubic superstructure-I of tetrabutylammonium fluoride $(C_4H_9)_4NF•29.7H_2O$ clathrate hydrate. J Inclusion Phenom Macrocyclic Chem. 2007;59:11-5.

[5] Rodionova T, Komarov V, Villevald G, Aladko L, Karpova T, Manakov A. Calorimetric and structural studies of tetrabutylammonium chloride ionic clathrate hydrates. J Phys Chemi B. 2010;114:11838-46.

[6] Lipkowski J, Komarov VY, Rodionova TV, Dyadin YA, Aladko LS. The structure of tetrabutylammonium bromide hydrate $(C_4H_9)_4NBr \cdot 2^1/_3H_2O$. J Supramolecular Chemistry. 2002;2:435-9.

[7] Oyama H, Shimada W, Ebinuma T, Kamata Y, Takeya S, Uchida T, et al. Phase diagram, latent heat, and specific heat of TBAB semiclathrate hydrate crystals. Fluid Phase Equilib. 2005;234:131-5.

[8] Shin K, Cha JH, Seo Y, Lee H. Physicochemical properties of ionic clathrate hydrates. Chem Asian J. 2010;5:22-34.

[9] Fan S, Li Q, Nie J, Lang X, Wen Y, Wang Y. Semiclathrate hydrate phase equilibrium for CO_2/CH_4 gas mixtures in the presence of tetrabutylammonium halide (bromide, chloride, or fluoride). J Chem Eng Data. 2013;58:3137-41.

[10] Park S, Lee S, Lee Y, Seo Y. CO_2 capture from simulated fuel gas mixtures using semiclathrate hydrates formed by quaternary ammonium salts. Environ Sci Technol. 2013;47:7571-7.

[11] Deschamps J, Dalmazzone D. Hydrogen storage in semiclathrate hydrates of tetrabutyl ammonium chloride and tetrabutyl phosphonium bromide. J Chem Eng Data. 2010;55:3395-9.

[12] Li S, Fan S, Wang J, Lang X, Wang Y. Semiclathrate hydrate phase equilibria for CO2 in the presence of tetra-n-butyl ammonium halide (bromide, chloride, or fluoride). J Chem Eng Data. 2010;55:3212-5.

[13] Li XS, Xu CG, Chen ZY, Wu HJ. Tetra-n-butyl ammonium bromide semi-clathrate hydrate process for post-combustion capture of carbon dioxide in the presence of dodecyl trimethyl ammonium chloride. Energy. 2010;35:3902-8.

[14] Linga P, Kumar R, Lee JD, Ripmeester J, Englezos P. A new apparatus to enhance the rate of gas hydrate formation: Application to capture of carbon dioxide. Int J Greenhouse Gas Control. 2010;4:630-7.

[15] Lee S, Lee Y, Park S, Kim Y, Lee JD, Seo Y. Thermodynamic and spectroscopic identification of guest gas enclathration in the double tetra-n-butylammonium fluoride semiclathrates. J Phys Chem B. 2012;116:9075-81.

[16] Deschamps J, Dalmazzone D. Dissociation enthalpies and phase equilibrium for TBAB semi-clathrate hydrates of N_2, CO_2, $N_2 + CO_2$ and $CH_4 + CO_2$. J Therm Anal Calorim. 2009;98:113-8.

[17] Sfaxi IBA, Durand I, Lugo R, Mohammadi AH, Richon D. Hydrate phase equilibria of $CO_2 + N_2$ + aqueous solution of THF, TBAB or TBAF system. Int. J. Greenhouse Gas Control. 2014;26:185-92.

[18] Lee S, Park S, Lee Y, Lee J, Lee H, Seo Y. Guest gas enclathration in semiclathrates of tetra-n-butylammonium bromide: stability condition and spectroscopic analysis. Langmuir. 2011;27:10597-603.

[19] Sato K, Tokutomi H, Ohmura R. Phase equilibrium of ionic semiclathrate hydrates formed with tetrabutylammonium bromide and tetrabutylammonium chloride. Fluid Phase Equilib. 2013;337:115-8.

[20] Makino T, Yamamoto T, Nagata K, Sakamoto H, Hashimoto S, Sugahara T, Ohgaki K. Thermodynamic stabilities of tetra-n-butyl ammonium chloride + H_2, N_2, CH_4, CO_2, or C_2H_6 semiclathrate hydrate systems. J Chem Eng Data. 2009;55:839-41.

[21] Nakayama H. Solid-liquid and liquid-liquid phase equilibria in the symmetrical tetraalkylammonium halide-water systems. Bull. Chem. Soc. Jpn. 1981;54:3717-22.

[22] Sun ZG, Liu CG, Zhou B, Xu LZ. Phase equilibrium and latent heat of tetra-n-butylammonium chloride semi-clathrate hydrate. J Chem Eng Data. 2011;56:3416-8.

[23] Aladko LS, Dyadin YA, Rodionova TV, Terekhova IS. Clathrate hydrates of tetrabutylammonium and tetraisoamylammonium halides. J Struct Chem. 2002;43:990-4.

[24] Zhang J, Lee JW. Equilibrium of hydrogen + cyclopentane and carbon dioxide + cyclopentane binary hydrates. J Chem Eng Data. 2008;54:659-61.

[25] Manakov A, Rodionova T, Terekhova I, Komarov V, Burdin A, Sizikov A. Structural and physico-chemical studies of ionic clathrate hydrates of tetrabutyl-and tetraisoamylammonium salts. Proceedings of the 7th International Conference on Gas Hydrates. Edinburgh, Scotland, UK; 2011.

[26] Nakayama H. Hydrates of Organic Compounds. XI. Determination of the melting point and hydration numbers of the clathrate-like hydrate of tetrabutylammonium chloride by differential scanning calorimetry. Bull. Chem. Soc. Jpn. 1987;60:839-43.

[27] S. Kim, I.-H. Baek, J.-K. You, Y. Seo, Guest gas enclathration in tetra-n-butyl ammonium chloride (TBAC) semiclathrates: Potential application to natural gas storage and CO_2 capture, Appl. Energy 140 (2015) 107-112.

[28] Park S, Lee S, Lee Y, Seo Y. CO_2 capture from simulated fuel gas mixtures using semiclathrate hydrates formed by quaternary ammonium salts. Environ Sci Technol 2013;47:7571-7.

[29] Adisasmito S, Frank III RJ, Sloan Jr ED. Hydrates of carbon dioxide and methane mixtures. J Chem Eng Data. 1991;36:68-71.

[30] Kamran-Pirzaman A, Pahlavanzadeh H, Mohammadi AH. Hydrate phase equilibria of furan, acetone, 1, 4-dioxane, TBAC and TBAF. J Chem Thermodyn. 2013;64:151-8.

[31] Ye N, Zhang P. Phase equilibrium and morphology characteristics of hydrates formed by tetra-n-butyl ammonium chloride and tetra-n-butyl phosphonium chloride with and without CO_2. Fluid Phase

Equilib. 2014;361:208-14.

[32] A. Van Cleeff, G. Diepen, Gas hydrates of nitrogen and oxygen, Recl. Trav. Chim. Pays-Bas 1060;79:582-6.

[33] A. Mohammadi, M. Manteghian, A.H. Mohammadi, Phase equilibria of semiclathrate hydrates for methane + tetra n-butylammonium chloride (TBAC), carbon dioxide + TBAC, and nitrogen + TBAC aqueous solution systems, Fluid Phase Equilib. 2014;381:102-7.

[34] Shimada W, Ebinuma T, Oyama H, Kamata Y, Takeya S, Uchida T, et al. Separation of gas molecule using tetra-n-butyl ammonium bromide semi-clathrate hydrate crystals. Jpn J Appl Phys 2003;42:L129.

[35] S. Lee, Y. Lee, S. Park, Y. Kim, J.D. Lee, Y. Seo, Thermodynamic and spectroscopic identification of guest gas enclathration in the double tetra-n-butylammonium fluoride semiclathrates, J. Phys. Chem. B 2012;116: 9075-9081.

[36] Ripmeester JA, Ratcliffe CI. On the contributions of NMR spectroscopy to clathrate science. J Struct Chem. 1999;40:654-62.

[37] C.-l. Liu, H.-l. Lu, Y.-g. Ye, Raman spectroscopy of nitrogen clathrate hydrates, Chin. J. Chem. Phys. 29;22:353-8.

[38] K. Sugahara, Y. Tanaka, T. Sugahara, K. Ohgaki, Thermodynamic stability and structure of nitrogen hydrate crystal, J. Supramolecular Chemistry 2002;2:365-8.

Chapter 4. References

[1] Spigarelli BP, Kawatra SK. Opportunities and challenges in carbon dioxide capture. J CO2 Util 2013;1:69-87.

[2] Eslamimanesh A, Mohammadi AH, Richon D, Naidoo P, Ramjugernath D. Application of gas hydrate formation in separation precesses: A review of experimental studies. J Chem Thermodyn 2012;46:62-72.

[3] Dashti H, Zhehao Yew L, Lou X. Recent advances in gas hydrate-based CO_2 capture. J Nat Gas Sci Eng 2015;23:195-207.

[4] Kim S, Baek I-H, You J-K, Seo Y. Guest gas enclathration in tetra-n-butyl ammonium chloride (TBAC) semiclathrates: Potential application to natural gas storage and CO_2 capture. Appl Energy 2015;140:107-12.

[5] Aladko L, Dyadin YA, Rodionova T, Terekhova I. Clathrate hydrates of tetrabutylammonium and tetraisoamylammonium halides. J Struct Chem 2002;43:990-4.

[6] Lipkowski J, Komarov VY, Rodionova TV, Dyadin YA, Aladko LS. The Structure of Tetrabutylammonium Bromide Hydrate $(C_4H_9)_4NBr^{\cdot 2}1/3\ H_2O$. J Supramolecular Chemistry 2002;2:435-9.

[7] Komarov VY, Rodionova T, Terekhova I, Kuratieva N. The cubic superstructure-I of tetrabutylammonium fluoride $(C_4H_9)_4F^{\cdot 2}9.7H_2O$ clathrate hydrate. J Inclusion Phenom Macrocyclic Chem 2007;59:11-5.

[8] Fowler D, Loebenstein W, Pall D, Kraus CA. Some unusual hydrates of quaternary ammonium salts. J Am Chem Soc 1940;62:1140-2.

[9] Shimada W, Ebinuma T, Oyama H, Kamata Y, Takeya S, Uchida T, et al. Separation of gas molecule using tetra-n-butyl ammonium bromide semi-clathrate hydrate crystals. Jpn J Appl Phys 2003;42:L129.

[10] Deschamps J, Dalmazzone D. Dissociation enthalpies and phase equilibrium for TBAB semi-clathrate hydrates of N_2, CO_2, $N_2 + CO_2$ and $CH_4 + CO_2$. J Therm Anal Calorim 2009;98:113-8.

[11] Gholinezhad J, Chapoy A, Tohidi B. Separation and capture of carbon dioxide from CO_2/H_2 syngas mixture using semi-clathrate hydrates. Chem Eng Res Des 2011;89:1747–51.

[12] Li X-S, Xu C-G, Chen Z-Y, Cai J. Synergic effect of cyclopentane and tetra-nbutyl ammonium bromide on hydrate-based carbon dioxide separation from fuel gas mixture by measurements of gas uptake and X-ray diffraction patterns. Int J Hydrogen Energy 2012;37:720–7.

[13] Park S, Lee S, Lee Y, Lee Y, Seo Y. Hydrate-based pre-combustion capture of carbon dioxide in the presence of a thermodynamic promoter and porous silica gels. Int J Greenhouse Gas Control 2013;14:193–9.

[14] Komatsu H, Ota M, Sato Y, Watanabe M, Smith RL. Hydrogen and carbon dioxide adsorption with tetra-n-butyl ammonium semi-clathrate hydrates for gas separations. AIChE J 2014.

[15] Park S, Lee S, Lee Y, Seo Y. CO_2 capture from simulated fuel gas mixtures using semiclathrate hydrates formed by quaternary ammonium salts. Environ Sci Technol 2013;47:7571–7.

[16] Lee Y, Lee S, Lee J, Seo Y. Structure identification and dissociation enthalpy measurements of the $CO_2 + N_2$ hydrates for their application to CO_2 capture and storage. Chem Eng J 2014;246:20-6.

[17] Liu CL, Lu HL, Ye YG. Raman spectroscopy of nitrogen clathrate hydrates. Chin. J. Chem. Phys 2009;22:353-8.

[18] Cha I, Lee S, Lee JD, Lee GW, Seo Y. Separation of SF_6 from gas mixtures using gas hydrate formation. Environ. Sci. Technol 2010;44:6117-22.

[19] Sugahara K, Tanaka Y, Sugahara T, Ohgaki K. Thermodynamic stability and structure of nitrogen hydrate crystal. J. Supramolecular Chemistry 2002;2:365-8.

[20] Kumar R, Englezos P, Moudrakovski I, Ripmeester JA. Structure and composition of CO_2/H_2 and $CO_2/H_2/C_3H_8$ hydrate in relation to simultaneous CO_2 capture and H_2 production. AIChE J 2009;55:1584-94.

[21] Lee S, Park S, Lee Y, Lee J, Lee H, Seo Y. Guest gas enclathration in semiclathrates of tetra-n-

butylammonium bromide: stability condition and spectroscopic analysis. Langmuir 2011;27:10597-603.

[22] Rodionova T, Komarov V, Villevald G, Aladko L, Karpova T, Manakov A. Calorimetric and structural studies of tetrabutylammonium chloride ionic clathrate hydrates. J Phys Chem B2010;114:11838-46.

[23] Sun Z-G, Liu C-G, Zhou B, Xu L-Z. Phase equilibrium and latent heat of tetra-n-butylammonium chloride semi-clathrate hydrate. J Chem Eng Data 2011;56:3416-8.

[24] Sfaxi IBA, Durand I, Lugo R, Mohammadi AH, Richon D. Hydrate phase equilibria of CO_2 + N_2 + aqueous solution of THF, TBAB or TBAF system. Int J Greenhouse Gas Control 2014;26:185-92.

[25] Komatsu H, Ota M, Sato Y, Watanabe M, Smith RL. Hydrogen and carbon dioxide adsorption with tetra-n-butyl ammonium semi-clathrate hydrates for gas separations. AIChE J 2014.

Chapter 5. References

[1] Aaron D, Tsouris C. Separation of CO_2 from flue gas: a review. Separ Sci Technol, 40 (1–3) (2005), pp. 321–348

[2] Freund P, Ormerod W.G.. Progress toward storage of carbon dioxide. Energ Convers Manage 1997;38:199-204

[3] Eslamimanesh A, Mohammadi AH, Richon D. Thermodynamic modeling of phase equilibria of semi-clathrate hydrates of CO_2, CH_4, or N_2 + tetra-n-butylammonium bromide aqueous solution. Chem. Eng. Sci 2012;81:319-2.

[4] Li XS, Xu CG, Chen ZY, Wu HJ. Tetra-n-butyl ammonium bromide semi-clathrate hydrate process for post-combustion capture of carbon dioxide in the presence of dodecyl trimethyl ammonium chloride. Energy 2010;35:3902-8.

[5] Shimada W, Ebinuma T, Oyama H, Kamata Y, Takeya S, Uchida T, et al. Separation of gas molecule using tetra-n-butyl ammonium bromide semi-clathrate hydrate crystals. Jpn. J. Appl. Phys., Part 2 2003;42:L129.

[6] Oyama H, Shimada W, Ebinuma T, Kamata Y, Takeya S, Uchida T, et al. Phase diagram, latent heat, and specific heat of TBAB semiclathrate hydrate crystals. Fluid Phase Equilib 2005;234:131-5.

[7] Lee S, Lee Y, Park S, Kim Y, Lee JD, Seo Y. Thermodynamic and spectroscopic identification of guest gas enclathration in the double tetra-n-butylammonium fluoride semiclathrates. J. Phys. Chem. B 2012;116:9075-81.

[8] Chapoy A, Anderson R, Tohidi B. Low-pressure molecular hydrogen storage in semi-clathrate hydrates of quaternary ammonium compounds. J. Am. Chem. Soc 2007;129:746-7.

[9] Mohammadi A, Manteghian M, Mohammadi AH. Dissociation data of semiclathrate hydrates for the systems of tetra-n-butylammonium fluoride (TBAF) + methane + water, TBAF + carbon dioxide + water, and TBAF + nitrogen + water. J. Chem. Eng. Data 2013;58:3545-50.

[10] Lee S, Park S, Lee Y, Lee J, Lee H, Seo Y. Guest gas enclathration in semiclathrates of tetra-n-butylammonium bromide: stability condition and spectroscopic analysis. Langmuir 2011;27:10597-603.

[11] Gholinezhad J, Chapoy A, Tohidi B. Separation and capture of carbon dioxide from CO_2/H_2 syngas mixture using semi-clathrate hydrates. Chem. Eng. Res. Des 2011;89:1747-51.

[12] Park S, Lee S, Lee Y, Seo Y. CO_2 capture from simulated fuel gas mixtures using semiclathrate hydrates formed by quaternary ammonium salts. Environ. Sci. Technol 2013;47:7571-7.

[13] Sfaxi IBA, Durand I, Lugo R, Mohammadi AH, Richon D. Hydrate phase equilibria of $CO_2 + N_2$ + aqueous solution of THF, TBAB or TBAF system. Int. J. Greenhouse Gas Control 2014;26:185-92.

[14] Li XS, Xu CG, Chen ZY, Wu HJ. Hydrate-based pre-combustion carbon dioxide capture process in the system with tetra-n-butyl ammonium bromide solution in the presence of cyclopentane. Energy 2011;36:1394-403.

[15] Li XS, Xu CG, Chen ZY, Cai J. Synergic effect of cyclopentane and tetra-n-butyl ammonium bromide on hydrate-based carbon dioxide separation from fuel gas mixture by measurements of gas uptake and X-ray diffraction patterns. Int. J. Hydrogen Energy 2012;37:720-7.

[16] Sloan ED, Koh C. Clathrate Hydrates of Natural Gases, 3th ed. Boca Raton: Taylor &Francis; 2007.

[17] Herslund PJ, Thomsen K, Abildskov J, Solms N. Modelling of cyclopentane promoted gas hydrate systems for carbon dioxide capture processes. Fluid Phase Equilib 2014;375:89-103

[18] Babu P, Linga P, Kumar R, Englezos P. A review of the hydrate based gas separation (HBGS) process for carbon dioxide pre-combustion captue. Energy 2015;85:261-79

[19] Seo Y, Kang SP, Lee S, Lee H. Experimental measurements of hydrate phase equilibria for carbon dioxide in the presence of THF, propylene oxide, and 1,4-dioxane. J. Chem. Eng. Data 2008;53:2833-7.

[20] Kang SP, Lee H, Lee CS, Sung WM. Hydrate phase equilibria of the guest mixtures containing CO_2, N_2 and tetrahydrofuran. Fluid Phase Equilib 2001;185:101-9.

[21] Delahaye A, Fournaison L, Marinhas S, Chatti I, Petitet JP, Dalmazzone D, et al. Effect of THF on equilibrium pressure and dissociation enthalpy of CO_2 hydrates applied to secondary refrigeration. Ind. Eng. Chem. Res 2005;45:391-7.

[22] Lee Y, Lee S, Lee J, Seo Y. Structure identification and dissociation enthalpy measurements of the $CO_2 + N_2$ hydrates for their application to CO_2 capture and storage. Chem Eng J

2014;246:20-6.

Chapter 6. References

[1] R. Kumar, H.J. Wu, P. Englezos, Incipient hydrate phase equilibrium for gas mixtures cont aining hydrogen, carbon dioxide and propane, Fluid Phase Equilibria, 244 (2) (2006), 167–171

[2] Park S, Lee S, Lee Y, Seo Y. CO_2 capture from simulated fuel gas mixtures using semiclathrate hydrates formed by quaternary ammonium salts. Environ Sci Technol. 2013;47:7571-7.

[3] N. Mayoufi, D. Dalmazzone, W. Fürst, A. Delahaye, L. Fournaison, CO_2 enclathration in hydrat es of peralkyl-(ammonium/phosphonium) salts: stability conditions and dissociation enthalpies, J. Eng. Data 55 (2009) 1271-1275.

[4] J. Deschamps, D. Dalmazzone, Hydrogen storage in semiclathrate hydrates of tetrabutyl a mmonium chloride and tetrabutyl phosphonium bromide, J. Chem. Eng. Data 55 (2010) 3395-3399.

Education

- M.S. in Environmental Engineering (2011. 03 – 2013. 02) Advisor: Prof. Taehyeung Kim
  Department of Environmental Engineering,Changwon National University
  Thesis Title: “Investigation of Odor Dispersion from Industrial area in Changwon City”
- B.S. in Environmental Engineering (2007. 03 – 2011. 02)
  Department of Environmental Engineering, Changwon National University

Membership

- Korean Institute of Chemical Engineering (KIChE)
- Korean Society of Environmental Engineers (KSEE)

Journal publications

[1] Prueksakorn, K., Kim, T., **Kim, S.**, Kim, H., Kim, K. Y., Son, W., Vongmahadlek, C., “Review of Air Dispersion Modeling Approaches to Assess the Risk of Wind-borne Spread of Foot-and mouth Disease Virus”, *Journal of Environmental Protection*, **3**, 1260-1267 (2012).

[2] **Kim, S.**, Baek I., You, J., Seo, Y. "Guest gas enclathration in tetra-n-butyl ammonium chloride (TBAC) semiclathrates: Potential application to natural gas storage and CO_2 capture" *Applied Energy*, **140**, 107-112 (2015).

[3] **Kim, S.**, Kang, S., Seo, Y. "Semiclathrate-based CO_2 capture from flue gas in the presence of tetra-n-butyl ammonium chloride (TBAC)", *Chemical Engineering Journal*, **276**, 205–212, (2015).

[4] **Kim, S.**, Seo, Y. "Semiclathrate-based CO_2 capture from flue gas mixtures: An experimental approach with thermodynamic and Raman spectroscopic analyses", *Applied Energy*, **154**, 987-994 (2015)

[5] **Kim, S.**, Baek I., You, J., Seo, Y. “Phase equilibria, dissociation enthalpies, and Raman spectroscopic analyses of N_2 + tetra-n-butyl ammonium chloride (TBAC) semiclathrates”, Fluid Phase Equilibria, **413**, 86-91(2016)

[6] **Kim, S.**, Choi S-D., Seo, Y., “CO_2 capture from flue gas using clathrate formation in the presence of thermodynamic promoters”, Energy **(In press)**

[7] **Kim, S., Seo, Y.**, “Guest gas enclathration in tetra-iso-amyl ammonium bromide (TiAAB) semiclathrates: potential application to natural gas storage and CO_2 capture” **(In preparation)**

[8] **Kim, S., Seo, Y.**, “Phase equilibria and spectroscopic analysis of tetra-iso-amyl ammonium bromide (TiAAB) semiclathrates with CO_2, N_2, and CO_2 + N_2” **(In preparation)**

[9] **Kim, S., Seo, Y.**, “CO_2 capture from CO_2 + H_2 gas mixture using tetra-n-butyl ammonium chloride semiclathrate” **(In preparation)**

Conference

International

[1] **Kim, S.,** Kim, E., Seo, Y.T., Kang, S-P., Lee, J-w., Seo, Y., "CO_2 CAPTURE FROM CO_2 + N_2 GAS MIXTURES USING QUATERNARY AMMONIUM SALT SEMICLATHRATE HYDRATES", Proceedings of the 8th International Conference on Gas Hydrates (ICGH8-2014), Beijing, China, 28 July - 1 August (2014)

[2] **Kim, S.** and Seo, Y., "CO_2 CAPTURE FROM CO_2 + N_2 GAS MIXTURES USING TETRA-n-BUTYLAMMONIUM CHLORIDE SEMICLATHRATES", 10th International Conference on Separation Science and Technology (ICSST14) Nara, Japan, 30 October -1 November (2014)

[3] Seo, Y., **Kim, S.**, Kang, S-P., "Guest gas enclathration in the tetra-n-butyl ammonium chloride (TBAC) semiclathrates: potential application to CO_2 capture", Spring 2015 National Meeting & Expo, Denver, CO, USA, Mar 22-26 (2015)

[4] Kim, E., **Kim, S.**, Lee, Y., Jin, Y-K., Seo, Y., "Influences of large molecular alcohols on phase behavior and structural characteristics of CO_2 hydrates", 13th International Conference on Carbon Dioxide Utilization, Singapore, July 05 – 09 (2015)

[5] **Kim, S.**, Lee, Y., Kim, E., Kang, S-P., Seo, Y., "Quaternary Ammonium Salt Semiclathrates-Based CO_2 Capture from Flue Gas Mixtures", 13th International Conference on Carbon Dioxide Utilization, Singapore, July 05 – 09 (2015)

[6] **Kim, S.**, Seo, Y., "CO_2 Capture from Flue Gas using Quaternary Ammonium Salts Semi-clathrate", 3th International Environmental Engineering Conference, Korea, October 28 – 30 (2015)

[7] **Kim, S.**, Lee, Y., Seo, Y "Guest Gas Enclathration in Tetra-n-butylammonium Chloride (TBAC) Semiclathrates as Revealed by Phase Equilibria and Spectroscopic Analyses.", 8th International Conference on Separation Science and Technology, China, July 05-10, 2016

Domestic

[1] **Kim, S.**, Kim, T., Prueksakorn, K., Park, N., "Investigation of Odor Dispersion from Industrial Area over the Complex Terrain of Changwon City", Korean Society of Odor Research and Engineering, Nov.2012

[2] Park, N., Kim, T., **Kim, S.,** Choi, J., "The Study of the Actual State of Odor in ChangWon City, Korean Society of Odor Research and Engineering, Nov.2012

[3] Kim, Y., Lee, Y., **Kim, S.**, Kim, E., Seo, Y., "Themodynamic and Microscopic Analyses of the CH_4 + CO_2 Mixed Gas Hydrate Containing Neohexane, 15th Asian Chemical Congress, Aug.2013

[4] Lee, Y., Kim, Y., **Kim, S.**, Kim, E., Seo, Y., "Structural Transition of structure H Hydrate to structure I hydrate in the CO_2 + N_2 + 2,2 dimethylbutane + Water System", Korean Institute of Chemical Engineers (KIChE) Fall Meeting, Oct.2013

[5] Kim, Y., **Kim, S.**, Lee, Y., Kim, E., Seo, Y., "기체 조성에 따른 CH_4 + CO_2 + 액상탄화수소 혼합가스 하이드레이트의 구조전이 현상규명", Korean Institute of Chemical Engineers (KIChE) Fall Meeting, Oct. 2013

[6] **Kim, S.**, Kim, Y., Lee, Y., Kim, E., Seo, Y., "Guest Gas Enclathration in the Tetra-n-butyl Ammonium Chlorid (TBAC) Semi-clathrates: Thermodynamic and Spectroscopic Analyses", Korean Institute of Chemical Engineers (KIChE) Fall Meeting, Oct.2013

[7] Lee, Y., Yunju Kim, **Kim, S.**, Kim, E., Seo, Y., "Structural Transition and Dissociation Enthalpies of the Mixed CO_2 + N_2 Neohexanxe Hydrates Using a Micro Differential Scanning Calorimeter, Korean Society For New And Renewable Energy (KSNRE) Fall Meeting, Nov.2013

[8] **Kim, S.**, Kim, Y., Lee, Y., Kim, E., Seo, Y., "TBAC Semi-clathrate를 이용한 CO_2 + N_2 혼합가스 분리 및 회수", Korean Society For New And Renewable Energy (KSNRE) Fall Meeting, Nov. 2013

[9] **Kim, S.**, Lee, Y., Kim, E., Seo, Y., "Selective Partitioning of CO_2 in the Flue Gas Mixtures by TBAC Semi-clathrates Formation" Korean Institute of Chemical Engineers (KIChE) Spring Meeting, Apr.2014, Changwon

[10] Lee, Y., **Kim, S.**, Kim, E., Seo, Y., "CO_2 as a Co-guest of Structure H Hydrates Formed from the CO_2 + N_2 – dimethybutane + Water Mixtures", Korean Institute of Chemical Engineers (KIChE) Spring Meeting, Apr.2014, Changwon

[11] Kim, E., **Kim, S.**, Kim, Y., Lee, Y., Yongkeun Jin, Seo, Y., "Phase-Equilibrium and Structural Chracteristics of Gas Hydrates with Pinacolyl Alcohol and tert-Amyl Alcohol", Korean Institute of Chemical Engineers (KIChE) Spring Meeting, Apr.2014 , Changwon

[12] **Kim, S.**, Lee, Y., Kim, E., Seo, Y., "QAS계 Semiclathrate를 이용한 연소 배가스로부터의 CO_2 + N_2 혼합가스 분리, Korean Society For New And Renewable Energy (KSNRE) Spring Meeting, May.2014, Busan

[13] Kim, E., **Kim, S.**, Lee, Y., Seo, Y., "Structural analyses and phase behaviors of gas hydrates with pinacolyl alcohol and tert-butyl alcohol", Korean Society For New And Renewable Energy (KSNRE) Spring Meeting, May 2014, Busan

[14] Kim, E., **Kim, S.**, Lee, Y., Seo, Y., 'Effect of large moleculer alcohols on phase behavior and structural characteristics of CO_2 and N_2 hydrates, Korean Institute of Chemical Engineers (KIChE) Fall Meeting, Oct.2014, Daejeon

[15] Lee, D., Lee, J., Lee, Y., **Kim, S.**, Kim, E., Seo, Y., "Structure Transition of Gas Hydrates in the CO_2 + N_2 + Methylcyclopentane + Water Systems", Korean Institute of Chemical Engineers (KIChE) Fall Meeting, Oct.2014, Daejeon

[16] Lee, J., Lee, D., Lee, Y., **Kim, S.**, Kim, E., Seo, Y., "Thermodynamic and Spectroscopic Analyses of Cyclopentane Hydrates in the Presence of Small Guest Molecules", Korean Institute of Chemical Engineers (KIChE) Fall Meeting, Oct.2014, Daejeon

[17] Lee, Y., **Kim, S.**, Kim, E., Seo, Y., "Experimental Verification of the CH_4-Flue Gas Replacement in the Structure H Hydrate System", Korean Institute of Chemical Engineers (KIChE) Fall Meeting, Oct.2014, Daejeon

[18] **Kim, S.**, Lee, Y., Kim, E., Seo, Y., "Quaternary Ammonium Salt Semiclathrate-Based CO_2 Capture from Flue Gas Mixtures", Korean Institute of Chemical Engineers (KIChE) Fall Meeting, Oct.2014, Daejeon

[19] **Kim, S.**, Seo, Y., "Effects of Thermodynamic Promotors on Clathrate-based CO_2 Capture from Flue Gas", Korean Institute of Chemical Engineers (KIChE) Spring Meeting, Apr.2015, Jeju

[20] Lee, J., Lee, Y., **Kim, S.**, Seo, Y., "Experimental Verification of Cyclopentane Hydrates with Guest Molecules for Potential Applications to Desalination and Gas Storage", Korean Institute of Chemical Engineers (KIChE) Spring Meeting, Apr.2015, Jeju

[21] **Kim, S.**, Seo, Y., "Post-combustion CO_2 Capture Using Clathrate Formation: Effects of Thermodynamic Promoters", Korean Institute of Chemical Engineers (KIChE) Fall Meeting, Oct.2015, Ilsan

[22] 고결, 김은애, 김소영, 임지연, 김나영, 서용원, 유정균, 백일현, "아민 계열 CO_2 흡수제의 열

변성 및 거품 생성 현상 관찰", The Korean Institute of Chemical Engineers, Apr.2016, Busan, Republic of Korea (poster)

[23] Lee, J., **Kim, S.**, Lee, Y., Seo, Y., "Thermodynamic and Spectroscopic Analyses of Cyclopentane Hydrate with Guest Molecules for Potential Application in Gas Storage and Desalination", The Korean Institute of Chemical Engineers, Apr.2016, Busan, Republic of Korea (poster)

[24] **Kim, S.**, Kim, K., Seo, Y, "Guest Gas Enclathration in Tetra-iso-amyl Ammonium Bromide (TiAAB) semi-clathrate: Thermodynamic and Spectroscopic Approaches", The Korean Institute of Chemical Engineers, Apr.2016, Busan, Republic of Korea (poster)

[25] Lee, J., Lee, Y., **Kim, S.**, Seo, Y.,, "Phase behavior and characterization of the pure CP and CP + CO_2 hydrates in the presence of NaCl for desalination", The Korean Institute of Chemical Engineers, Oct.2016, Dajeon, Republic of Korea (poster)

[26] **Kim, S.**, Seo, Y., "CO_2 Capture from CO_2 + H_2 Gas Mixture using Tetra-n-butyl Ammonium Chloride Semi-clathrate", The Korean Institute of Chemical Engineers, Oct.2016, Dajeon, Republic of Korea (poster)

[27] 이준섭, 이요한, 김소영, 서용원, "담수화와 기체저장으로의 응용을 위한 사이클로펜테인 하이드레이트의 열역학적 및 분광학적 분석", The Korean Society of New and Renewable Evergy, Nov. 2016, Gwangju, Republic of Korea

Awards and Honors

[1] Oral Presentation Award, Korean Society of Odor Research and Engineering, Nov. 2012

[2] Flash-Presentation Award, The Korean Institute of Chemical Engineers, Oct. 2013

Acknowledgment

박사과정을 열심히 하겠다는 각오를 다진지 얼마 지나지 않은 것 같은데 벌써 4년이라는 시간이 지나 졸업을 앞두게 되었습니다. 이 논문이 완성되기까지 지난 4년간 미숙한 저를 지도하여 주신 서용원 교수님께 깊은 감사를 드립니다. 또한 논문심사를 통하여 많은 조언과 격려를 주신 강성필 박사님, 권영남 교수님, 차채녕 교수님, 최성득 교수님께 깊이 감사드립니다.

항상 옆에서 든든한 지원군이 되어준 부모님, 의젓한 내동생에게 사랑한다고 전하고 싶습니다. 앞으로도 모두 항상 건강하고 행복이 넘치길 기도하겠습니다. 그리고 4년동안 많은 일도 있었지만, 소중한 추억과 인연이되어버린 함께한 연구실 동료들에게도 감사의 마음을 전합니다. 짧으면 짧고 길면 길수 있는 학위기간 동안 인연을 맺었던 선생님, 친구들, 이 지면에는 다 표현 할수 없는 도움을 주신 모든 분들께 감사드리며 앞으로도 지켜봐 주실 것을 부탁드립니다. 힘들고 지칠 때 울산까지 찾아와 힘이되어준 소중한 진서와 은진이, 앞으로도 항상 행복하길 바랍니다.

학위과정을 마치며 작성한 이 논문을 세상에 내어놓기에 부끄러움이 앞서지만, 저의 인생에 있어 2017년은 학위과정이 마무리 되며 또 다른 시작을 하게되는 해입니다. 희망찬 시작을 앞두고, 앞으로의 삶이 부끄럽지 않도록 저를 통해 계획하신대로 살아갈수 있도록 기도드리며 이만 줄이겠습니다.

2017년 1월